Origin and Evolution of the Universe

Week 2

COSMIC DISTANCES, SURVEYS, & BIG BANG NUCLEOSYNTHESIS

Joel Primack

University of California, Santa Cruz

Picturing the History of the Universe: The Backward Lightcone

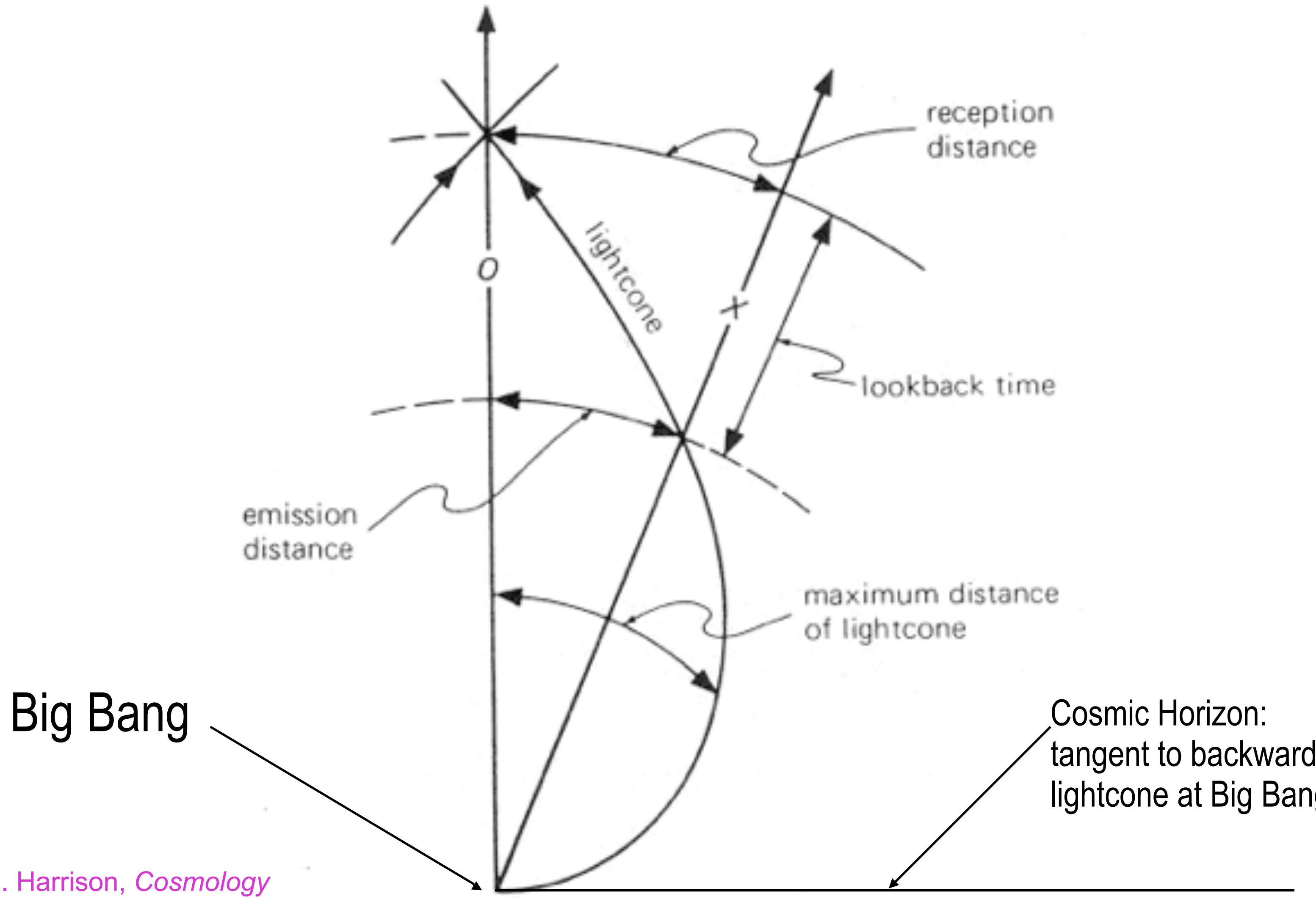

From E. Harrison, *Cosmology* (Cambridge UP, 2000).

Picturing the History of the Universe: The Backward Lightcone

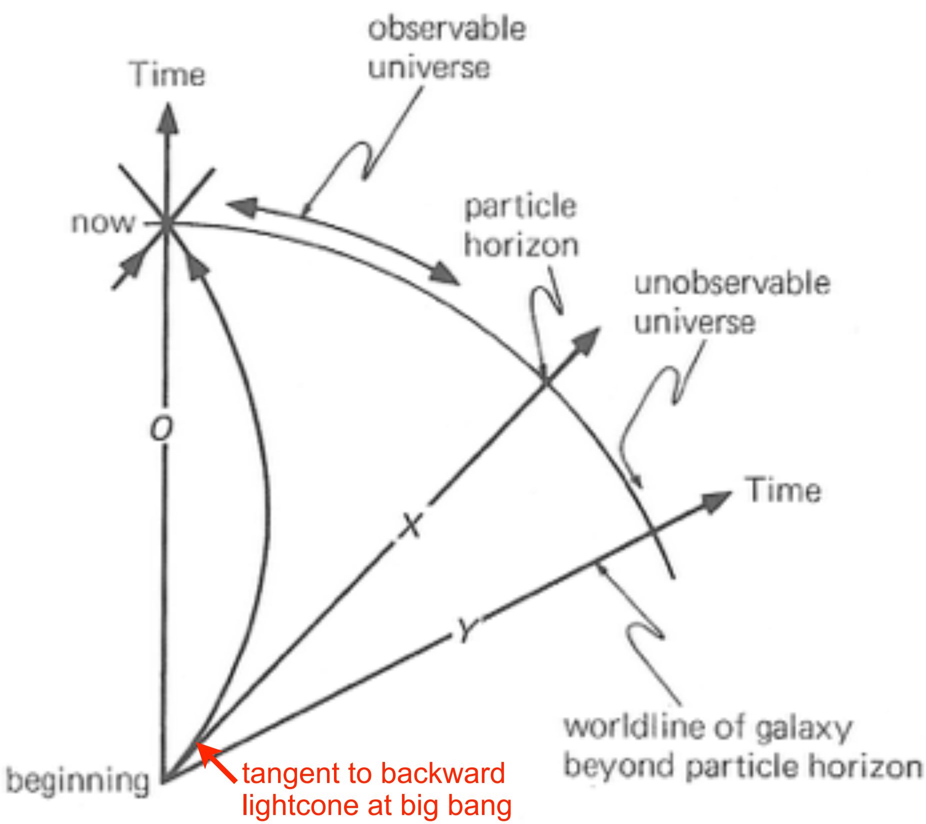

Figure 21.11. At the instant labeled "now" the particle horizon is at worldline X. In a big bang universe, all galaxies at the particle horizon have infinite redshift.

From E. Harrison, *Cosmology* (Cambridge UP, 2000).

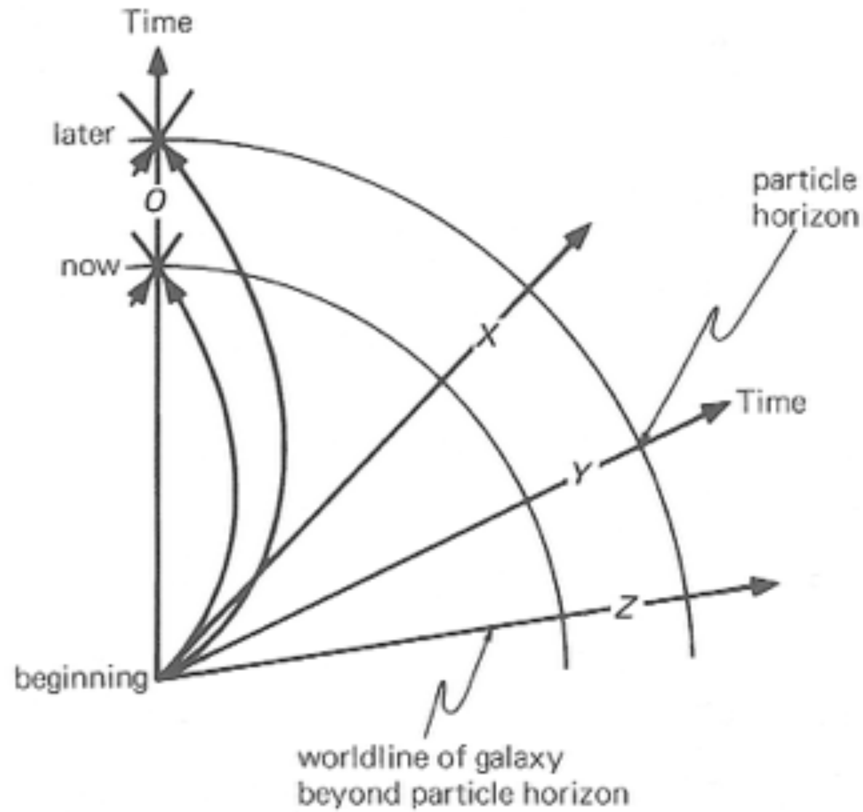

Figure 21.12. At the instant labeled "later" the particle horizon has receded to world line Y. Notice the distance of the particle horizon is always a reception distance, and the particle horizon always overtakes the galaxies and always the fraction of the universe observed increases.

Distances in an Expanding Universe

Proper distance = physical distance = d_p

$d_p(t_0)$ = (physical distance at t_0) = $a(t_0)\, r_e = r_e$

$\chi(t_e)$ = (comoving distance of galaxy emitting at time t_e)

$$\chi(t_e) = \int_0^{r_e} dr = r_e = c\int_{t_e}^{t_0} dt/a = c\int_{a_e}^{1} da/(a^2 H)$$

because

$$dt = (dt/da)\, da = (a\, dt/da)\, da/a = da/(aH)$$

$d_p(t_e)$ = (physical distance at t_e) = $a(t_e)\, r_e = a_e\, r_e$

The Hubble radius $d_H = c\, H_0^{-1}$ = $4.29\, h_{70}^{-1}$ Gpc = $13.97 h_{70}^{-1}$ Glyr

For E-dS, where $H = H_0\, a^{-3/2}$,

$$\chi(t_e) = r_e = d_p(t_0) = 2d_H\,(1-a_e^{1/2})$$

$$d_p(t_e) = 2d_H\, a_e\,(1-a_e^{1/2})$$

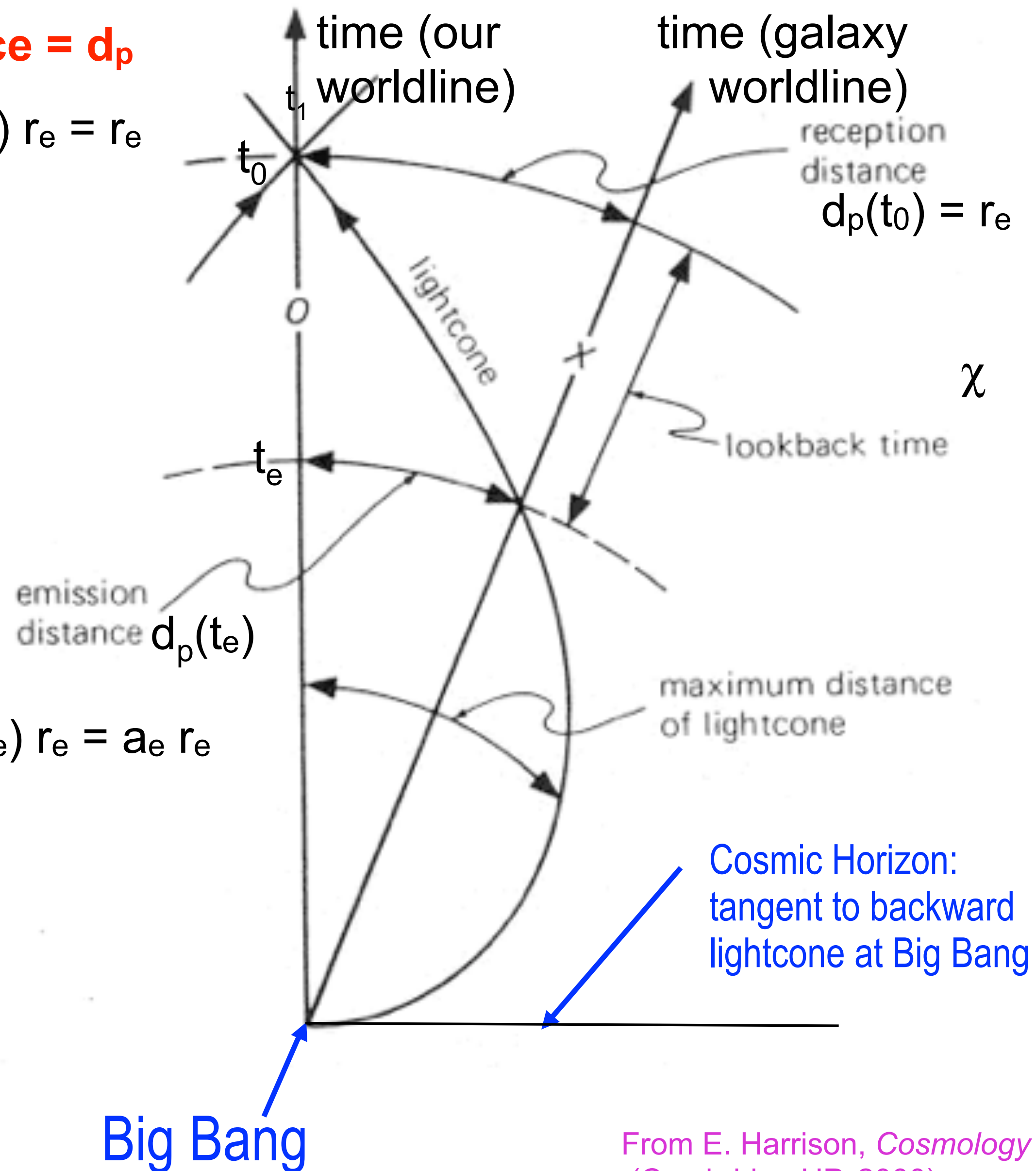

From E. Harrison, *Cosmology* (Cambridge UP, 2000).

Our Particle Horizon

FRW: $ds^2 = -c^2\, dt^2 + a(t)^2\, [dr^2 + r^2\, d\theta^2 + r^2 \sin^2\theta\, d\phi^2]$ for curvature K=0 so $\sqrt{g_{rr}} = a(t)$

Particle Horizon

$\mathbf{d_p}$(horizon) = (physical distance at time t_0) = $a(t_0)\, r_p = r_p$

$$\mathbf{d_p}(\text{horizon}) = \int_0^{r_{horizon}} dr = r_{horizon} = c\int_0^{t_0} dt/a = c\int_0^{1} da/(a^2H)$$

For E-dS, where $H = H_0\, a^{-3/2}$,

$$r_{horizon} = \lim_{a_e \to 0} 2d_H\, (1-a_e^{1/2}) = 2d_H =$$

$= 8.58\, h_{70}^{-1}$ Gpc $= 27.94\, h_{70}^{-1}$ Glyr

For the Benchmark Model with h=0.70,
$r_{horizon}$ = 13.9 Gpc = 45.2 Glyr.

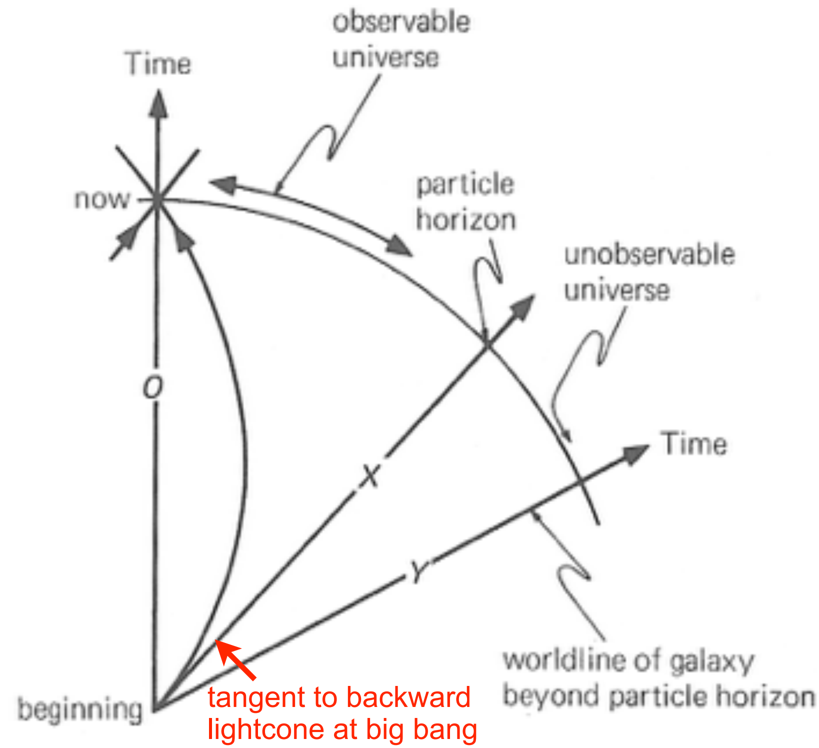

Figure 21.11. At the instant labeled "now" the particle horizon is at worldline X. In a big bang universe, all galaxies at the particle horizon have infinite redshift.

For WMAP5 parameters h = 0.70, Ω_m = 0.28, k = 0, t_0 = 13.7 Gyr, $r_{horizon}$ = 46.5 Glyr.
For Planck parameters h = 0.678, Ω_m = 0.31, k = 0, t_0 = 13.8 Gyr, $r_{horizon}$ = 46.1 Glyr.

Distances in an Expanding Universe

FRW: $ds^2 = -c^2\,dt^2 + a(t)^2\,[dr^2 + r^2\,d\theta^2 + r^2 \sin^2\theta\ \ d\phi^2]$ for curvature k=0

$$\chi(t_1) = (\text{comoving distance at time } t_1) = \int_0^{r_1} dr\,\sqrt{g_{rr}} = a(t_1)\,r_1 \qquad \left(\sqrt{g_{rr}} = a(t_1) \text{ for } k=0\right)$$

$$\boldsymbol{\chi = (\textbf{comoving distance at time } t_0) = r_1} \qquad [\text{since } a(t_0)=1]$$

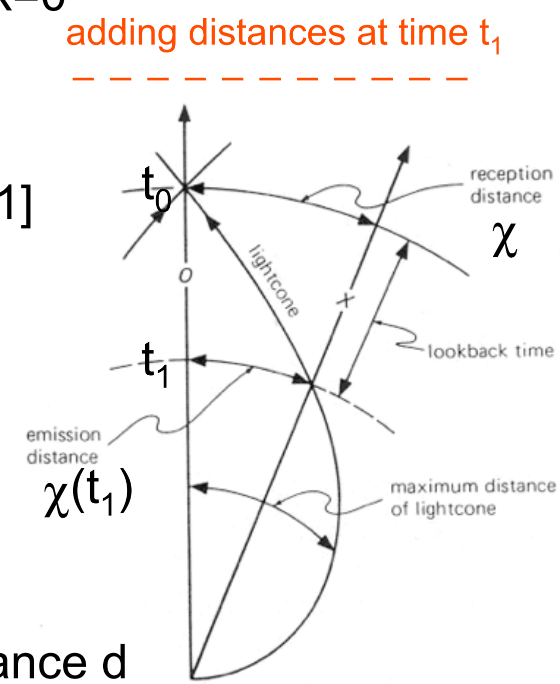

From the FRW metric above, the distance D across a source at distance r_1 which subtends an angle $d\theta$ is $D=a(t_1)\,r_1\,d\theta$. The angular diameter distance d_A is defined by $d_A = D/d\theta$, so

$$\mathbf{d_A = a(t_1)\,r_1 = r_1/(1+z_1)}$$

In Euclidean space, the luminosity L of a source at distance d is related to the apparent luminosity ℓ by

ℓ = Power/Area = $L/4\pi d^2$

so the luminosity distance d_L is defined by $d_L = (L/4\pi\ell)^{1/2}$.

Weinberg, *Gravitation and Cosmology*, pp. 419-421, shows that in FRW

$$\ell = \text{Power/Area} = L\,[a(t_1)/a(t_0)]^2\,[4\pi a(t_0)^2\,r_1^{\,2}]^{-1} = L/4\pi d_L^{\,2}$$

$[a(t_1)/a(t_0)]^2$: (redshift of each photon)(delay in arrival)

$[4\pi a(t_0)^2\,r_1^{\,2}]^{-1}$: fraction of photons reaching unit area at t_0

Thus

$$\mathbf{d_L = r_1/a(t_1) = r_1\,(1+z_1)}$$

Distances in an Expanding Universe

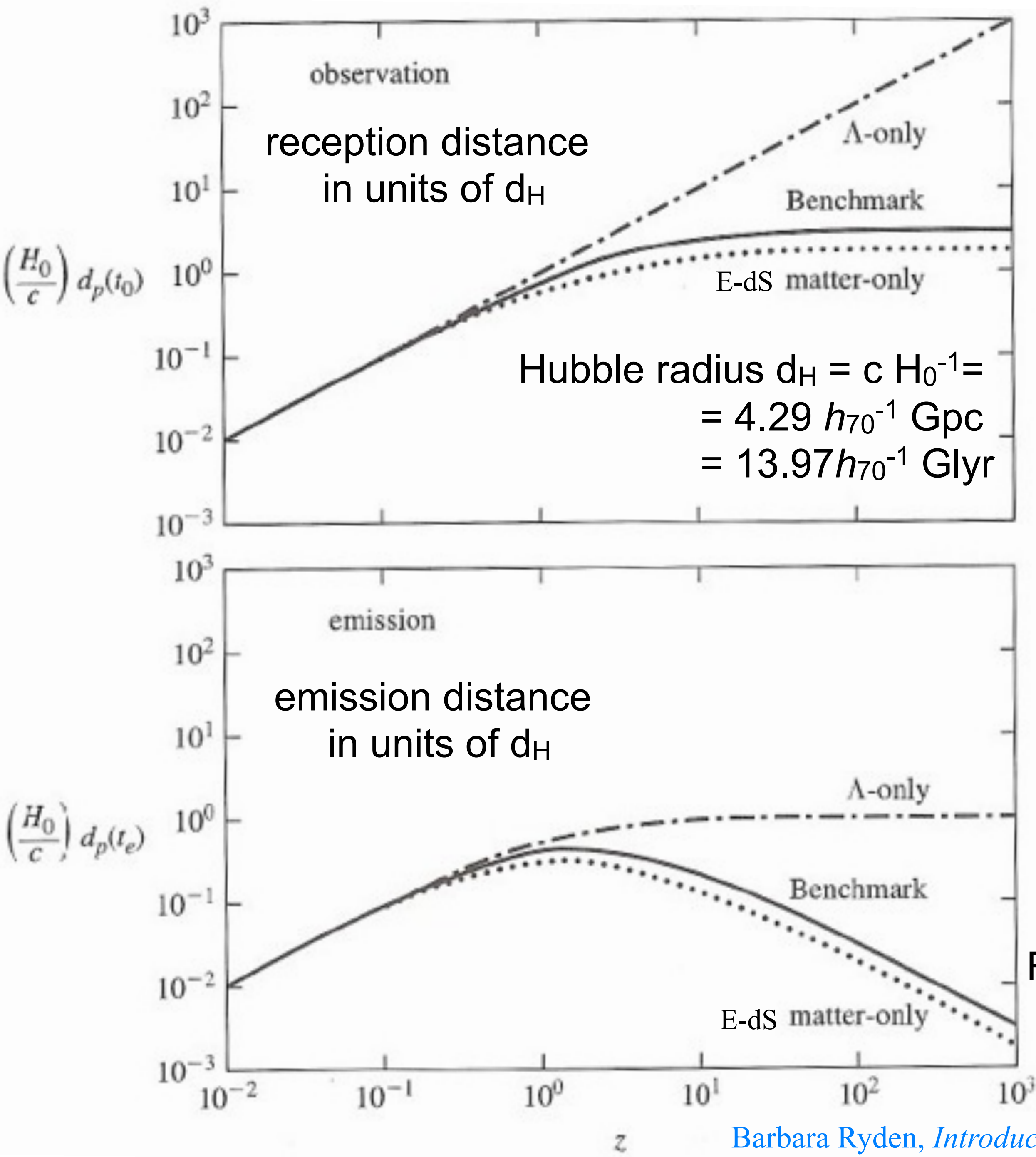

Hubble radius $d_H = c\,H_0^{-1} =$
$= 4.29\ h_{70}^{-1}$ Gpc
$= 13.97 h_{70}^{-1}$ Glyr

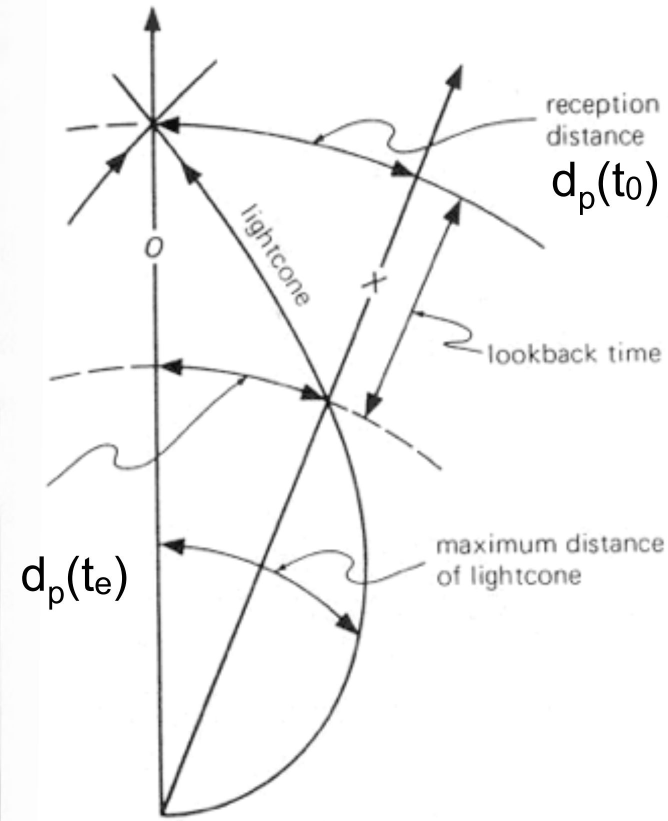

For E-dS, where $H = H_0\, a^{-3/2}$,

$\chi(t_e) = r_e = d_p(t_0) = 2d_H\,(1 - a_e^{1/2})$

$d_p(t_e) = 2d_H\, a_e\,(1 - a_e^{1/2})$

Barbara Ryden, *Introduction to Cosmology* (Addison-Wesley, 2003)

Distances in a Flat (k=0) Expanding Universe

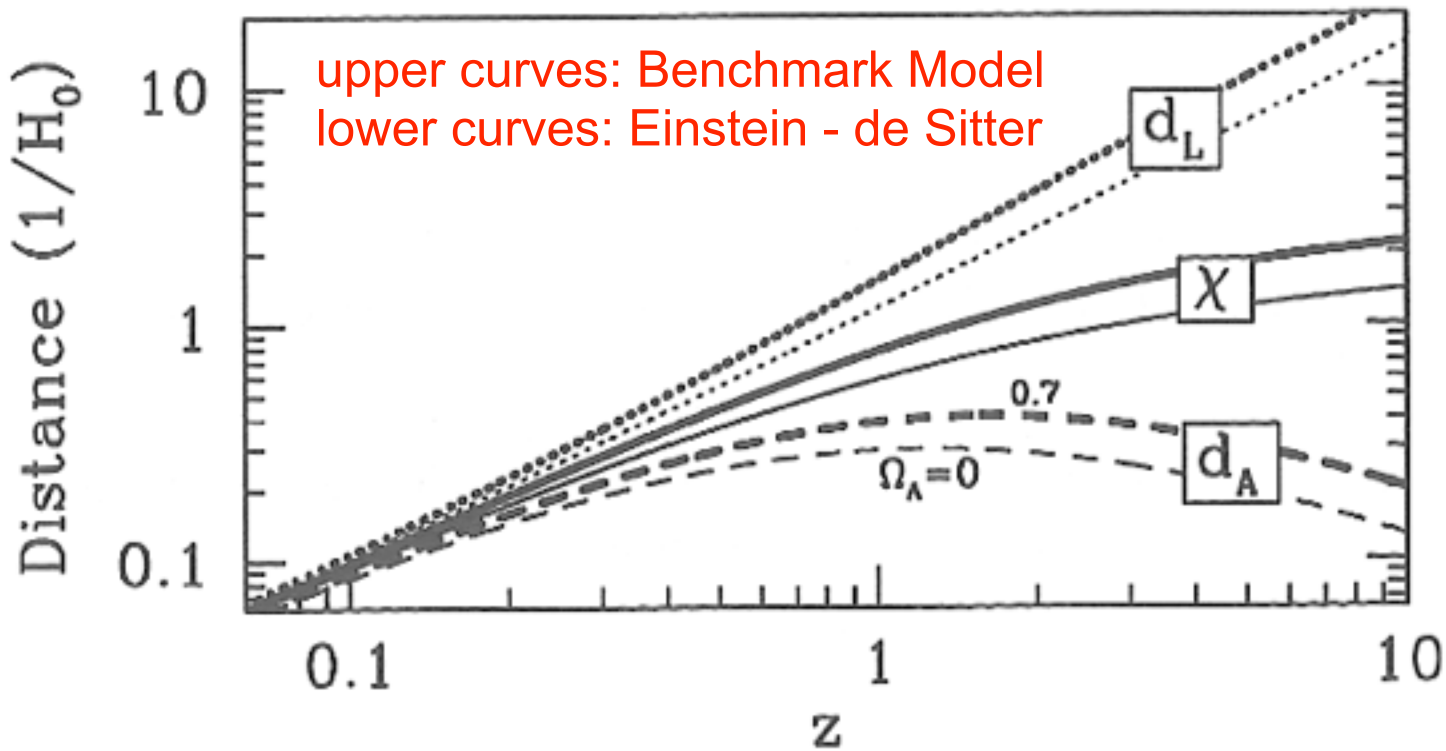

Figure 2.3. Three distance measures in a flat expanding universe. From top to bottom, the luminosity distance, the comoving distance, and the angular diameter distance. The pair of lines in each case is for a flat universe with matter only (light curves) and 70% cosmological constant Λ (heavy curves). In a Λ-dominated universe, distances out to fixed redshift are larger than in a matter-dominated universe.

Scott Dodelson, *Modern Cosmology* (Academic Press, 2003)

Distances in the Expanding Universe

D_{now} = proper distance, D_L = luminosity distance,

D_A = angular diameter distance, $D_{ltt} = c(t_0 - t_z)$

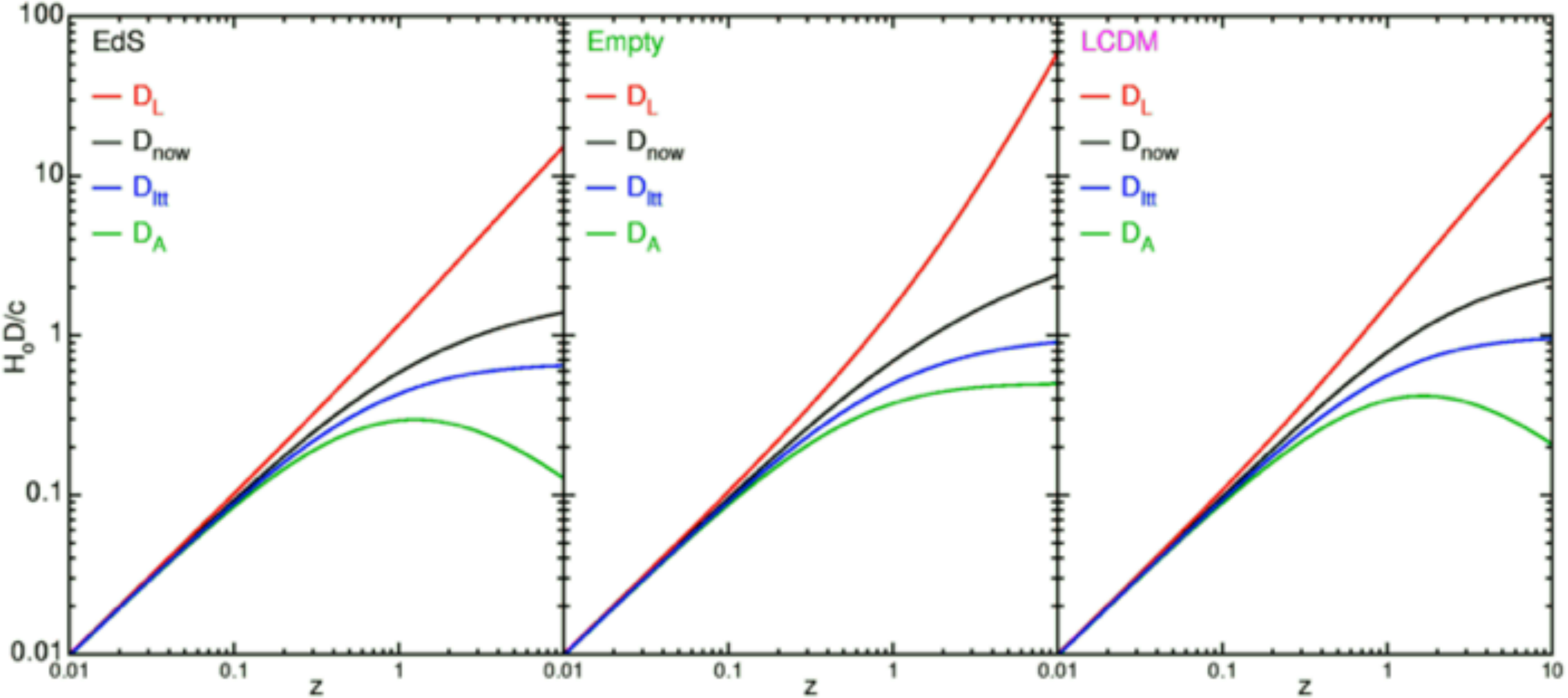

http://www.astro.ucla.edu/~wright/cosmo_02.htm#DH

Horizons

PARTICLE HORIZON

Spherical surface that at time t separates ***worldlines*** into observed vs. unobserved

FRW

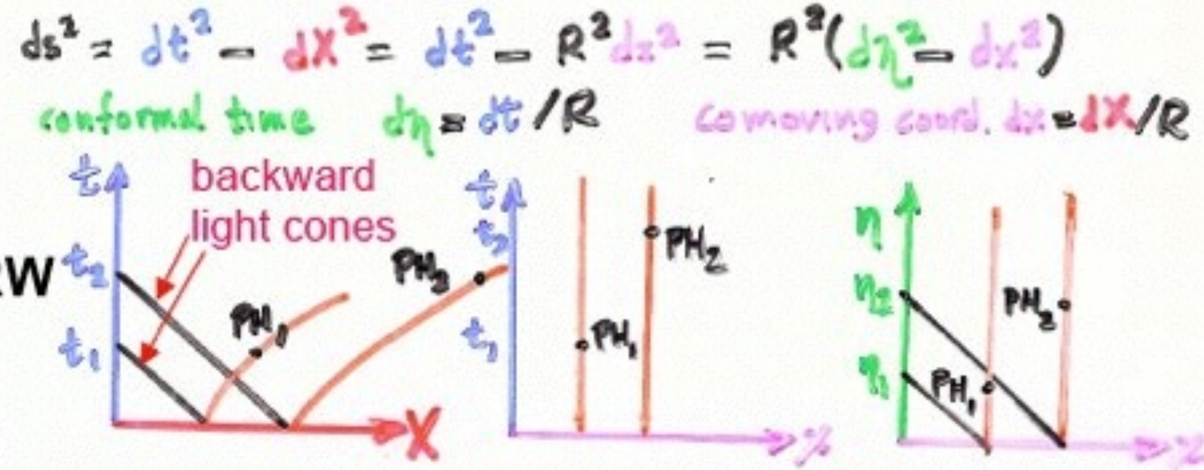

EVENT HORIZON

Backward lightcone that separates *events* that will someday be observed from those never observed

deS

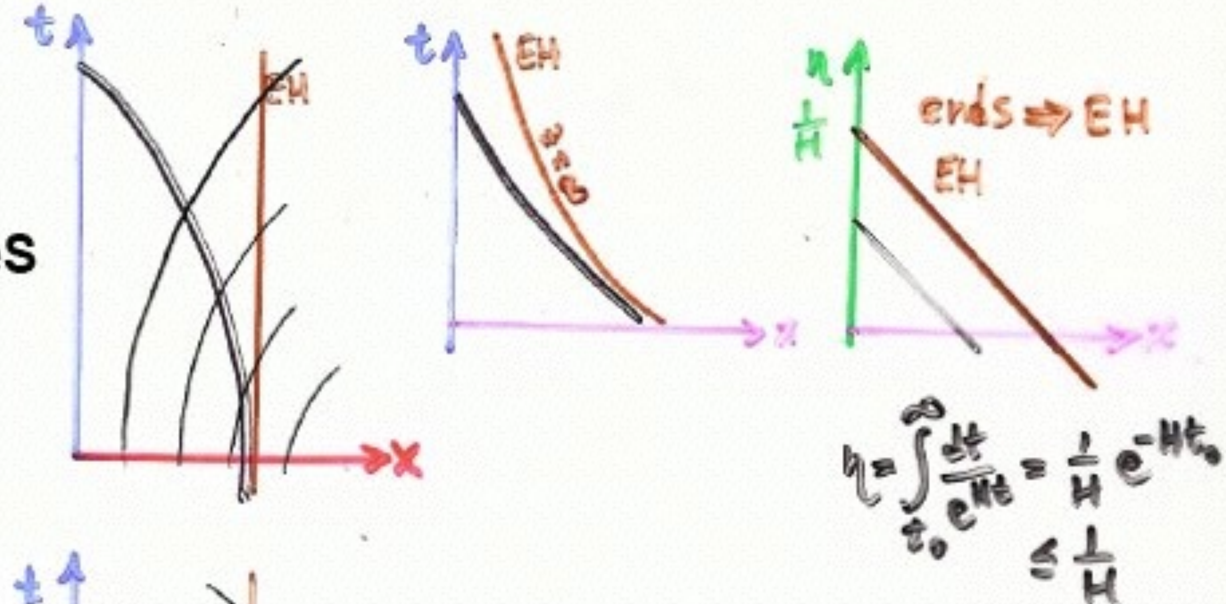

Schwarzschild

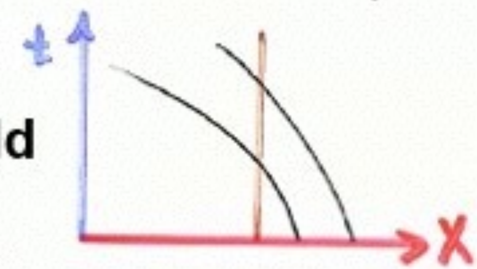

See Harrison, *Cosmology*
Rindler, *Relativity*

Velocities in an Expanding Universe

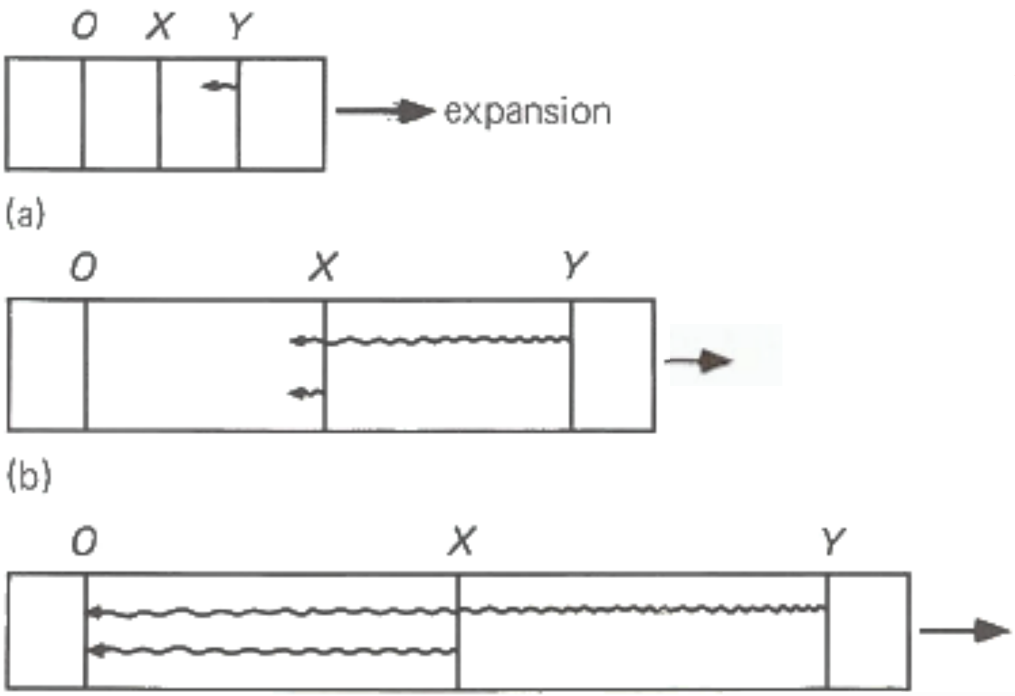

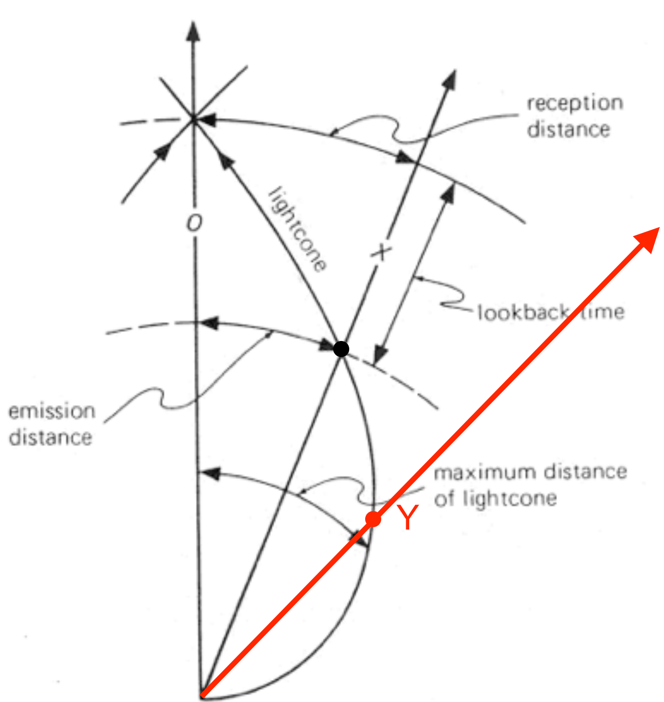

From E. Harrison, *Cosmology* (Cambridge UP, 2000).

Figure 15.12. On an elastic strip let O represent our position, and X and Y the positions of two galaxies. If signals from X and Y are to reach us at the same instant, then Y, which is farther away, must emit before X. In (a), Y emits a signal. In (b), X emits a signal at a later instant when it is farther away than Y was when it emitted its signal. In (c), both signals arrive simultaneously at O. Y's signal has the greater redshift (it has been stretched more) although Y was closer than X at the time of emission. This odd situation occurs at large redshifts in all big bang universes.

Velocities in an Expanding Universe

The velocity away from us now of a galaxy whose light we receive with redshift z_e, corresponding to scale factor $a_e = 1/(1 + z_e)$, is

$$v(t_0) = H_0\, d_p(t_0)$$

The velocity away from us that this galaxy had when it emitted the light we receive now is

$$v(t_e) = H_e\, d_p(t_e)$$

The graph at right shows $v(t_0)$ and $v(t_e)$ for the E-dS cosmology.

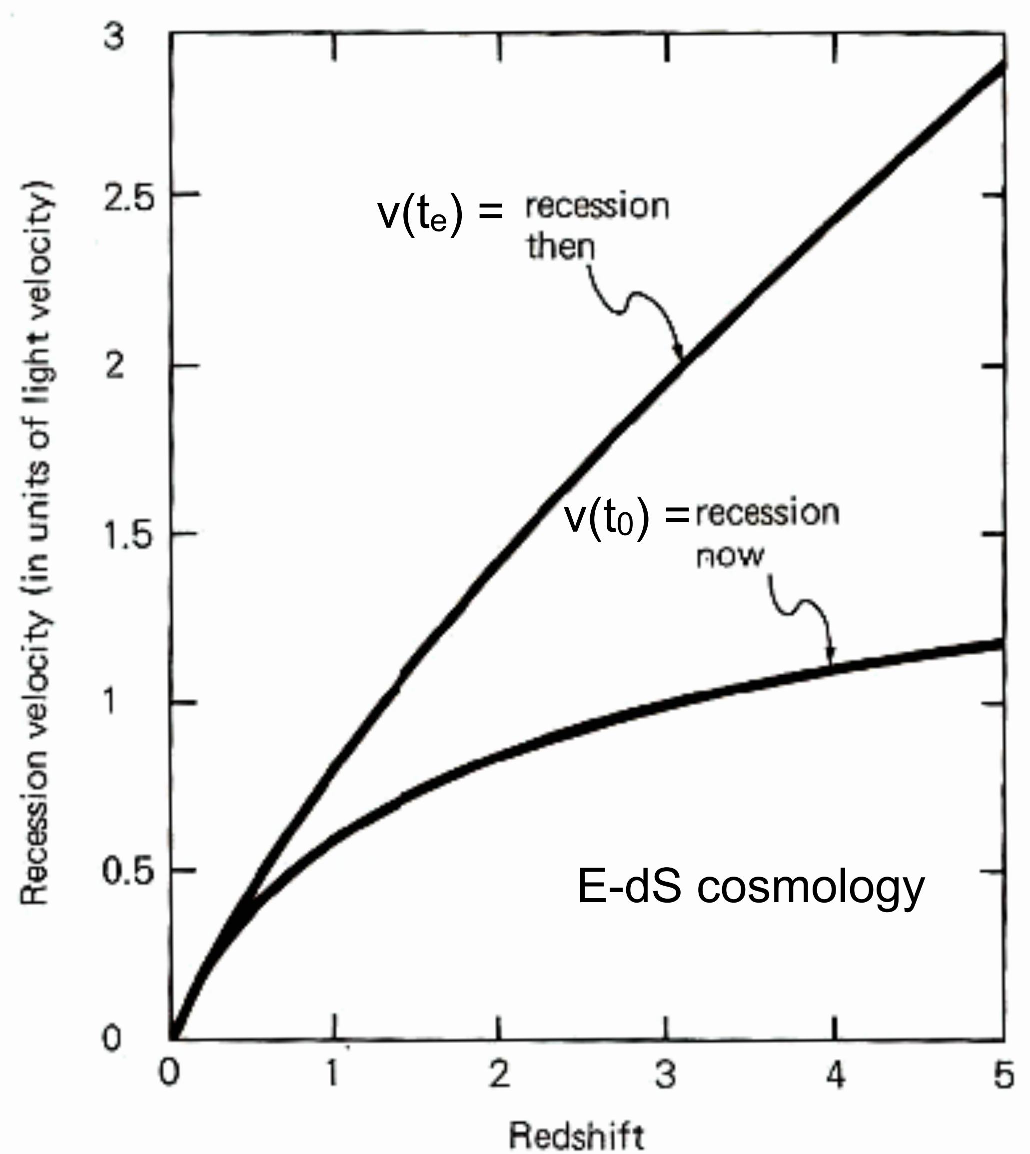

For E-dS, where $H = H_0\, a^{-3/2}$,

$$v(t_0) = H_0\, d_p(t_0) = 2c\,(1-a^{1/2})$$

$$v(t_e) = H_e\, d_p(t_e)$$

$$= H_0\, a_e^{-3/2}\, a_e\, 2c\,(1-a^{1/2})/H_0 = 2c\,(a^{-1/2} - 1)$$

Distances in the Expanding Universe:
Ned Wright's Javascript Calculator

Enter values, hit a button

70 H_o

0.30 $Omega_M$

0.83 z

Open | Flat

0.70 $Omega_{vac}$

General

Open sets $Omega_{vac}$ = 0 giving an open Universe [if you entered $Omega_M$ < 1]

Flat sets $Omega_{vac}$ = 1-$Omega_M$ giving a flat Universe.

General uses the $Omega_{vac}$ that you entered.

For H_o = 70, $Omega_M$ = 0.300, $Omega_{vac}$ = 0.700, z = 0.830

- It is now 13.462 Gyr since the Big Bang.
- The age at redshift z was 6.489 Gyr.
- The light travel time was 6.974 Gyr.
- The comoving radial distance, which goes into Hubble's law, is 2868.9 Mpc or 9.357 Gly.
- The comoving volume within redshift z is 98.906 Gpc^3.
- The angular size distance D_A is 1567.7 Mpc or 5.1131 Gly.
- This gives a scale of 7.600 kpc/".
- The luminosity distance D_L is 5250.0 Mpc or 17.123 Gly.

1 Gly = 1,000,000,000 light years or 9.461×10^{26} cm.
1 Gyr = 1,000,000,000 years.
1 Mpc = 1,000,000 parsecs = 3.08568×10^{24} cm, or 3,261,566 light years.

$H_0 D_L(z=0.83)$
$=17.123/13.97$
$=1.23$

Tutorial: Part 1 | Part 2 | Part 3 | Part 4
FAQ | Age | Distances | Bibliography | Relativity

Ned Wright's home page

© 1999-2003 Edward L. Wright. Last modified on 08/13/2003 11:58:51

http://www.astro.ucla.edu/~wright/CosmoCalc.html

See also David W. Hogg, "Distance Measures in Cosmology" http://arxiv.org/abs/astro-ph/9905116

CosmoCalc

By Eli Rykoff

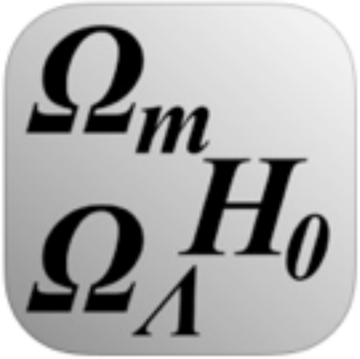

View In iTunes

Free

Category: Education
Updated: Sep 18, 2013
Version: 3.0
Size: 0.6 MB
Language: English
Seller: Eli Rykoff
© Eli Rykoff
Rated 4+

Compatibility: Requires iOS 6.1 or later. Compatible with

iPhone Screenshots

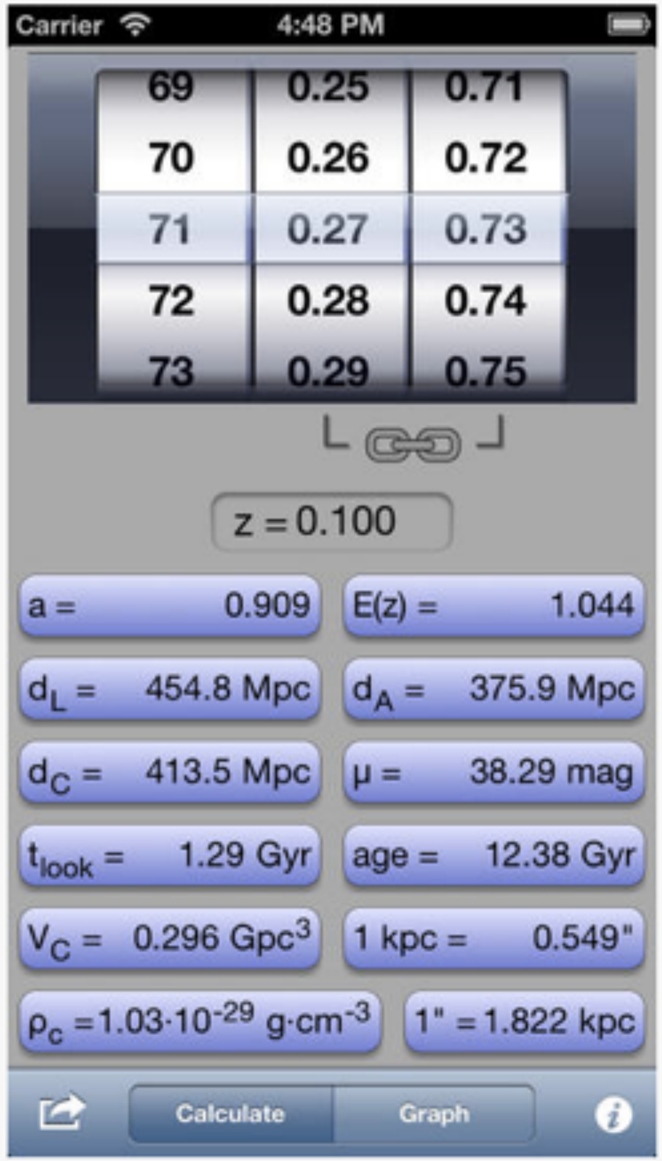

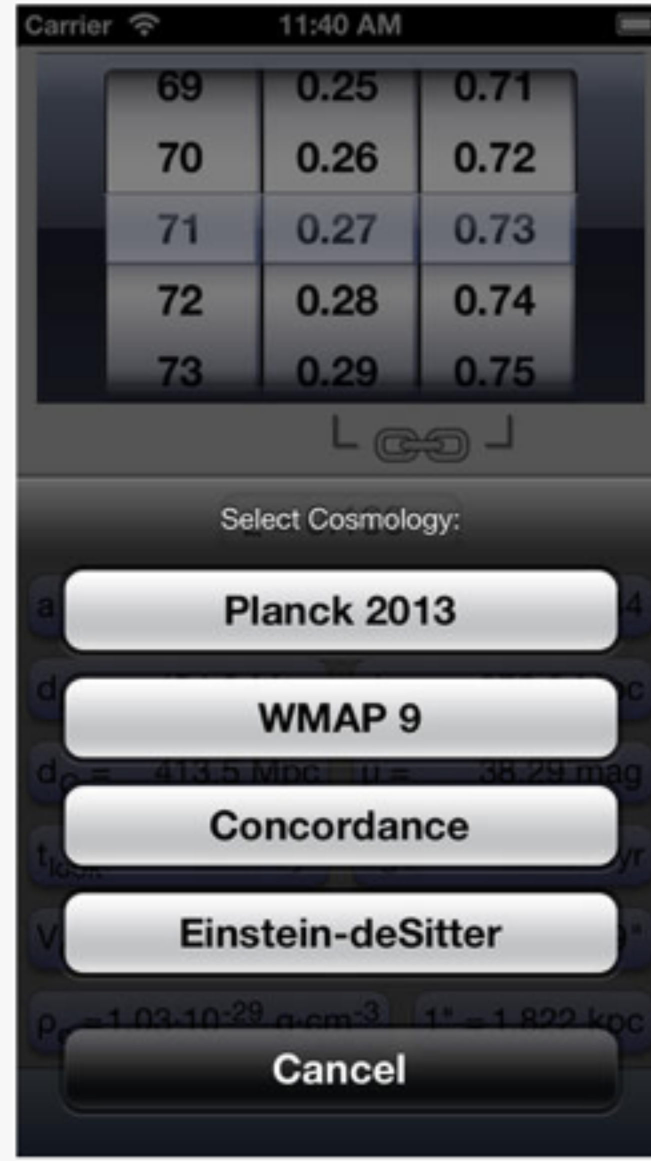

The Age of the Universe

In the mid-1990s there was a crisis in cosmology, because the age of the old Globular Cluster stars in the Milky Way, then estimated to be 16±3 Gyr, was higher than the expansion age of the universe, which for a critical density (Ω_m = 1) universe is 9±2 Gyr (with the Hubble parameter h=0.72±0.07).

But when the data from the Hipparcos astrometric satellite became available in 1997, it showed that the distance to the Globular Clusters had been under-estimated, which implied that their ages are 12±3 Gyr. Cosmology started to make sense!

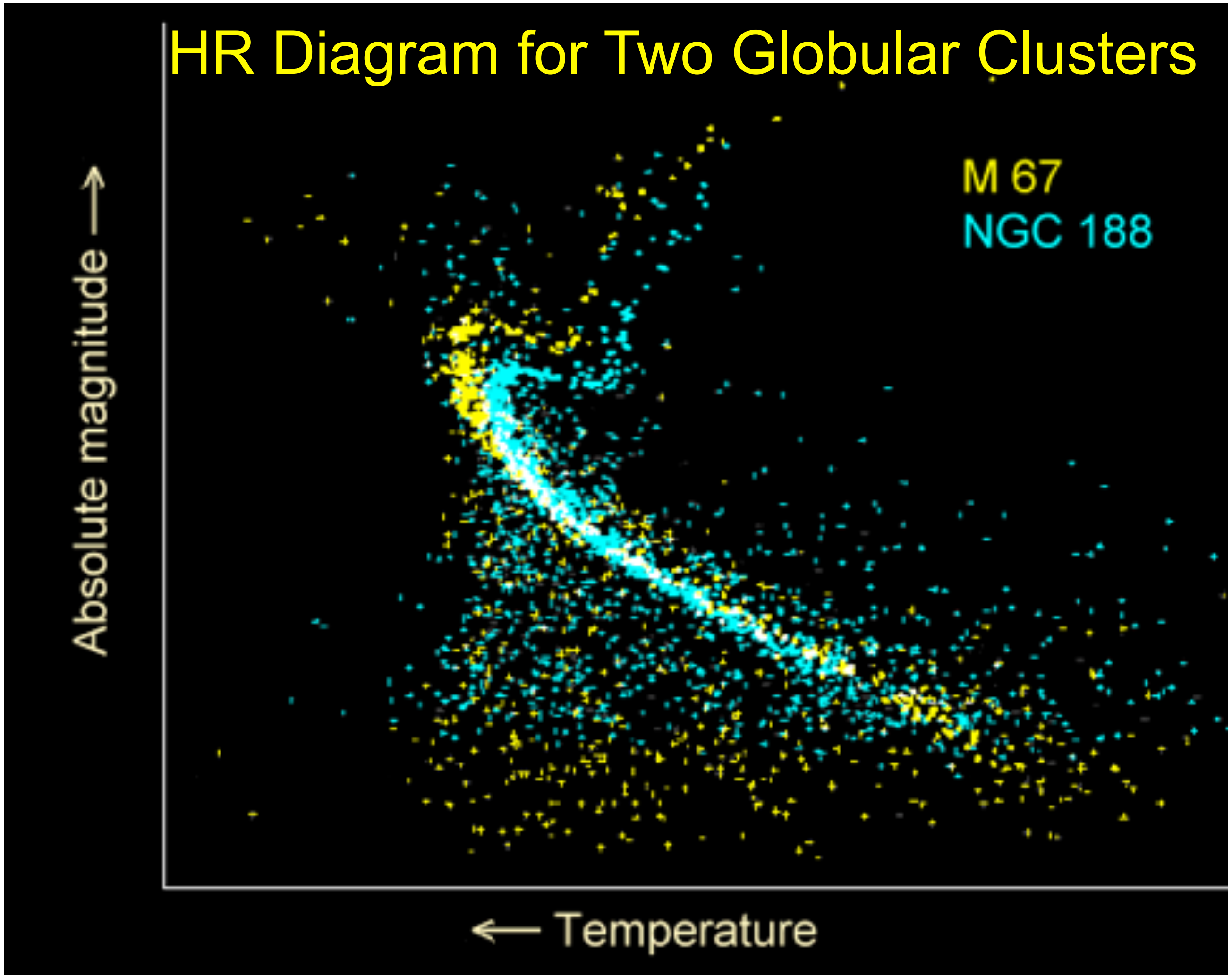

The Age of the Universe

In the mid-1990s there was a crisis in cosmology, because the age of the old Globular Cluster stars in the Milky Way, then estimated to be 16±3 Gyr, was higher than the expansion age of the universe, which for a critical density ($\Omega_m = 1$) universe is 9±2 Gyr (with the Hubble parameter h=0.72±0.07). But when the data from the Hipparcos astrometric satellite became available in 1997, it showed that the distance to the Globular Clusters had been underestimated, which implied that their ages are 12±3 Gyr.

Several lines of evidence now show that the universe does not have $\Omega_m = 1$ but rather $\Omega_{tot} = \Omega_m + \Omega_\Lambda = 1.0$ with $\Omega_m \approx 0.3$, which gives an expansion age of about 14 Gyr.

Moreover, a new type of age measurement based on radioactive decay of Thorium-232 (half-life 14.1 Gyr) measured in a number of stars gives a completely independent age of 14±3 Gyr. A similar measurement, based on the first detection in a star of Uranium-238 (half-life 4.47 Gyr), gives 12.5±3 Gyr (Cayrel et al. 2001; cf. Frebel & Kratz 2009).

All the recent measurements of the age of the universe are thus in excellent agreement. It is reassuring that three completely different clocks – stellar evolution, expansion of the universe, and radioactive decay – agree so well.

General Relativity

GR follows from the principle of equivalence and Einstein's equation $G_{\mu\nu} \equiv R_{\mu\nu} - \frac{1}{2}Rg_{\mu\nu} = -8\pi G T_{\mu\nu}$.* Einstein had intuited the local equivalence of gravity and acceleration in 1907 (Pais, p. 179), but it was not until November 1915 that he developed the final form of the GR equation.

(*Gravitation & Cosmology*)

It can be derived from the following assumptions (Weinberg, p. 153):

1. The l.h.s. $G_{\mu\nu}$ is a tensor
2. $G_{\mu\nu}$ consists only of terms linear in second derivatives or quadratic in first derivatives of the metric tensor $g_{\mu\nu}$ ($\Leftrightarrow$ $G_{\mu\nu}$ has dimension L^{-2})
3. Since $T_{\mu\nu}$ is symmetric in $\mu\nu$, so is $G_{\mu\nu}$
4. Since $T_{\mu\nu}$ is conserved (covariant derivative $T^{\mu}{}_{\nu;\mu}=0$) so also $G^{\mu}{}_{\nu;\mu}=0$
5. In the weak field limit where $g_{00} \approx -(1+2\phi)$, satisfying the Poisson equation $\nabla^2\phi=4\pi G\rho$ (i.e., $\nabla^2 g_{00}= -8\pi G T_{00}$), we must have $G_{00}= \nabla^2 g_{00}$

---

*Note: we're here using the metric –1, 1,1,1 as in Dodelson, Weinberg.

Einstein's equation can also be derived from an action principle, varying the total action $I = I_M + I_G$, where I_M is the action of matter and I_G is that of gravity:

$$I_G = -\frac{1}{16\pi G}\int R(x)\,\sqrt{g(x)}\,d^4x$$

(see, e.g., Weinberg, p. 364). The curvature scalar $R \equiv R_{\mu\nu}\,g^{\mu\nu}$ is the obvious term to insert in I_G since a scalar connected with the metric is needed and it is the only one, unless higher powers R^2, R^3 or higher derivatives $\Box R$ are used, which will lead to higher-order or higher-derivative terms in the gravity equation.

Einstein realized in 1916 that the 5th postulate above isn't strictly necessary – merely that the equation reduce to the Newtonian Poisson equation within observational errors, which allows the inclusion of a small cosmological constant term. In the action derivation, such a term arises if we just add a constant to R.

One elementary equivalence principle is the kind Newton had in mind when he stated that the property of a body called "mass" is proportional to the "weight", and is known as the weak equivalence principle (WEP). An alternative statement of WEP is that the trajectory of a freely falling "test" body (one not acted upon by such forces as electromagnetism and too small to be affected by tidal gravitational forces) is independent of its internal structure and composition. In the simplest case of dropping two different bodies in a gravitational field, WEP states that the bodies fall with the same acceleration (this is often termed the Universality of Free Fall, or UFF).

The Einstein equivalence principle (EEP) is a more powerful and far-reaching concept; it states that:

1. WEP is valid.

2. The outcome of any local non-gravitational experiment is independent of the velocity of the freely-falling reference frame in which it is performed.

3. The outcome of any local non-gravitational experiment is independent of where and when in the universe it is performed.

The second piece of EEP is called local Lorentz invariance (LLI), and the third piece is called local position invariance (LPI).

For example, a measurement of the electric force between two charged bodies is a local non-gravitational experiment; a measurement of the gravitational force between two bodies (Cavendish experiment) is not.

The Einstein equivalence principle is the heart and soul of gravitational theory, for it is possible to argue convincingly that if EEP is valid, then gravitation must be a "curved spacetime" phenomenon, in other words, the effects of gravity must be equivalent to the effects of living in a curved spacetime. As a consequence of this argument, the only theories of gravity that can fully embody EEP are those that satisfy the postulates of "metric theories of gravity", which are:

1. Spacetime is endowed with a symmetric metric.

2. The trajectories of freely falling test bodies are geodesics of that metric.

3. In local freely falling reference frames, the non-gravitational laws of physics are those written in the language of special relativity.

Friedmann-Robertson-Walker Framework (homogeneous, isotropic universe)

FRW E(00) $\frac{\dot{a}^2}{a^2} = \frac{8\pi}{3}G\rho - \frac{k}{a^2} + \frac{\Lambda}{3}$ ⟵ Friedmann equation

FRW E(ii) $\frac{2\ddot{a}}{a} + \frac{\dot{a}^2}{a^2} = -8\pi G p - \frac{k}{a^2} + \Lambda$

$$H_0 \equiv 100h\,\mathrm{km\,s^{-1}\,Mpc^{-1}} \equiv 70h_{70}\,\mathrm{km\,s^{-1}\,Mpc^{-1}}$$

$$\frac{E(00)}{H_0^2} \Rightarrow 1 = \Omega_0 - \frac{k}{H_0^2} + \Omega_\Lambda \text{ with } H \equiv \frac{\dot{a}}{a},\ a_0 \equiv 1,\ \Omega_0 \equiv \frac{\rho_0}{\rho_c}, \Omega_\Lambda \equiv \frac{\Lambda}{3H_0^2},$$

$$\rho_{c,0} \equiv \frac{3H_0^2}{8\pi G} = 1.36 \times 10^{11} h_{70}^2 M_\odot \mathrm{Mpc}^{-3}$$

$$E(ii) - E(00) \Rightarrow \frac{2\ddot{a}}{a} = -\frac{8\pi}{3}G\rho - 8\pi G p + \frac{2}{3}\Lambda$$

$$\text{Divide by } 2E(00) \Rightarrow \quad q_0 \equiv -\left(\frac{\ddot{a}}{a}\frac{a^2}{\dot{a}^2}\right)_0 = \frac{\Omega_0}{2} - \Omega_\Lambda$$

$$E(00) \Rightarrow t_0 = \int_0^1 \frac{da}{a}\left[\frac{8\pi}{3}G\rho - \frac{k}{a^2} + \frac{\Lambda}{3}\right]^{-\frac{1}{2}} = H_0^{-1}\int_0^1 \frac{da}{a}\left[\frac{\Omega_0}{a^3} - \frac{k}{H_0^2 a^2} + \Omega_\Lambda\right]^{-\frac{1}{2}}$$

$$t_0 = H_0^{-1} f(\Omega_0, \Omega_\Lambda) \qquad H_0^{-1} = 9.78h^{-1}\mathrm{Gyr} = 13.97\ h_{70}^{-1}\ \mathrm{Gyr}$$

$$f(1,0) = \tfrac{2}{3}$$
$$f(0,0) = 1$$
$$f(0,1) = \infty$$
$$f(0.3, 0.7) = 0.964$$

$$[E(00)a^3]' \text{ vs. } E(ii) \Rightarrow \quad \frac{\partial}{\partial a}(\rho a^3) = -3pa^2 \text{ ("continuity")}$$

Given eq. of state $p = p(\rho)$, integrate to determine $\rho(a)$,
integrate $E(00)$ to determine $a(t)$

Matter: $p = 0 \Rightarrow \rho = \rho_0 a^{-3}$ (assumed above in q_0, t_0 eqs.)

Radiation: $p = \frac{\rho}{3}$, $k = 0 \Rightarrow \rho \propto a^{-4}$

Evolution of Densities of Radiation, Matter, & Λ

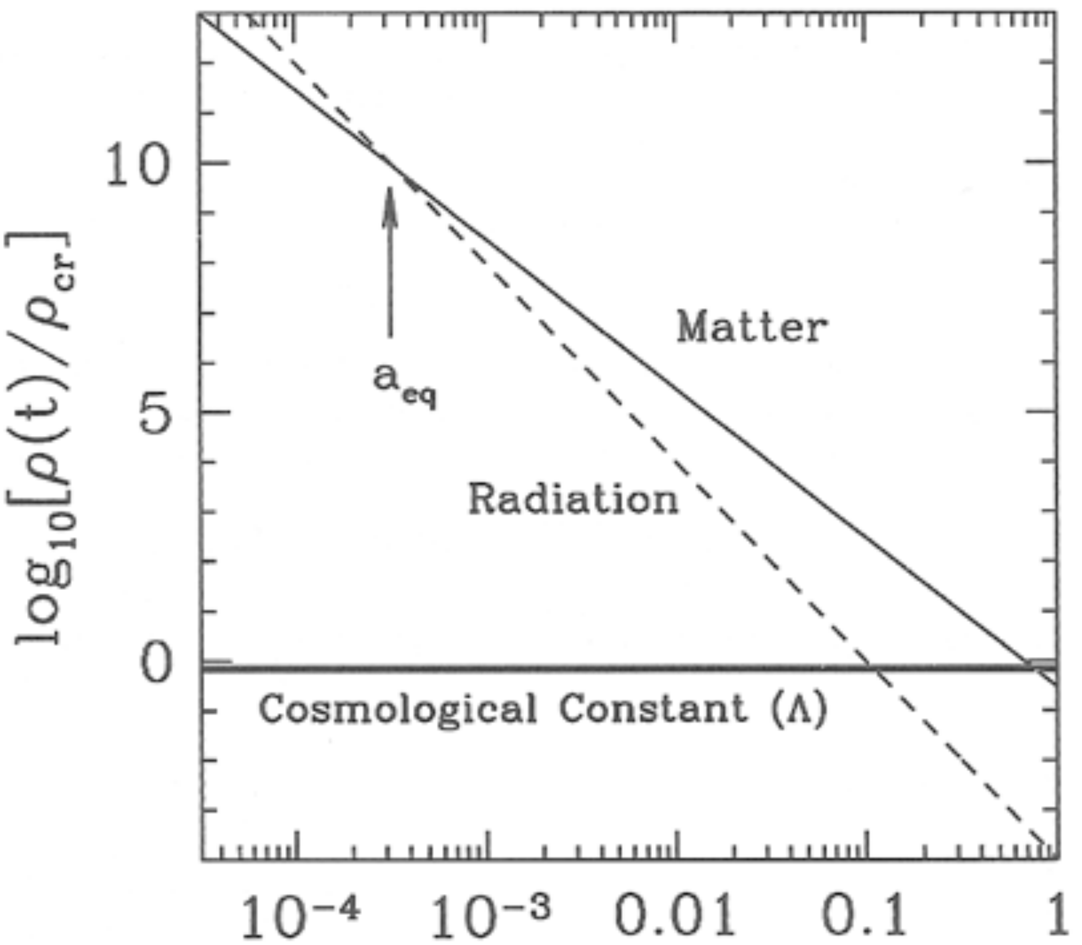

Scale Factor $a(t) = (1+z)^{-1}$ z = redshift

Figure 1.3. Energy density vs scale factor for different constituents of a flat universe. Shown are nonrelativistic matter, radiation, and a cosmological constant. All are in units of the critical density today. Even though matter and cosmological constant dominate today, at early times, the radiation density was largest. The epoch at which matter and radiation are equal is a_{eq}.

Dodelson, Chapter 1

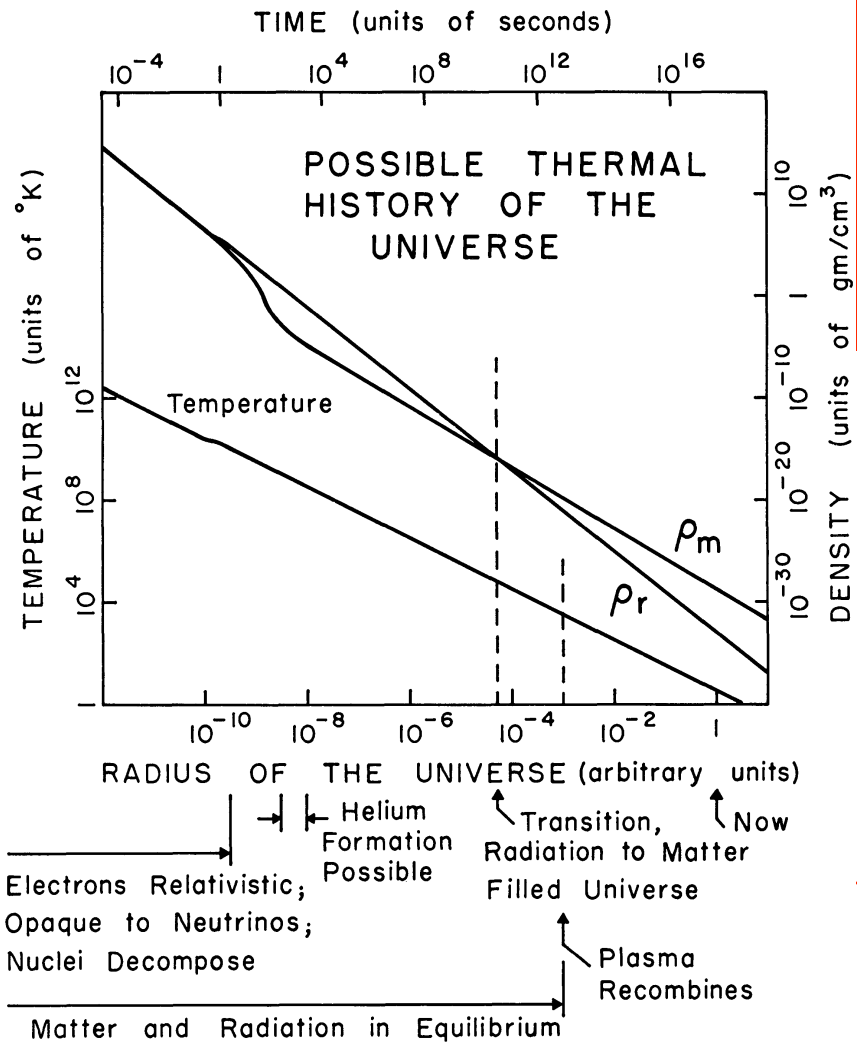

1965ApJ...142..414D

COSMIC BLACK-BODY RADIATION*

One of the basic problems of cosmology is the singularity characteristic of the familiar cosmological solutions of Einstein's field equations. Also puzzling is the presence of matter in excess over antimatter in the universe, for baryons and leptons are thought to be conserved. Thus, in the framework of conventional theory we cannot understand the origin of matter or of the universe. We can distinguish three main attempts to deal with these problems.

1. The assumption of continuous creation (Bondi and Gold 1948; Hoyle 1948), which avoids the singularity by postulating a universe expanding for all time and a continuous but slow creation of new matter in the universe.
2. The assumption (Wheeler 1964) that the creation of new matter is intimately related to the existence of the singularity, and that the resolution of both paradoxes may be found in a proper quantum mechanical treatment of Einstein's field equations.
3. The assumption that the singularity results from a mathematical over-idealization,

* This research was supported in part by the National Science Foundation and the Office of Naval Research of the U.S. Navy.

FIG 1 —Possible thermal history of the Universe. The figure shows the previous thermal history of the Universe assuming a homogeneous isotropic general-relativity cosmological model (no scalar field) with present matter density 2×10^{-29} gm/cm^3 and present thermal radiation temperature 3.5° K The bottom horizontal scale may be considered simply the proper distance between two chosen fiducial co-moving galaxies (*points*) The top horizontal scale is the proper world time. The line marked "temperature" refers to the temperature of the thermal radiation Matter remains in thermal equilibrium with the radiation until the plasma recombines, at the time indicated Thereafter further expansion cools matter not gravitationally bound faster than the radiation. The mass density in radiation is ρ_r. At present ρ_r is substantially below the mass density in matter, ρ_m, but, in the early Universe ρ_r exceeded ρ_m We have indicated the time when the Universe exhibited a transition from the characteristics of a radiation-filled model to those of a matter-filled model.

Looking back in time, as the temperature approaches 10^{10} ° K the electrons become relativistic, and thermal electron-pair creation sharply increases the matter density At temperatures somewhat greater than 10^{10} ° K these electrons should be so abundant as to assure a thermal neutrino abundance and a thermal neutron-proton abundance ratio. A temperature of this order would be required also to decompose the nuclei from the previous cycle in an oscillating Universe. Notice that the nucleons are non-relativistic here.

The thermal neutrons decay at the right-hand limit of the indicated region of helium formation. There is a left-hand limit on this region because at higher temperatures photodissociation removes the deuterium necessary to form helium The difficulty with this model is that most of the matter would end up in helium.

We deeply appreciate the helpfulness of Drs. Penzias and Wilson of the Bell Telephone Laboratories, Crawford Hill, Holmdel, New Jersey, in discussing with us the result of their measurements and in showing us their receiving system. We are also grateful for several helpful suggestions of Professor J. A. Wheeler.

R. H. DICKE
P. J. E. PEEBLES
P. G. ROLL
D. T. WILKINSON

May 7, 1965

PALMER PHYSICAL LABORATORY
PRINCETON, NEW JERSEY

History of Cosmic Expansion for General Ω_M & Ω_Λ

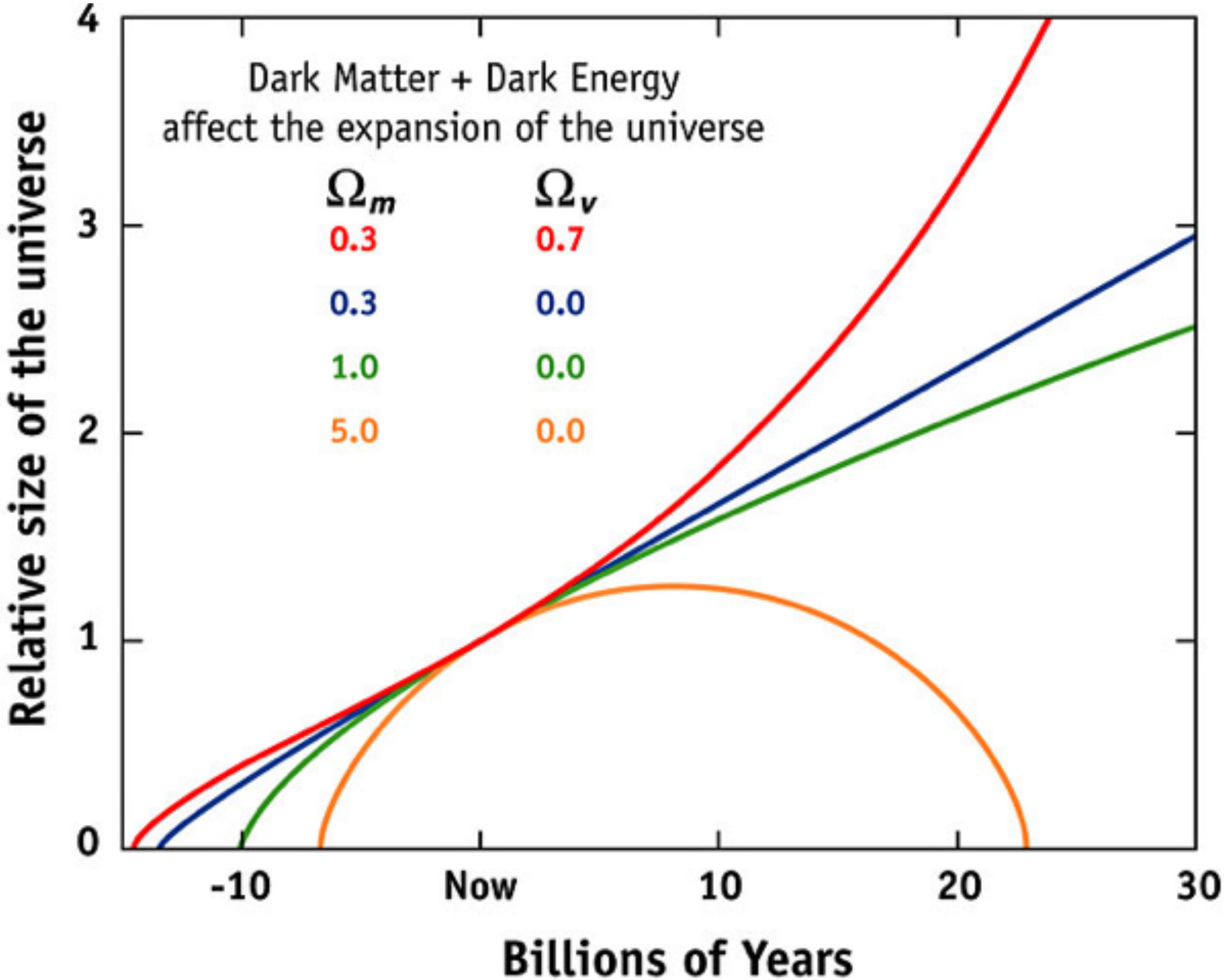

History of Cosmic Expansion for General Ω_M & Ω_Λ

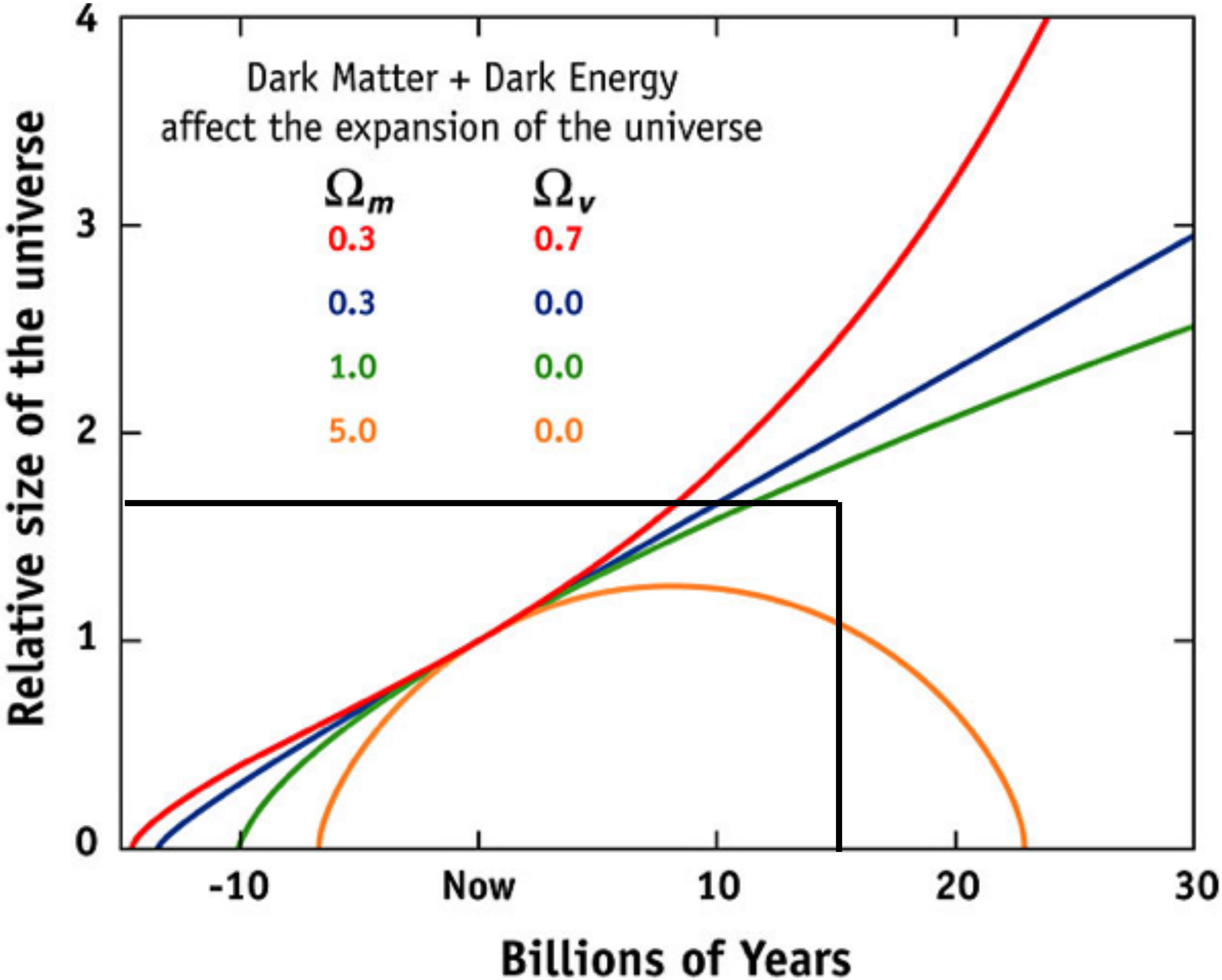

History of Cosmic Expansion for $\Omega_\Lambda = 1 - \Omega_M$

With $\Omega_\Lambda = 0$ the age of the decelerating universe would be only 9 Gyr, but $\Omega_\Lambda = 0.7$, $\Omega_m = 0.3$ gives an age of 14 Gyr, consistent with stellar and radioactive decay ages

Figure 4. The history of cosmic expansion, as measured by the high-redshift supernovae (the black data points), assuming flat cosmic geometry. The scale factor R of the universe is taken to be 1 at present, so it equals $1/(1 + z)$. The curves in the blue shaded region represent cosmological models in which the accelerating effect of vacuum energy eventually overcomes the decelerating effect of the mass density. These curves assume vacuum energy densities ranging from 0.95 ρ_c (top curve) down to 0.4 ρ_c. In the yellow shaded region, the curves represent models in which the cosmic expansion is always decelerating due to high mass density. They assume mass densities ranging (left to right) from 0.8 ρ_c up to 1.4 ρ_c. In fact, for the last two curves, the expansion eventually halts and reverses into a cosmic collapse.

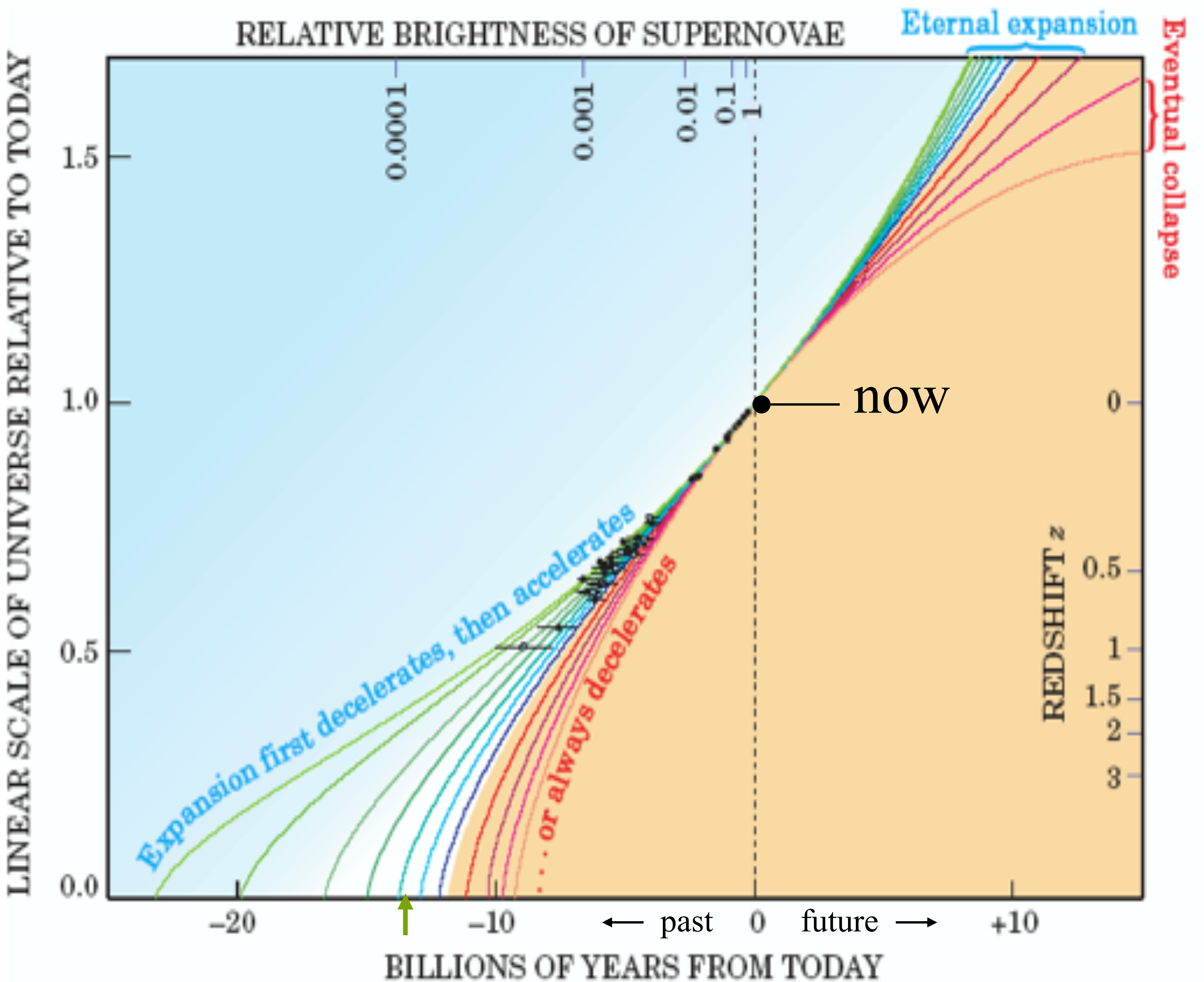

Saul Perlmutter, ***Physics Today***, Apr 2003

LCDM Benchmark Cosmological Model: Ingredients & Epochs

	List of Ingredients
photons:	$\Omega_{\gamma,0} = 5.0 \times 10^{-5}$
neutrinos:	$\Omega_{\nu,0} = 3.4 \times 10^{-5}$
total radiation:	$\Omega_{r,0} = 8.4 \times 10^{-5}$
baryonic matter:	$\Omega_{\text{bary},0} = 0.04$
nonbaryonic dark matter:	$\Omega_{\text{dm},0} = 0.26$
total matter:	$\Omega_{m,0} = 0.30$
cosmological constant:	$\Omega_{\Lambda,0} \approx 0.70$

Important Epochs

radiation-matter equality:	$a_{rm} = 2.8 \times 10^{-4}$	$t_{rm} = 4.7 \times 10^{4}$ yr
matter-lambda equality:	$a_{m\Lambda} = 0.75$	$t_{m\Lambda} = 9.8$ Gyr
Now:	$a_0 = 1$	$t_0 = 13.5$ Gyr

Barbara Ryden, *Introduction to Cosmology* (Addison-Wesley, 2003)

Benchmark Model: Scale Factor vs. Time

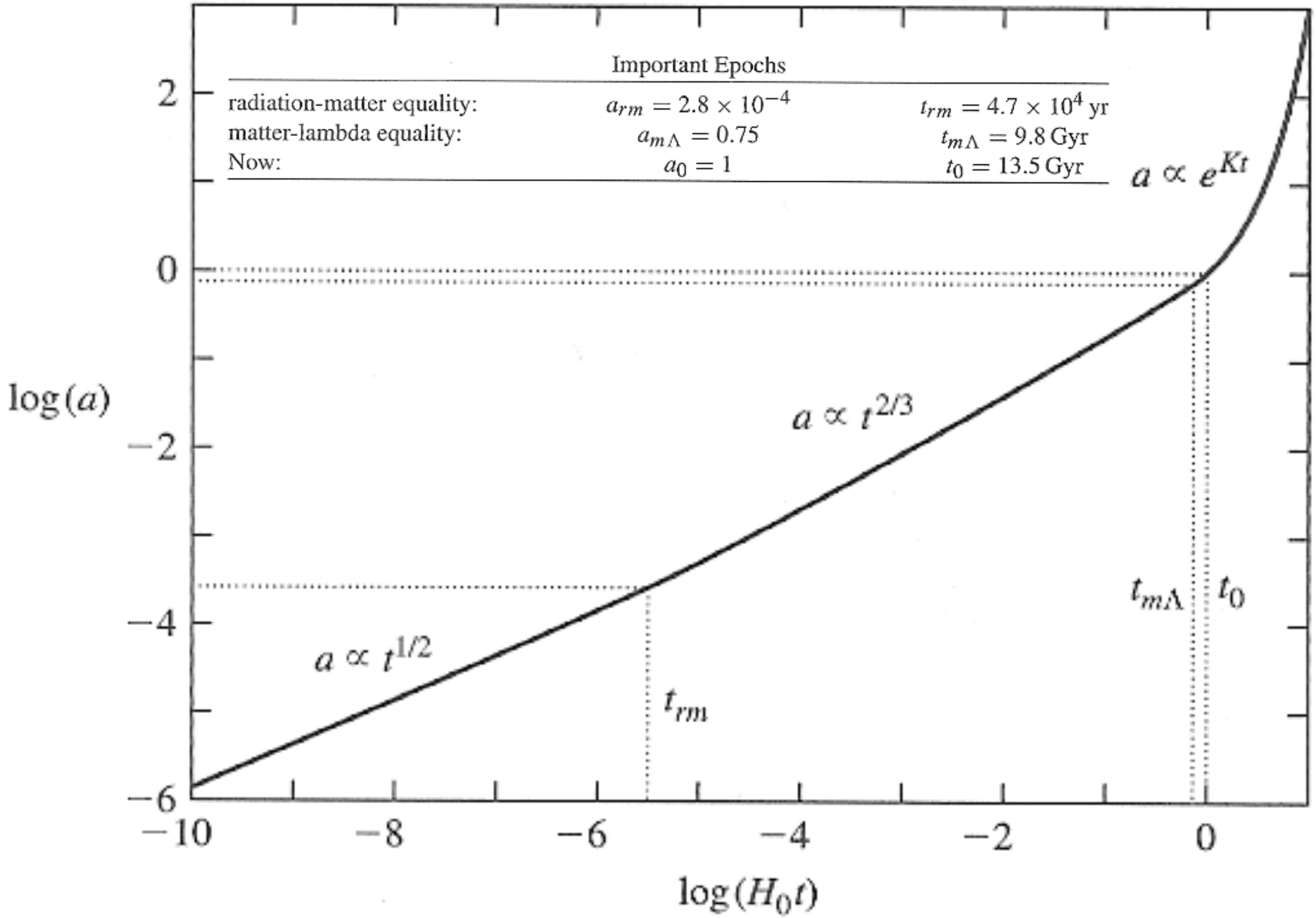

FIGURE 6.5 The scale factor a as a function of time t (measured in units of the Hubble time), computed for the Benchmark Model. The dotted lines indicate the time of radiation-matter equality, $a_{rm} = 2.8 \times 10^{-4}$, the time of matter-lambda equality, $a_{m\Lambda} = 0.75$, and the present moment, $a_0 = 1$.

Barbara Ryden, *Introduction to Cosmology* (Addison-Wesley, 2003)

Age of the Universe t_0 in FRW Cosmologies

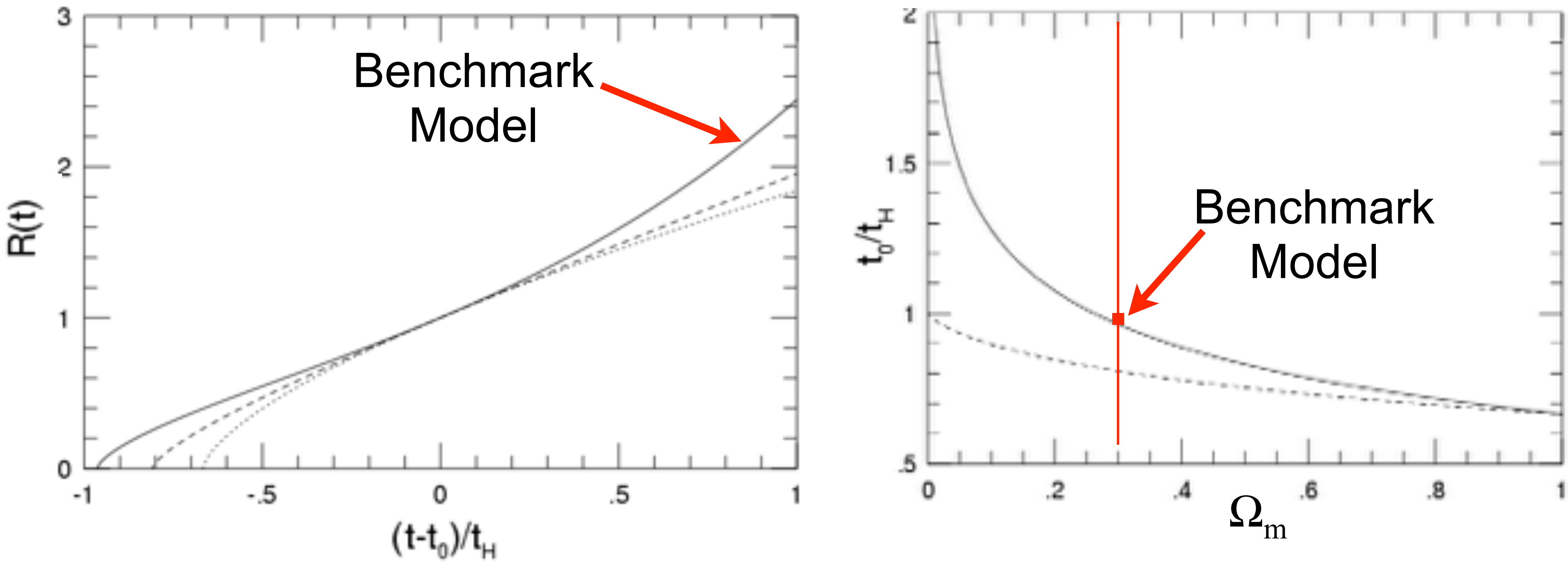

(a) Evolution of the scale factor $a(t)$ plotted vs. the time after the present $(t - t_0)$ in units of Hubble time $t_H \equiv H_0^{-1} = 9.78h^{-1}$ Gyr for three different cosmologies: Einstein-de Sitter ($\Omega_0 = 1, \Omega_\Lambda = 0$ dotted curve), negative curvature ($\Omega_0 = 0.3, \Omega_\Lambda = 0$: dashed curve), and low-Ω_0 flat ($\Omega_0 = 0.3$, $\Omega_\Lambda = 0.7$: solid curve). (b) Age of the universe today t_0 in units of Hubble time t_H as a function of Ω_0 for $\Lambda = 0$ (dashed curve) and flat $\Omega_0 + \Omega_\Lambda = 1$ (solid curve) cosmologies.

Age t_0 of the Double Dark Universe

$\Omega_{\Lambda,0}$

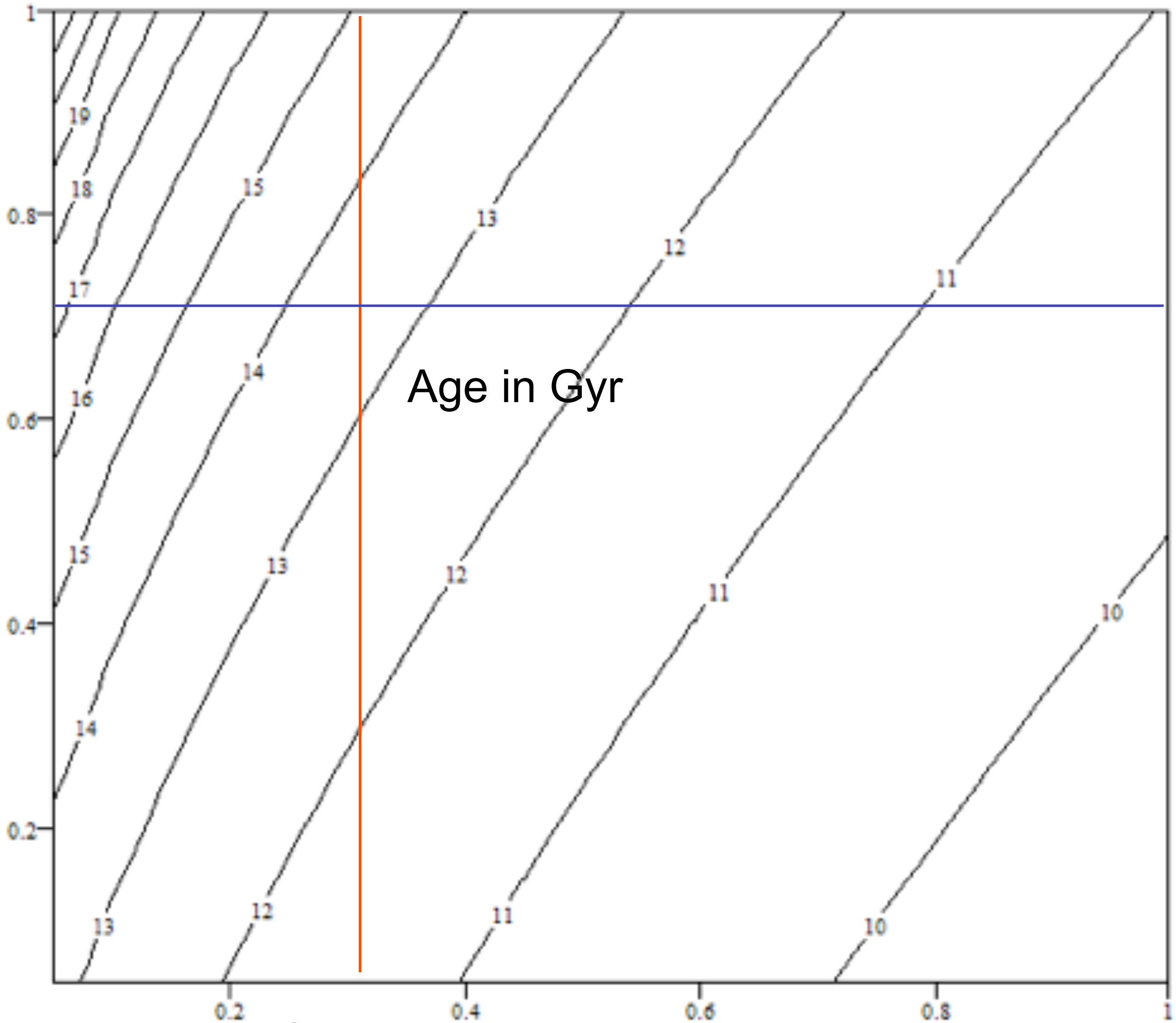

$\Omega_{m,0}$

Calculated for k=0 and h=0.7. For any other value of the Hubble parameter, multiply the age by (h/0.7).

Age of the Universe and Lookback Time

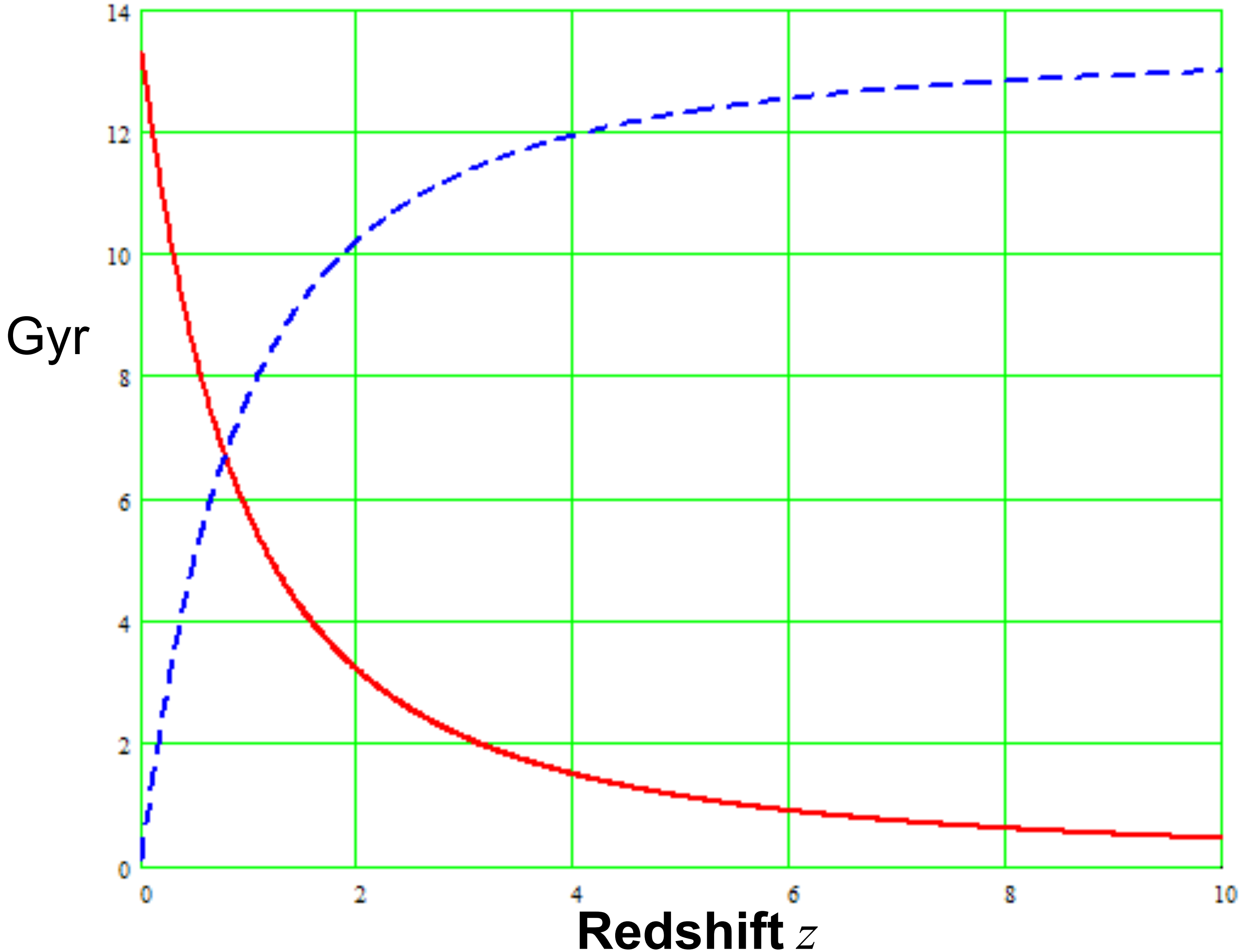

These are for the Benchmark Model $\Omega_{m,0}$=0.3, $\Omega_{\Lambda,0}$=0.7, h=0.7.

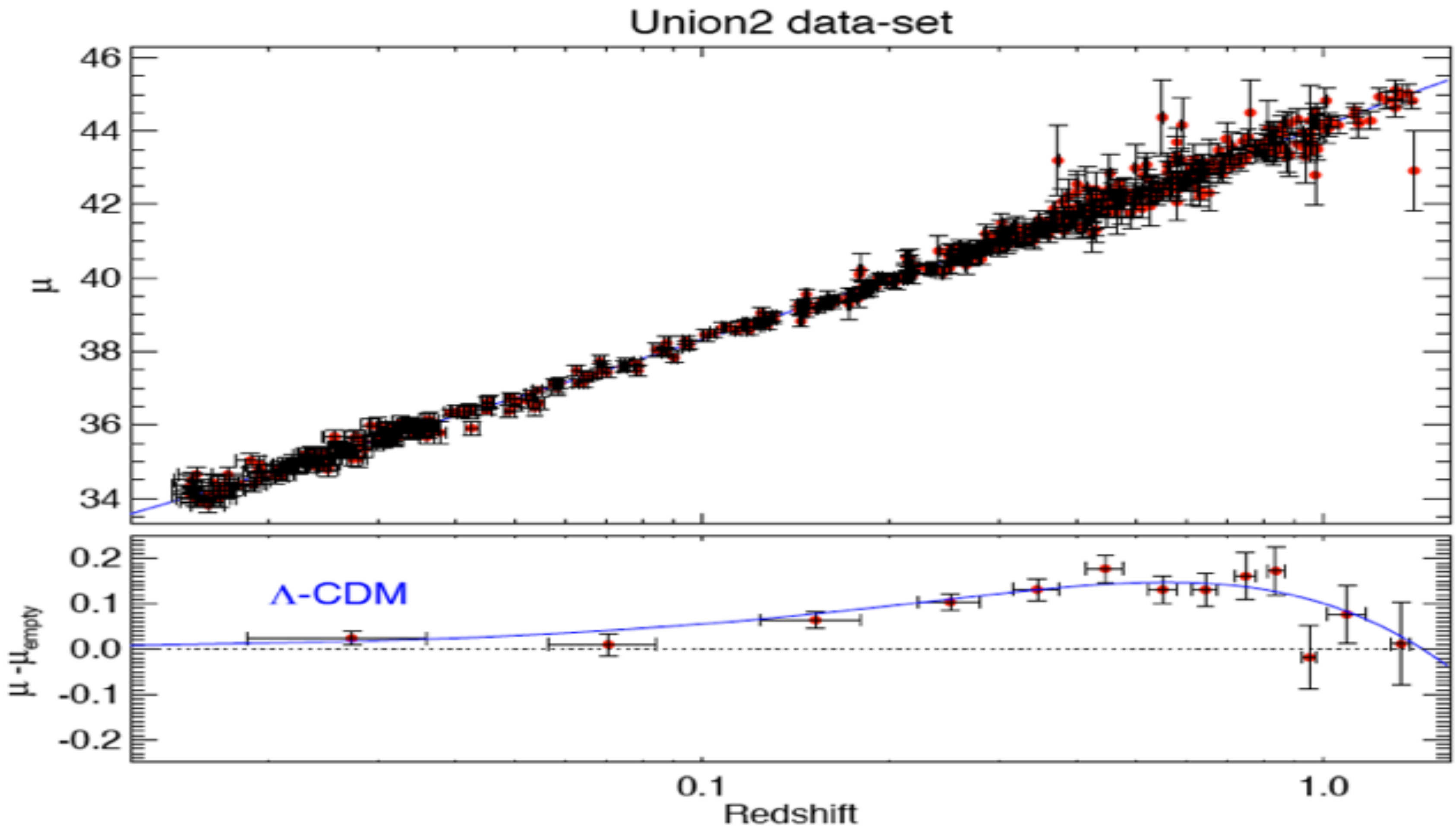

The Hubble diagram of Type Ia supernovae correlating distance modulus (μ) vs. redshift. The Union2 compilation (Amanullah R, et al., 2010) represents one of the largest SN Ia samples. The linear expansion in the local universe can be traced out to $z<0.1$. The distance relative to an empty universe model (μempty) is shown in the lower panel. The data are binned for clarity in this diagram. The blue curve shows the expectation from the best fit LCDM model with $\Omega_m=0.3$.

The distance modulus $\mu = m - M$ is the difference between the apparent magnitude m (ideally, corrected for the effects of interstellar absorption) and the absolute magnitude M of an astronomical object. It is related to the distance d in parsecs by $\mu = 5 \log_{10}(d) - 5$.

Brief History of the Universe

- Cosmic Inflation generates density fluctuations
- Symmetry breaking: more matter than antimatter
- All antimatter annihilates with almost all the matter (1s)
- Big Bang Nucleosynthesis makes light nuclei (10 min)
- Electrons and light nuclei combine to form atoms, and the cosmic background radiation fills the newly transparent universe (380,000 yr)

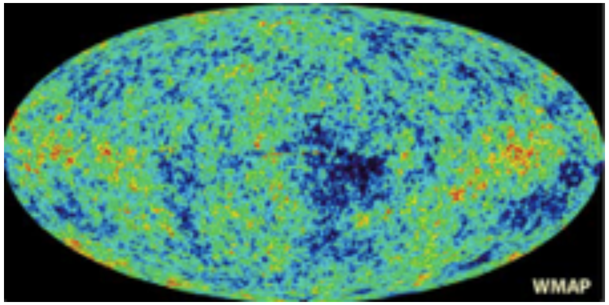

- Galaxies and larger structures form (~1 Gyr)
- Carbon, oxygen, iron, ... are made in stars
- Earth-like planets form around 2nd generation stars
- Life somehow starts (~4 Gyr ago) and evolves on earth

Mapping the large scale structure of the universe ...

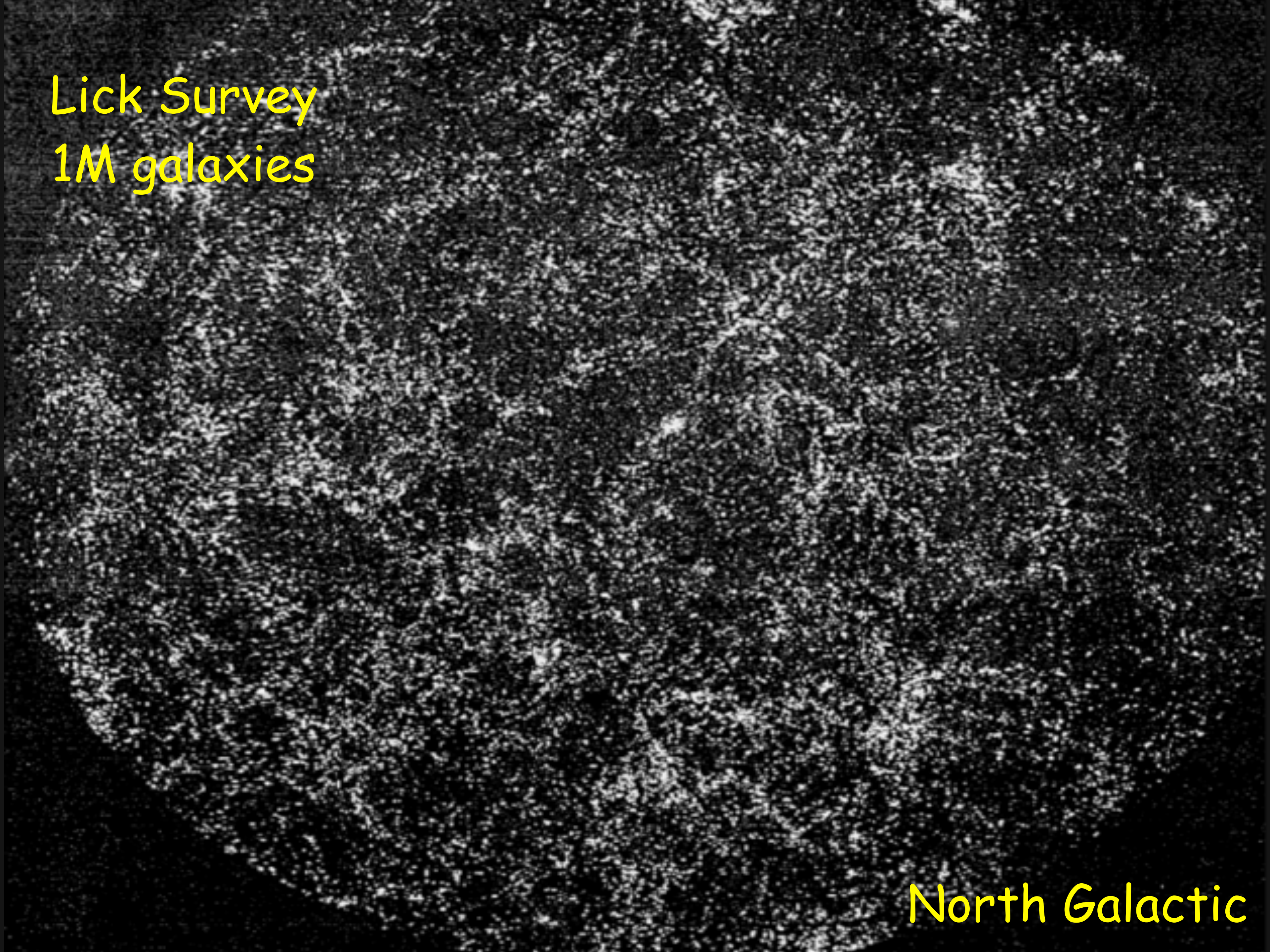
Lick Survey
1M galaxies
North Galactic

CfA survey: Great Wall

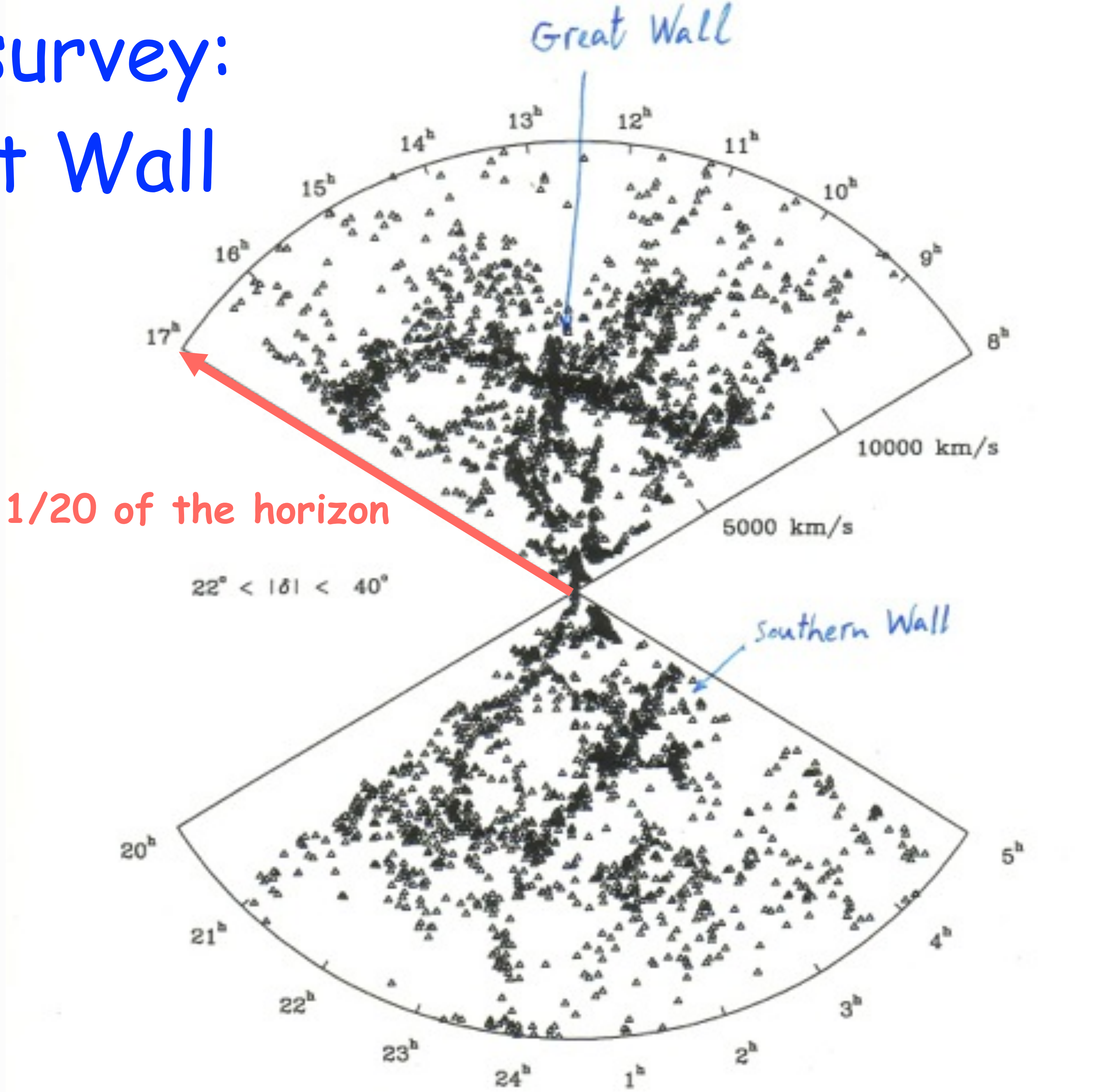

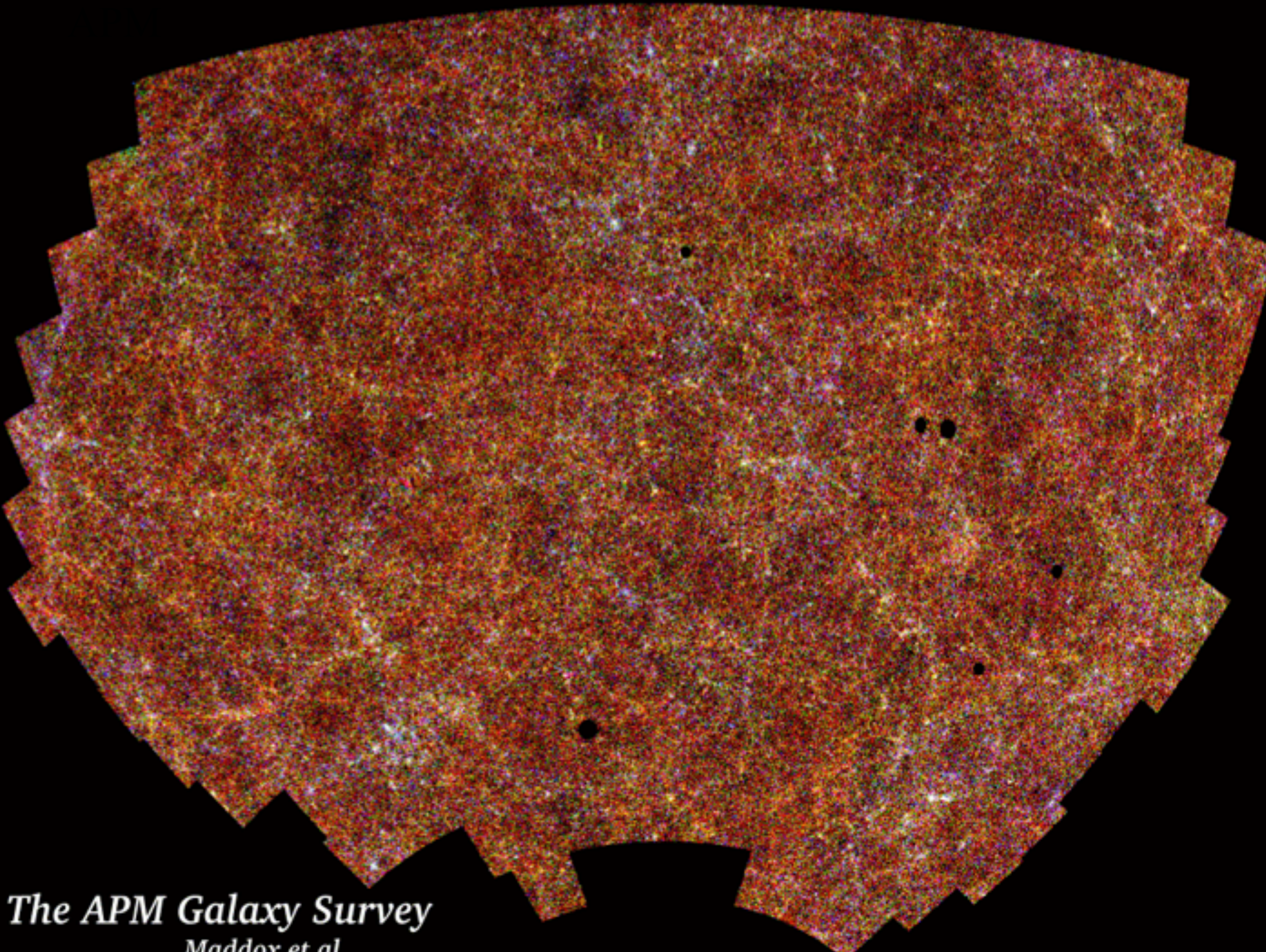

The APM Galaxy Survey

Maddox et al

2dF Galaxy Redshift Survey
¼ M galaxies 2003

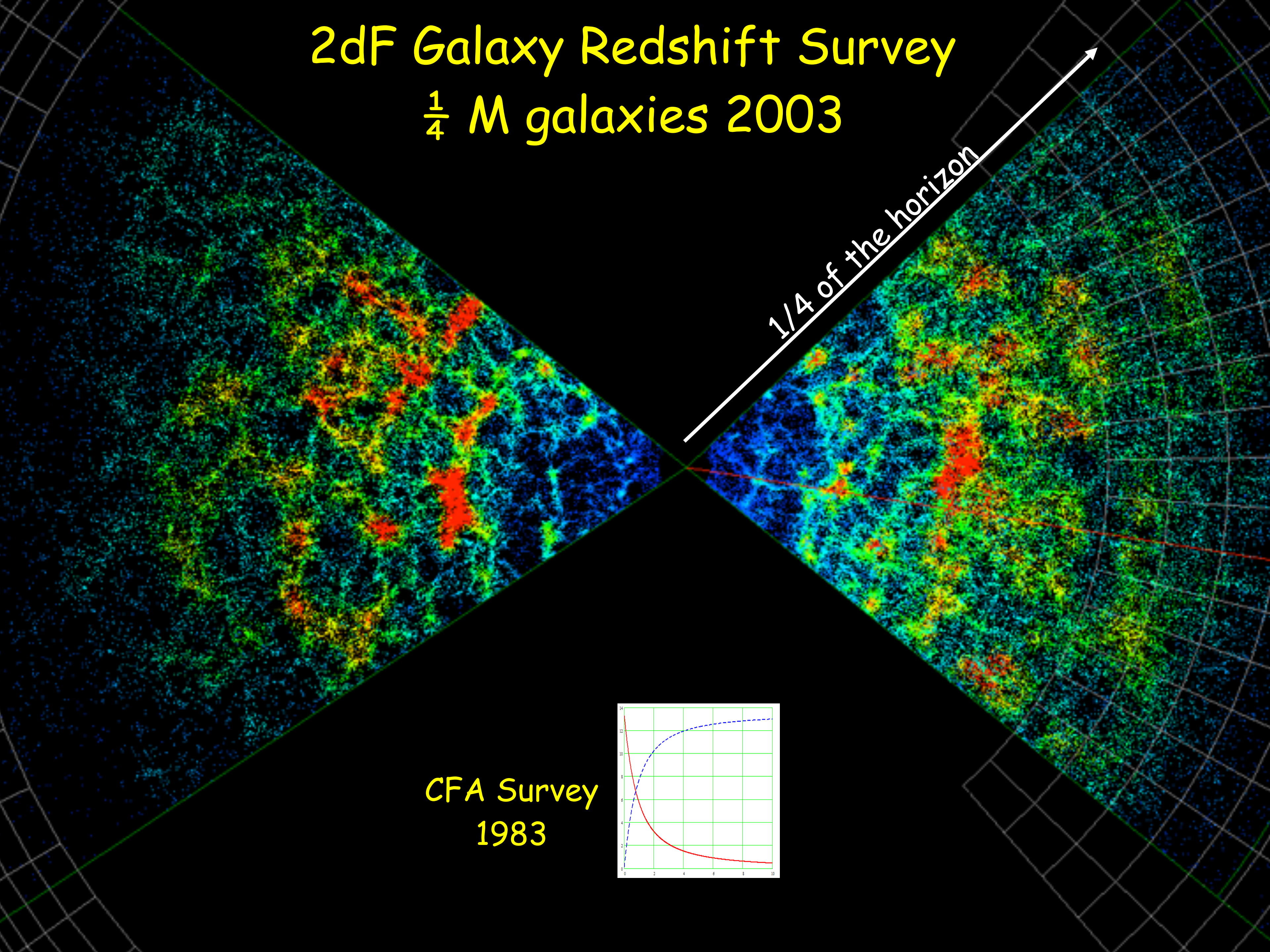

CFA Survey
1983

Mapping the Galaxies
Sloan Digital Sky Survey

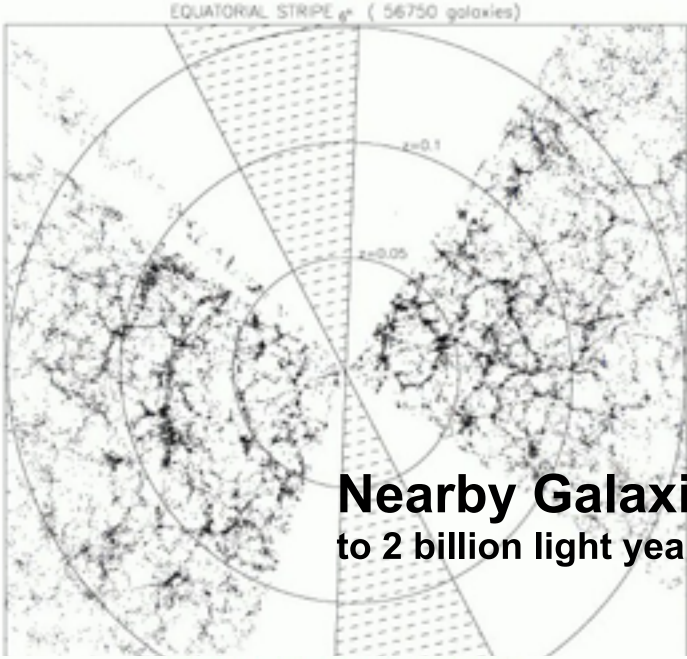

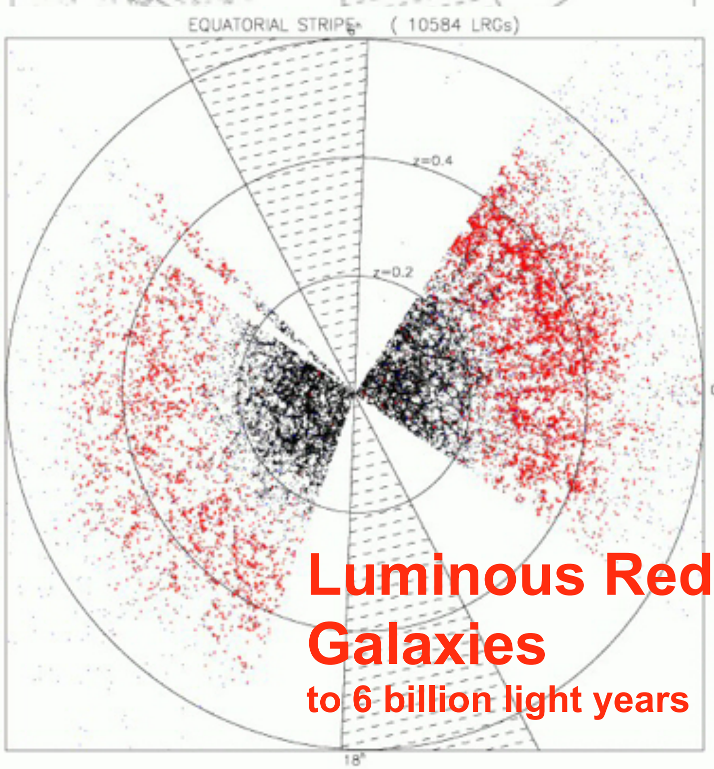

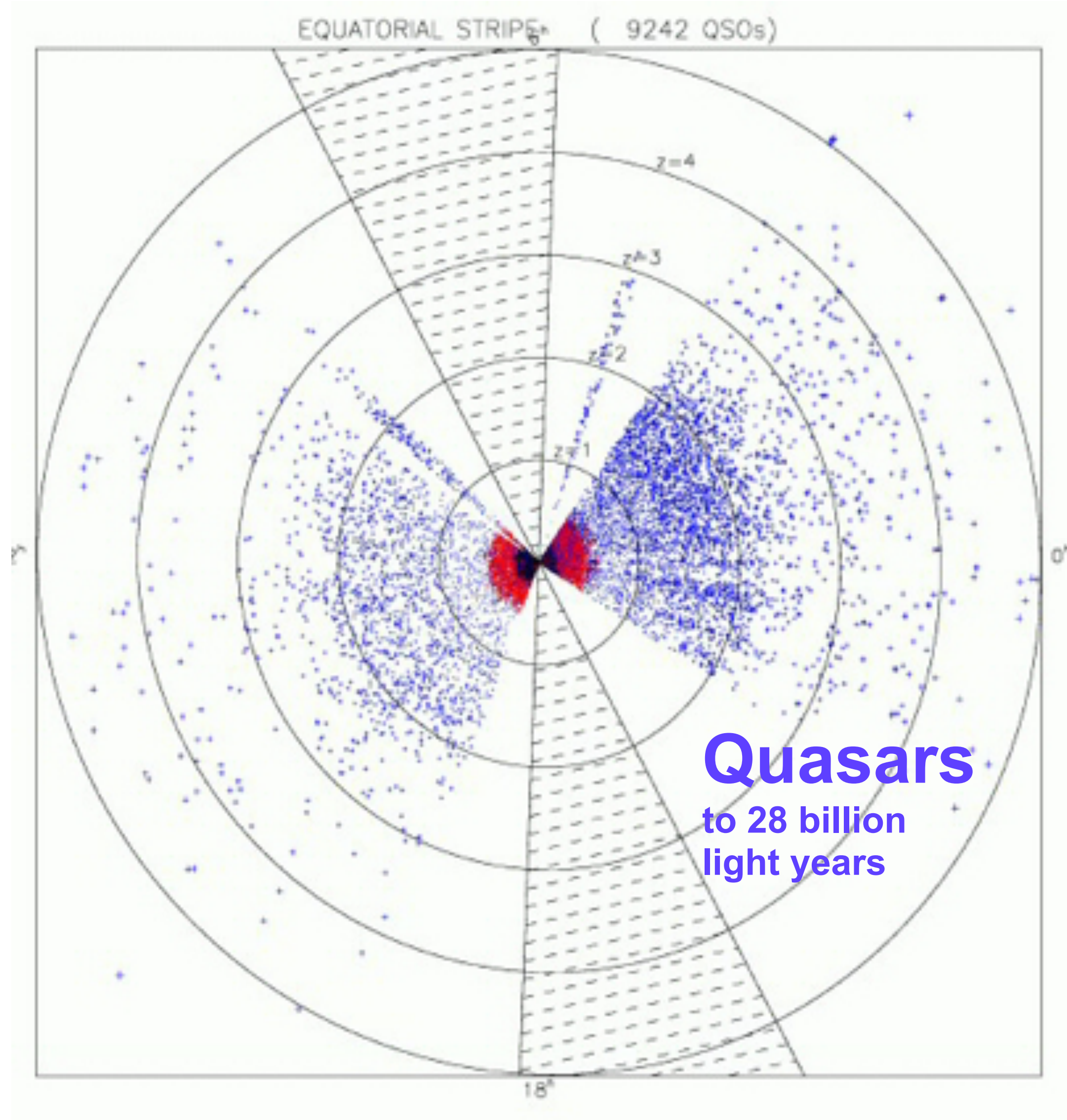

GALAXIES MAPPED BY THE SLOAN SURVEY

Data Release 4:

565,715 Galaxies & 76,403 Quasars

GALAXIES MAPPED BY THE SLOAN SURVEY

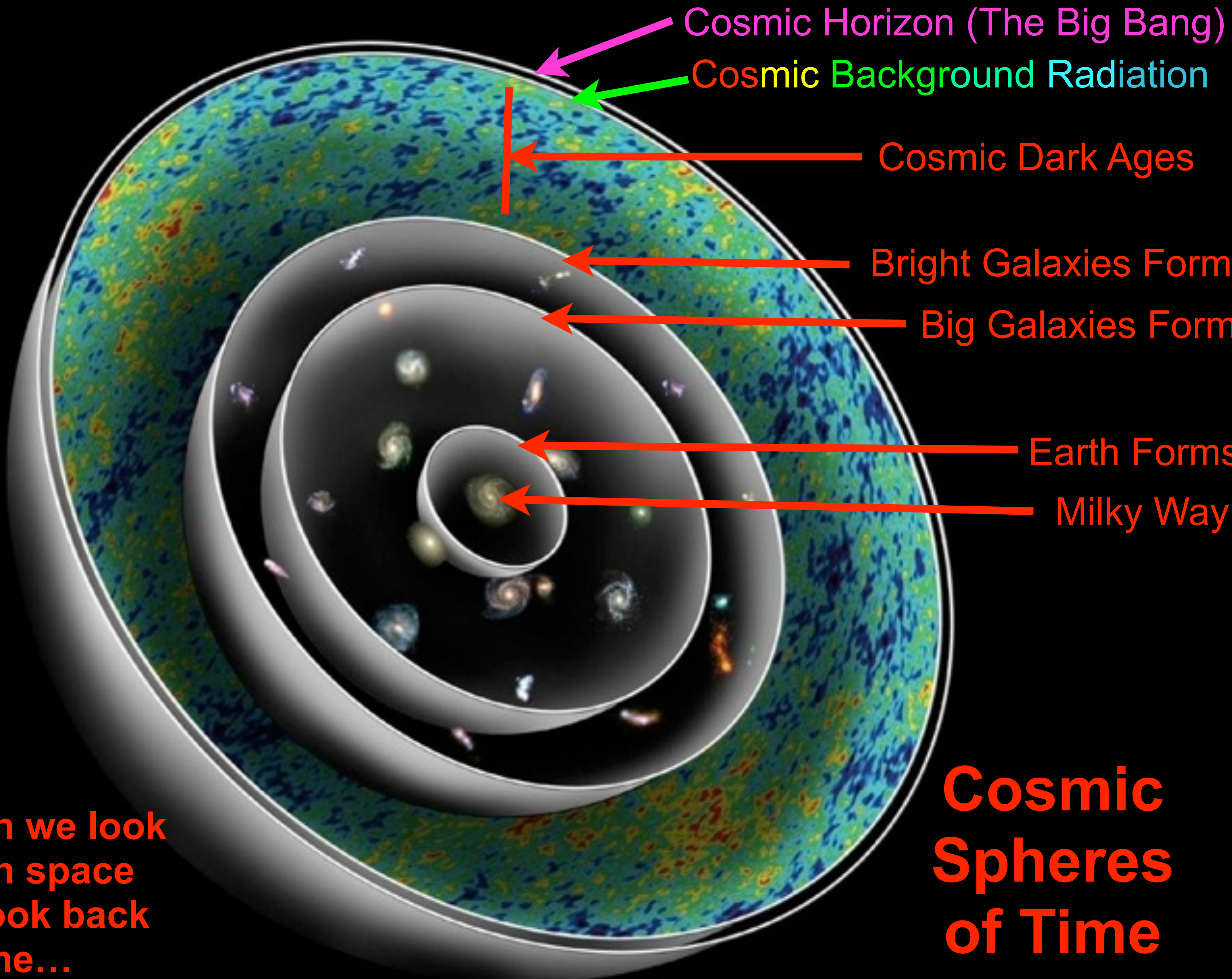

Cosmic Spheres of Time

When we look out in space we look back in time…

Medieval Universe

Neutrino Decoupling and Big Bang Nucleosynthesis, Photon Decoupling, and WIMP Annihilation

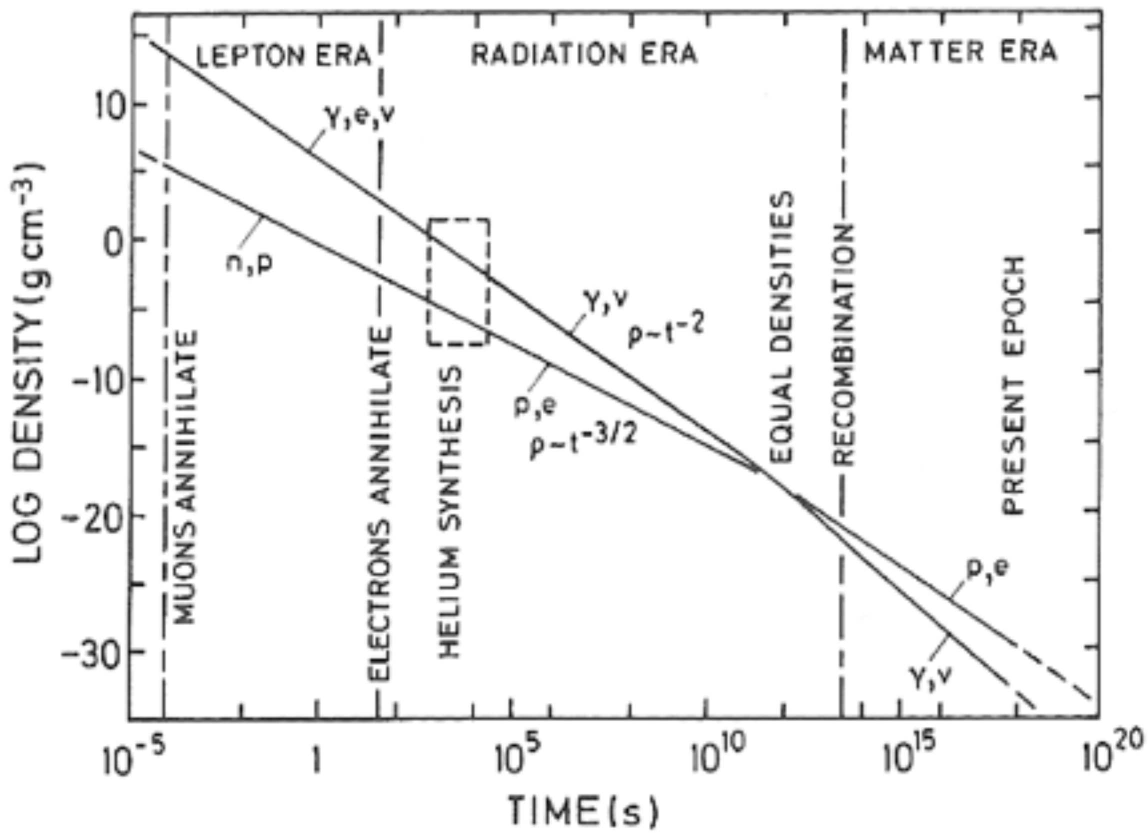

Fig. 3.1. The thermal history of the standard model. The densities of protons, electrons, photons, and neutrinos are shown at various stages of cosmological evolution [after Harrison (1973)]

Börner, *Early Universe* 4th Ed, p. 152

Big Bang Nucleosynthesis

BBN was conceived by Gamow in 1946 as an explanation for the formation of all the elements, but the absence of any stable nuclei with A=5,8 makes it impossible for BBN to proceed past Li. The formation of carbon and heavier elements occurs instead through the triple-α process in the centers of red giants (Burbidge[2], Fowler, & Hoyle 57). At the BBN baryon density of $2\times10^{-29}\ \Omega_b\ h^2\ (T/T_0)^3$ g cm^{-3} $\approx 2\times10^{-5}$ g cm^{-3}, the probability of the triple-α process is negligible even though $T \approx 10^9$K.

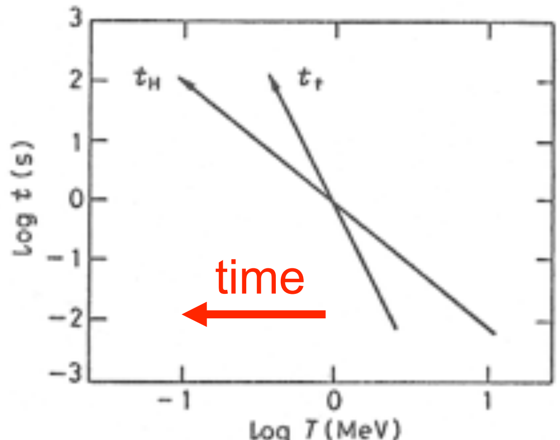

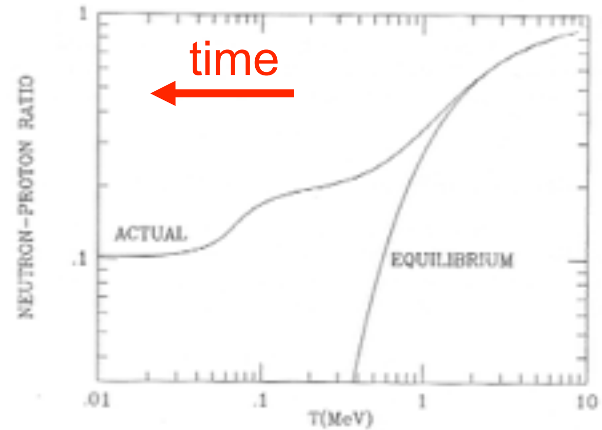

Kolb & Turner

Thermal equilibrium between n and p is maintained by weak interactions, which keeps $n/p = \exp(-Q/T)$ (where $Q = m_n - m_p = 1.293$ MeV) until about $t \approx 1$ s. But because the neutrino mean free time $t_\nu^{-1} \approx \sigma_\nu n_{e\pm} \approx (G_F T)^2 (T^3)$ is increasing as $t_\nu \propto T^{-5}$ (here the Fermi constant $G_F \approx 10^{-5}$ GeV^{-2}), while the horizon size is increasing only as $t_H \approx (G\rho)^{-1/2} \approx M_{Pl}\ T^{-2}$, these interactions freeze out when T drops below about 0.8 MeV. This leaves $n/(p+n) \approx 0.14$. The neutrons then decay with a mean lifetime 887 ± 2 s until they are mostly fused into D and then ^{4}He. The higher the baryon density, the higher the final abundance of ^{4}He and the lower the abundance of D that survives this fusion process. Since D/H is so sensitive to baryon density, David Schramm called deuterium the "baryometer." He and his colleagues also pointed out that since the horizon size increases more slowly with T^{-1} the larger the number of light neutrino species N_ν contributing to the energy density ρ, BBN predicted that $N_\nu \approx 3$ before N_ν was measured at accelerators by measuring the width of the Z^0 (Cyburt et al. 2005: $2.67 < N_\nu < 3.85$).

Neutrinos in the Early Universe

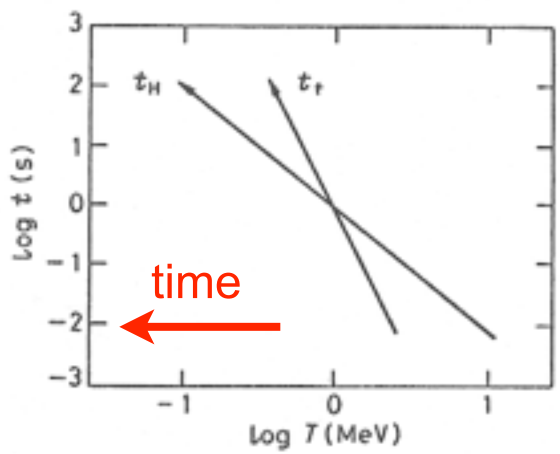

As we discussed, neutrino decoupling occurs at T ~ 1 MeV. After decoupling, the neutrino phase space distribution is

$f_\nu = [1+\exp(p_\nu c/T_\nu)]^{-1}$ (note: $\neq [1+\exp(E_\nu/T_\nu)]$ for NR neutrinos)

After e+e- annihilation, $T_\nu=(4/11)^{1/3}T_\gamma$ = 1.9K. Proof :

Number densities of primordial particles

FermiDirac/BoseEinstein factor

$n_\gamma(T) = 2\,\zeta(3)\,\pi^{-2}\,T^3 = 400\ \mathrm{cm}^{-3}\,(T/2.7K)^3$, $n_\nu(T) = (3/4)\,n_\gamma(T)$ including antineutrinos

Conservation of entropy s_I of interacting particles per comoving volume

$s_I = g_I(T)\,N_\gamma(T)$ = constant, where $N_\gamma = n_\gamma V$; we only include neutrinos for T>1 MeV.

Thus for T>1 MeV, $g_I = 2 + 4(7/8) + 6(7/8) = 43/4$ for γ, e+e-, and the three ν species, while for T< 1 MeV, $g_I = 2 + 4(7/8) = 11/2$. At e+e- annihilation, below about T=0.5 Mev, g_I drops to 2, so that $2N_{\gamma 0} = g_I(T<1\ \mathrm{MeV})\,N_\gamma(T<1\ \mathrm{MeV}) = (11/2)\,N_\gamma(T<1\ \mathrm{MeV}) = (11/2)(4/3)\,N_\nu(T<1\ \mathrm{MeV})$. Thus $n_{\nu 0} = (3/4)(4/11)\,n_{\gamma 0} = 109\ \mathrm{cm}^{-3}\,(T/2.7K)^3$, or

$T_\nu = (4/11)^{1/3}\,T = 0.714\,T$

Statistical Thermodynamics

$$n_i = \frac{g_i}{2\pi^2}\left(\frac{kT_i}{\hbar c}\right)^3 I_i^{11}(\pm), \quad \rho_i = \frac{g_i kT_i}{2\pi^2 c^2}\left(\frac{kT_i}{\hbar c}\right)^3 I_i^{21}(\pm), \quad \text{where}$$

$$I_i^{mn} \equiv \int_{\theta_i}^{\infty} x^m \left(x^2 - \theta_i^{-2}\right)^{n/2} \left(e^x \pm 1\right)^{-1} dx, \quad \theta_i = \frac{kT_i}{m_i c^2}, \quad g_i = \#\ \text{spin states}$$

+ Fermi-Dirac, - Bose-Einstein

$\theta_i >> 1$ (ER):

$$I^{11}(+) = \tfrac{3}{2}\zeta(3) = 1.803, \quad I^{21}(+) = 7\pi^4/120$$

$$I^{11}(-) = 2\zeta(3) = \tfrac{4}{3} I^{11}(+), \quad I^{21}(-) = \pi^4/15 = \tfrac{8}{7} I^{21}(+)$$

$\theta_i << 1$ (NR):

$$n_i = \frac{\rho_i}{m_i} = \frac{g_i}{(2\pi)^{3/2}}\left(\frac{kT_i}{\hbar c}\right)^3 \theta_i^{-3/2} e^{-\theta_i^{-1}} \quad (\text{not } \nu\text{'s})$$

[Note: $\zeta(3) = 1.2020569\cdots = \sum_{k=1}^{\infty} \frac{1}{k^3} = \prod_{\text{primes}} (1 - p^{-3})^{-1}$]

Boltzmann Equation

$$a^{-3}\frac{d(n_1a^3)}{dt} = \int\frac{d^3p_1}{(2\pi)^3 2E_1}\int\frac{d^3p_2}{(2\pi)^3 2E_2}\int\frac{d^3p_3}{(2\pi)^3 2E_3}\int\frac{d^3p_4}{(2\pi)^3 2E_4}$$

$$\times (2\pi)^4\delta^3(p_1+p_2-p_3-p_4)\delta(E_1+E_2-E_3-E_4)|\mathcal{M}|^2$$

$$\times \{f_3f_4[1\pm f_1][1\pm f_2] - f_1f_2[1\pm f_3][1\pm f_4]\}.$$

Dodelson (3.1)

In the absence of interactions (rhs=0) n_1 falls as a^{-3}

+ bosons
- fermions

We will typically be interested in T>> E-μ (where μ is the chemical potential). In this limit, the exponential in the Fermi-Dirac or Bose-Einstein distributions is much larger than the ±1 in the denominator, so that

$$f(E) \to e^{\mu/T}e^{-E/T}$$

and the last line of the Boltzmann equation above simplifies to

$$f_3f_4[1\pm f_1][1\pm f_2] - f_1f_2[1\pm f_3][1\pm f_4]$$

$$\to \quad e^{-(E_1+E_2)/T}\left\{e^{(\mu_3+\mu_4)/T} - e^{(\mu_1+\mu_2)/T}\right\}.$$

The number densities are given by $n_i = g_i e^{\mu_i/T}\int\frac{d^3p}{(2\pi)^3}e^{-E_i/T}$. For our applications, i's are

Table 3.1. Reactions in This Chapter: $1+2\leftrightarrow 3+4$

	1	2	3	4
Neutron-Proton Ratio	n	ν_e or e^+	p	e^- or $\bar{\nu}_e$
Recombination	e	p	H	γ
Dark Matter Production	X	X	l	l

The equilibrium number densities are given by

$$n_i^{(0)} \equiv g_i \int \frac{d^3p}{(2\pi)^3} e^{-E_i/T} = \begin{cases} g_i \left(\frac{m_i T}{2\pi}\right)^{3/2} e^{-m_i/T} & m_i \gg T \\ g_i \frac{T^3}{\pi^2} & m_i \ll T \end{cases}. \tag{3.6}$$

With this defintion, $e^{\mu_i/T}$ can be rewritten as $n_i/n_i^{(0)}$, so the last line of Eq. (3.1) is equal to

$$e^{-(E_1+E_2)/T} \left\{ \frac{n_3 n_4}{n_3^{(0)} n_4^{(0)}} - \frac{n_1 n_2}{n_1^{(0)} n_2^{(0)}} \right\}. \tag{3.7}$$

With these approximations the Boltzmann equation now simplifies enormously. Define the thermally averaged cross section as

$$\langle \sigma v \rangle \equiv \frac{1}{n_1^{(0)} n_2^{(0)}} \int \frac{d^3p_1}{(2\pi)^3 2E_1} \int \frac{d^3p_2}{(2\pi)^3 2E_2} \int \frac{d^3p_3}{(2\pi)^3 2E_3} \int \frac{d^3p_4}{(2\pi)^3 2E_4} e^{-(E_1+E_2)/T}$$

$$\times (2\pi)^4 \delta^3(p_1 + p_2 - p_3 - p_4) \delta(E_1 + E_2 - E_3 - E_4) \left|\mathcal{M}\right|^2. \tag{3.8}$$

Then, the Boltzmann equation becomes

$$a^{-3} \frac{d\left(n_1 a^3\right)}{dt} = n_1^{(0)} n_2^{(0)} \langle \sigma v \rangle \left\{ \frac{n_3 n_4}{n_3^{(0)} n_4^{(0)}} - \frac{n_1 n_2}{n_1^{(0)} n_2^{(0)}} \right\}. \tag{3.9}$$

If the reaction rate $n_2\langle \sigma v \rangle$ is much smaller than the expansion rate (~ H), then the {} on the rhs must vanish. This is called *chemical equilibrium* in the context of the early universe, *nuclear statistical equilibrium* (NSE) in the context of Big Bang nucleosynthesis, and the *Saha equation* when discussing recombination of electrons and protons to form neutral hydrogen.

As the temperature of the universe cools to 1 MeV, the cosmic plasma consists of:

- **Relativistic particles in equilibrium: photons, electrons and positrons.** These are kept in close contact with each other by electromagnetic interactions such as $e^+e^- \leftrightarrow \gamma\gamma$. Besides a small difference due to fermion/boson statistics, these all have the same abundances.
- **Decoupled relativistic particles: neutrinos.** At temperatures a little above 1 MeV, the rate for processes such as $\nu e \leftrightarrow \nu e$ which keep neutrinos coupled to the rest of the plasma drops beneath the expansion rate. Neutrinos therefore share the same temperature as the other relativistic particles, and hence are roughly as abundant, but they do not couple to them.
- **Nonrelativistic particles: baryons.** If there had been no asymmetry in the initial number of baryons and anti-baryons, then both would be completely depleted by 1 MeV. However, such an asymmetry did exist: $(n_b - n_{\bar{b}})/s \sim 10^{-10}$ initially,[1] and this ratio remains constant throughout the expansion. By the time the temperature is of order 1 MeV, all anti-baryons have annihilated away (Exercise 12) so

$$\eta_b \equiv \frac{n_b}{n_\gamma} = 5.5 \times 10^{-10} \left(\frac{\Omega_b h^2}{0.020}\right). \quad (3.11)$$

There are thus many fewer baryons than relativistic particles when $T \sim$ MeV.

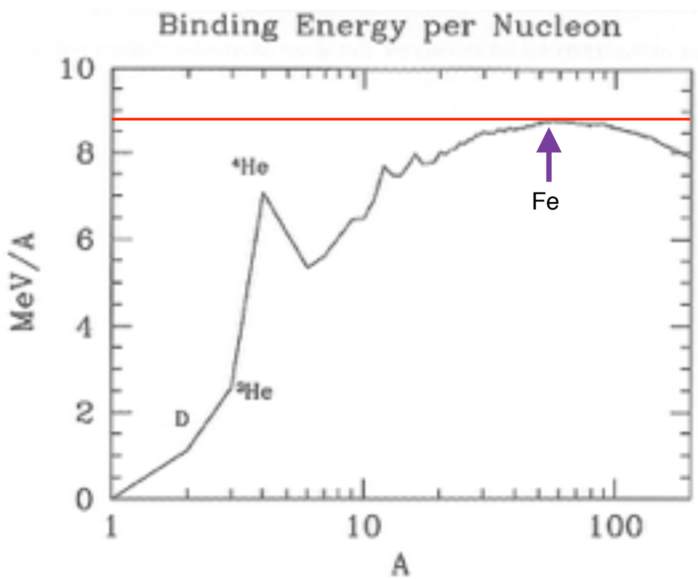

Figure 3.1. Binding energy of nuclei as a function of mass number. Iron has the highest binding energy, but among the light elements, ^{4}He is a crucial local maximum. Nucleosynthesis in the early universe essentially stops at ^{4}He because of the lack of tightly bound isotopes at $A = 5-8$. In the high-density environment of stars, three ^{4}He nuclei fuse to form ^{12}C, but the low baryon number precludes this process in the early universe.

GR follows from the principle of equivalence and Einstein's equation $G_{\mu\nu} \equiv R_{\mu\nu} - \frac{1}{2}Rg_{\mu\nu} = -8\pi G T_{\mu\nu}$.* Einstein had intuited the local equivalence of gravity and acceleration in 1907 (Pais, p. 179), but it was not until November 1915 that he developed the final form of the GR equation.

It can be derived from the following assumptions (Weinberg, p. 153):

1. The l.h.s. $G_{\mu\nu}$ is a tensor
2. $G_{\mu\nu}$ consists only of terms linear in second derivatives or quadratic in first derivatives of the metric tensor $g_{\mu\nu}$ ($\Leftrightarrow G_{\mu\nu}$ has dimension L^{-2})
3. Since $T_{\mu\nu}$ is symmetric in $\mu\nu$, so is $G_{\mu\nu}$
4. Since $T_{\mu\nu}$ is conserved (covariant derivative $T^{\mu}{}_{\nu;\mu}=0$) so also $G^{\mu}{}_{\nu;\mu}=0$
5. In the weak field limit where $g_{00} \approx -(1+2\phi)$, satisfying the Poisson equation $\nabla^2\phi = 4\pi G\rho$ (i.e., $\nabla^2 g_{00} = -8\pi G T_{00}$), we must have $G_{00} = \nabla^2 g_{00}$

---

*Note: we're here using the metric –1, 1,1,1 as in Dodelson, Weinberg.

$$\frac{n_D}{n_n n_p} = \frac{n_D^{(0)}}{n_n^{(0)} n_p^{(0)}}. \quad (3.14)$$

The integrals on the right, as given in Eq. (3.6), lead to

$$\frac{n_D}{n_n n_p} = \frac{3}{4}\left(\frac{2\pi m_D}{m_n m_p T}\right)^{3/2} e^{[m_n + m_p - m_D]/T}, \quad (3.15)$$

the factor of 3/4 being due to the number of spin states (3 for D and 2 each for p and n). In the prefactor, m_D can be set to $2m_n = 2m_p$, but in the exponential the small difference between $m_n + m_p$ and m_D is important: indeed the argument of the

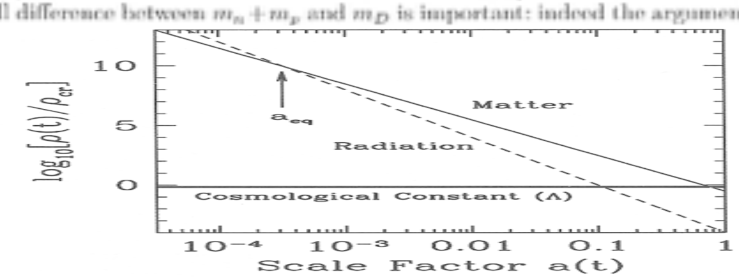

Figure 1.3. Energy density vs scale factor for different constituents of a flat universe. Shown are nonrelativistic matter, radiation, and a cosmological constant. All are in units of the critical density today. Even though matter and cosmological constant dominate today, at early times, the radiation density was largest. The epoch at which matter and radiation are equal is a_{eq}.

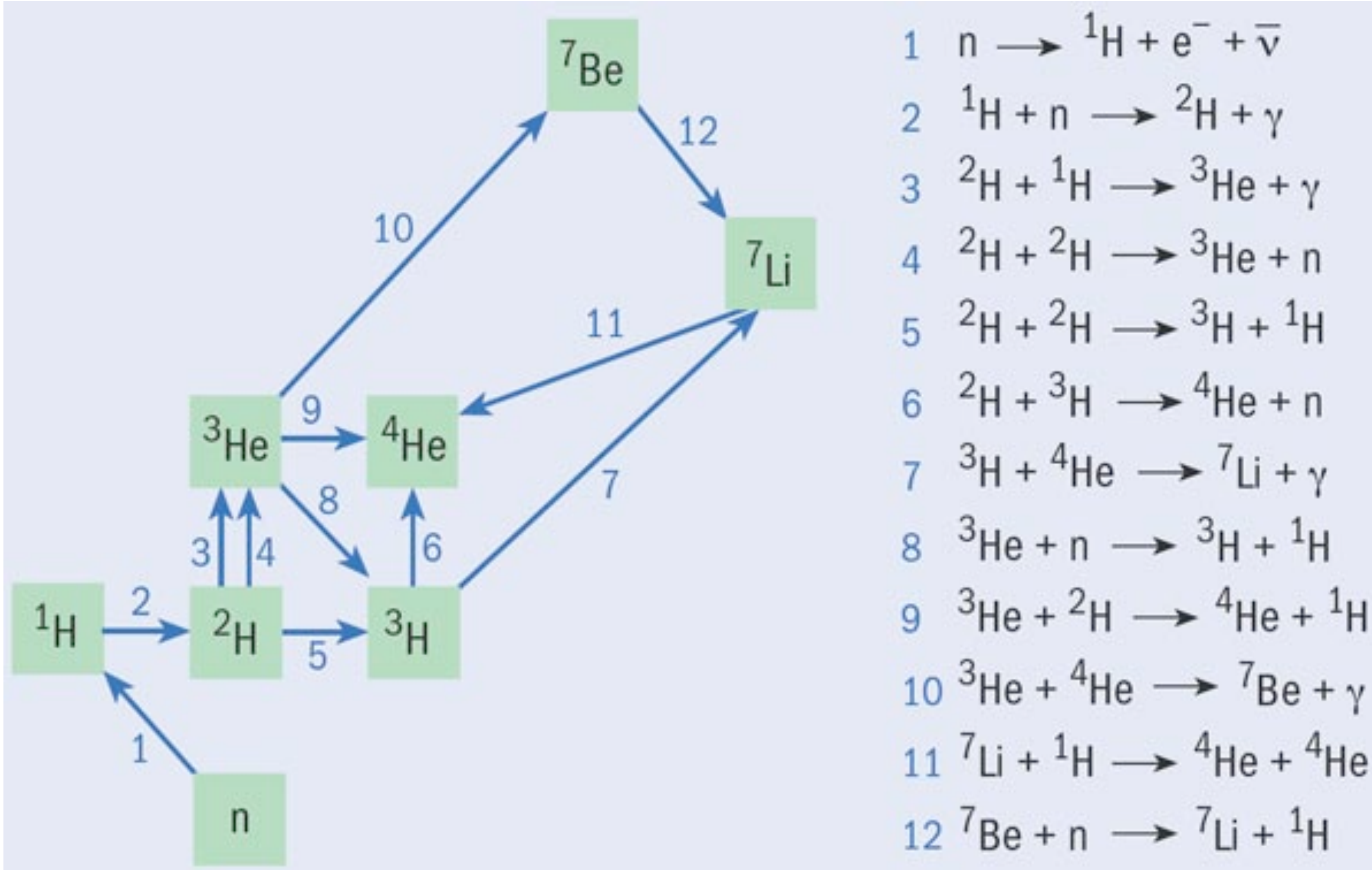

Deuterium nuclei (^{2}H) were produced by collisions between protons and neutrons, and further nuclear collisions led to every neutron grabbing a proton to form the most tightly bound type of light nucleus: ^{4}He. This process was complete after about five minutes, when the universe became too cold for nuclear reactions to continue. Tiny amounts of deuterium, ^{3}He, ^{7}Li, and ^{7}Be were produced as by-products, with the ^{7}Be undergoing beta decay to form ^{7}Li. Almost all of the protons that were not incorporated into ^{4}He nuclei remained as free particles, and this is why the universe is close to 25% ^{4}He and 75% H by mass. The other nuclei are less abundant by several orders of magnitude.

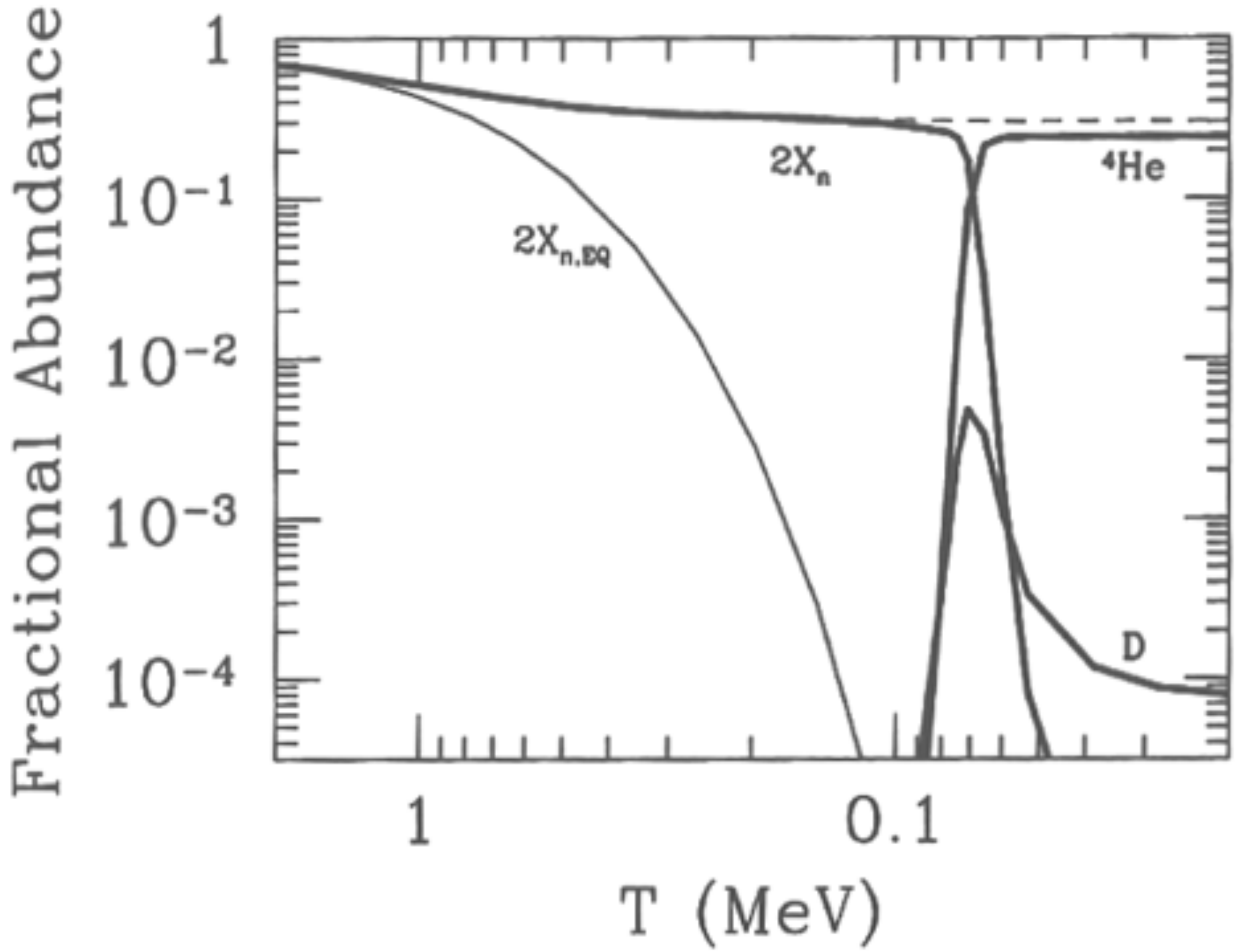

Figure 3.2. Evolution of light element abundances in the early universe. Heavy solid curves are results from Wagoner (1973) code; dashed curve is from integration of Eq. (3.27); light solid curve is twice the neutron equilibrium abundance. Note the good agreement of Eq. (3.27) and the exact result until the onset of neutron decay. Also note that the neutron abundance falls out of equilibrium at $T \sim$MeV.

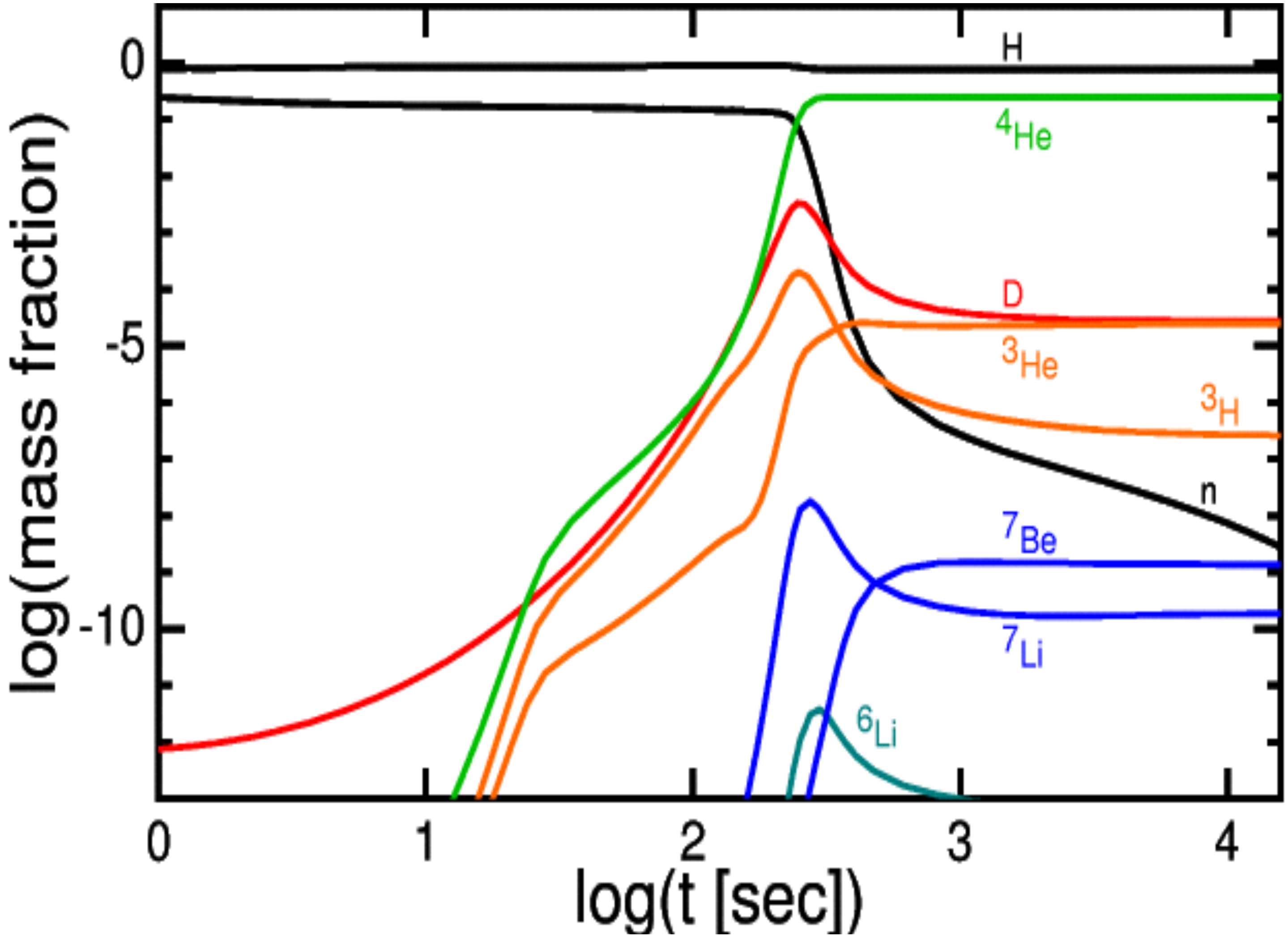

The detailed production of the lightest elements out of protons and neutrons during the first three minutes of the universe's history. The nuclear reactions occur rapidly when the temperature falls below a billion degrees Kelvin. Subsequently, the reactions are shut down, because of the rapidly falling temperature and density of matter in the expanding universe.

Ken Kawano's (1992) BBN code is available at
http://www-thphys.physics.ox.ac.uk/users/SubirSarkar/bbn.html

5 INDEPENDENT MEASURES AGREE: ATOMS ARE ONLY 4% OF THE COSMIC DENSITY

Einstein's equation can also be derived from an action principle, varying the total action $I = I_M + I_G$, where I_M is the action of matter and I_G is that of gravity:

$$I_G = -\frac{1}{16\pi G} \int R(x) \sqrt{g(x)}$$

(see, e.g., Weinberg p. 364). The curvature sc... obvious term to insert in I_G since a scalar conn... ...etric is needed and it is the only one, unless higher po... ...gher derivatives of R are used, which will lead to hig... ...her-derivative terms in the gravity equation.

Einstein realized in 1916 that the 5th postulate above isn't strictly necessary – merely that the equation reduce to the Newtonian Poisson equation within observational errors, which allows the inclusion of a small cosmological constant term. In the action derivation, such a term arises if we just add a constant to R.

WMAP Cosmic Microwave Background

Relative Height

Angular Power Spectrum

Galaxy Cluster in X-rays

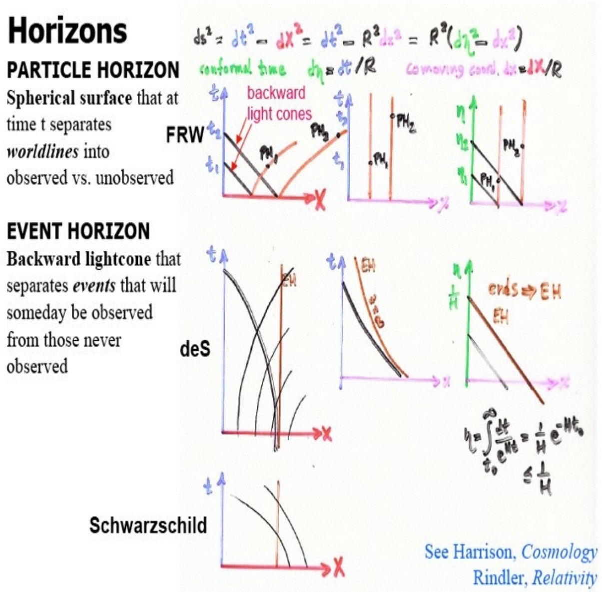

Absorption of Quasar Light

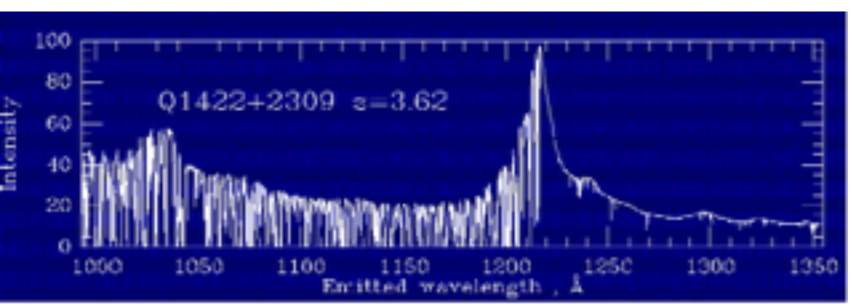

Deuterium Abundance + Big Bang Nucleosynthesis

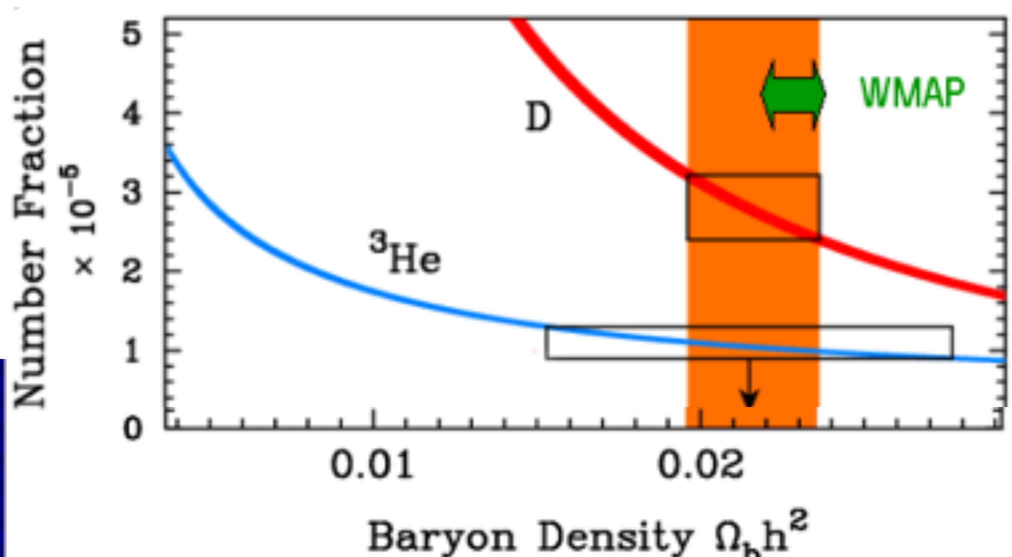

& WIGGLES IN GALAXY P(k)

BAO WIGGLES IN GALAXY P(k)

Sound waves that propagate in the opaque early universe imprint a characteristic scale in the clustering of matter, providing a “standard ruler” whose length can be computed using straightforward physics and parameters that are tightly constrained by CMB observations. Measuring the angle subtended by this scale determines a distance to that redshift and constrains the expansion rate.

The detection of the acoustic oscillation scale is one of the key accomplishments of the SDSS, and even this moderate signal-to-noise measurement substantially tightens constraints on cosmological parameters. Observing the evolution of the BAO standard ruler provides one of the best ways to measure whether the dark energy parameters changed in the past.

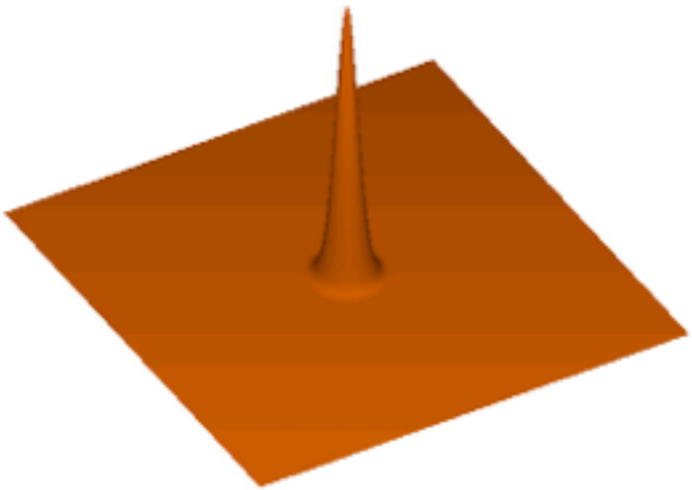

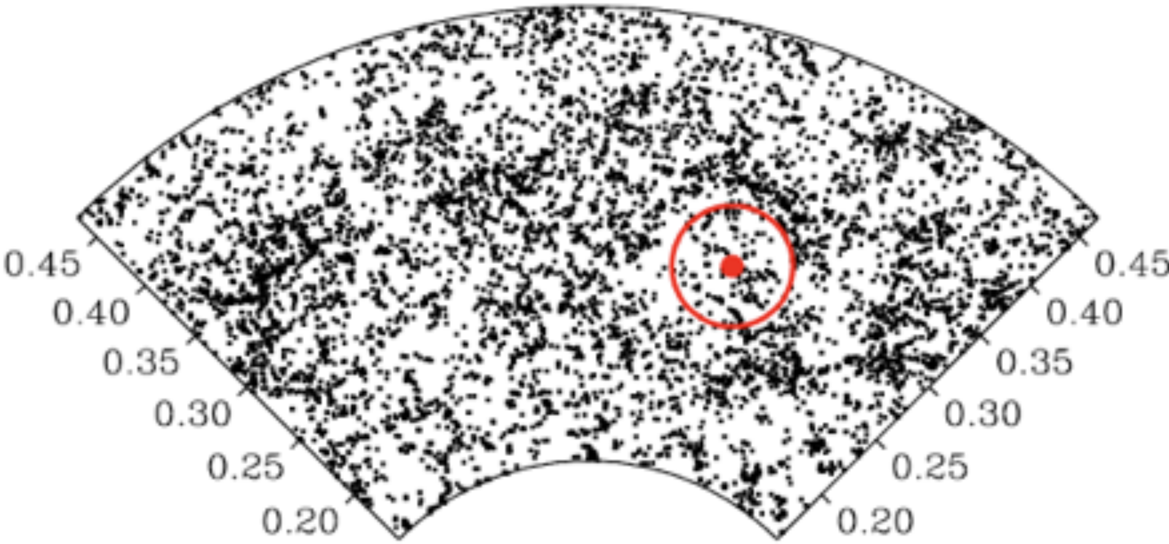

M. White lectures 08

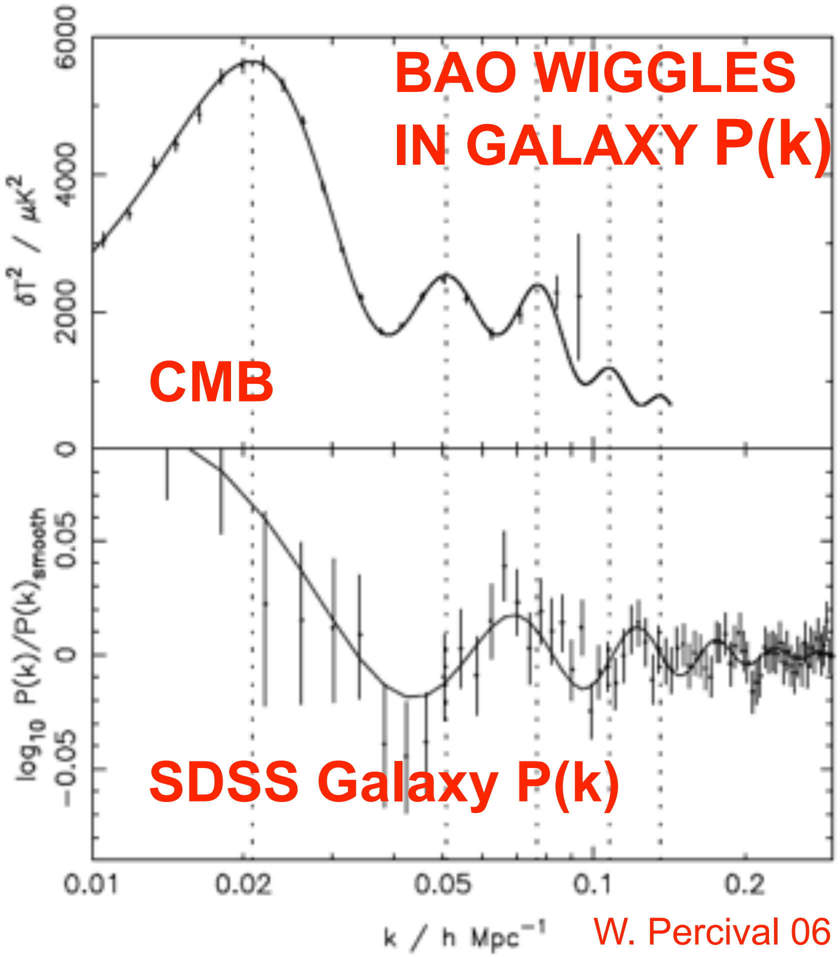

Fig. 3. Upper panel: The TT power spectrum recovered from the 3-year WMAP data (Hinshaw et al. 2006), projected into comoving space assuming a cosmological model with $\Omega_m = 0.25$ and $\Omega_V = 0.75$. For comparison, in the lower panel we plot the baryon oscillations calculated by dividing the SDSS power spectrum with a smooth cubic spline fit (Percival et al. 2007a). Vertical dotted lines show the positions of the peaks in the CMB power spectrum. As can be seen, there is still a long way to go before low redshift observations can rival the CMB in terms of the significance of the acoustic oscillation signal.

One elementary equivalence principle is the kind Newton had in mind when he stated that the property of a body called "mass" is proportional to the "weight", and is known as the weak equivalence principle (WEP). An alternative statement of WEP is that the trajectory of a freely falling "test" body (one not acted upon by such forces as electromagnetism and too small to be affected by tidal gravitational forces) is independent of its internal structure and composition. In the simplest case of dropping two different bodies in a gravitational field, WEP states that the bodies fall with the same acceleration (this is often termed the Universality of Free Fall, or UFF).

The Einstein equivalence principle (EEP) is a more powerful and far-reaching concept; it states that:

1. WEP is valid.
2. The outcome of any local non-gravitational experiment is independent of the velocity of the freely-falling reference frame in which it is performed.
3. The outcome of any local non-gravitational experiment is independent of where and when in the universe it is performed.

The second piece of EEP is called local Lorentz invariance (LLI), and the third piece is called local position invariance (LPI).

For example, a measurement of the electric force between two charged bodies is a local non-gravitational experiment; a measurement of the gravitational force between two bodies (Cavendish experiment) is not.

SDSS Galaxy ξ(k)

D. Eisenstein+05

The Einstein equivalence principle is the heart and soul of gravitational theory, for it is possible to argue convincingly that if EEP is valid, then gravitation must be a "curved spacetime" phenomenon, in other words, the effects of gravity must be equivalent to the effects of living in a curved spacetime. As a consequence of this argument, the only theories of gravity that can fully embody EEP are those that satisfy the postulates of "metric theories of gravity", which are:

1. Spacetime is endowed with a symmetric metric.
2. The trajectories of freely falling test bodies are geodesics of that metric.
3. In local freely falling reference frames, the non-gravitational laws of physics are those written in the language of special relativity.

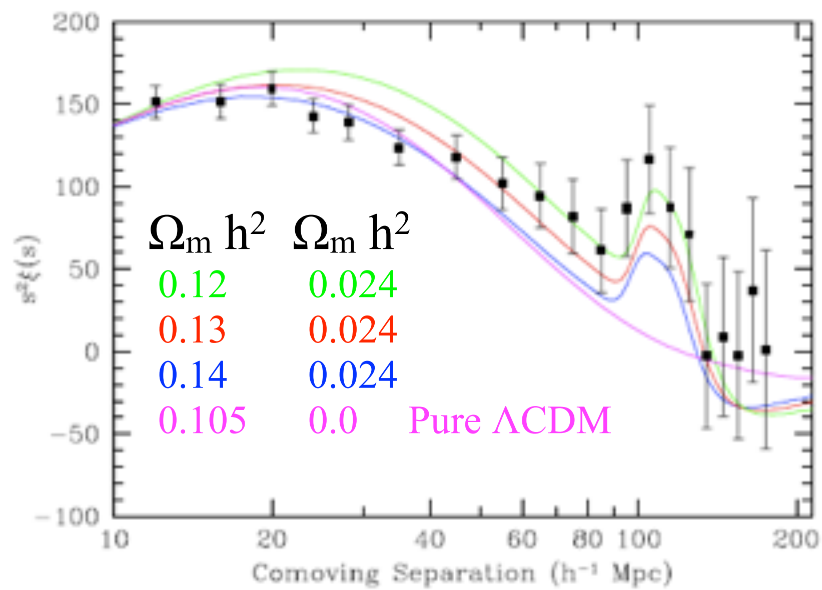

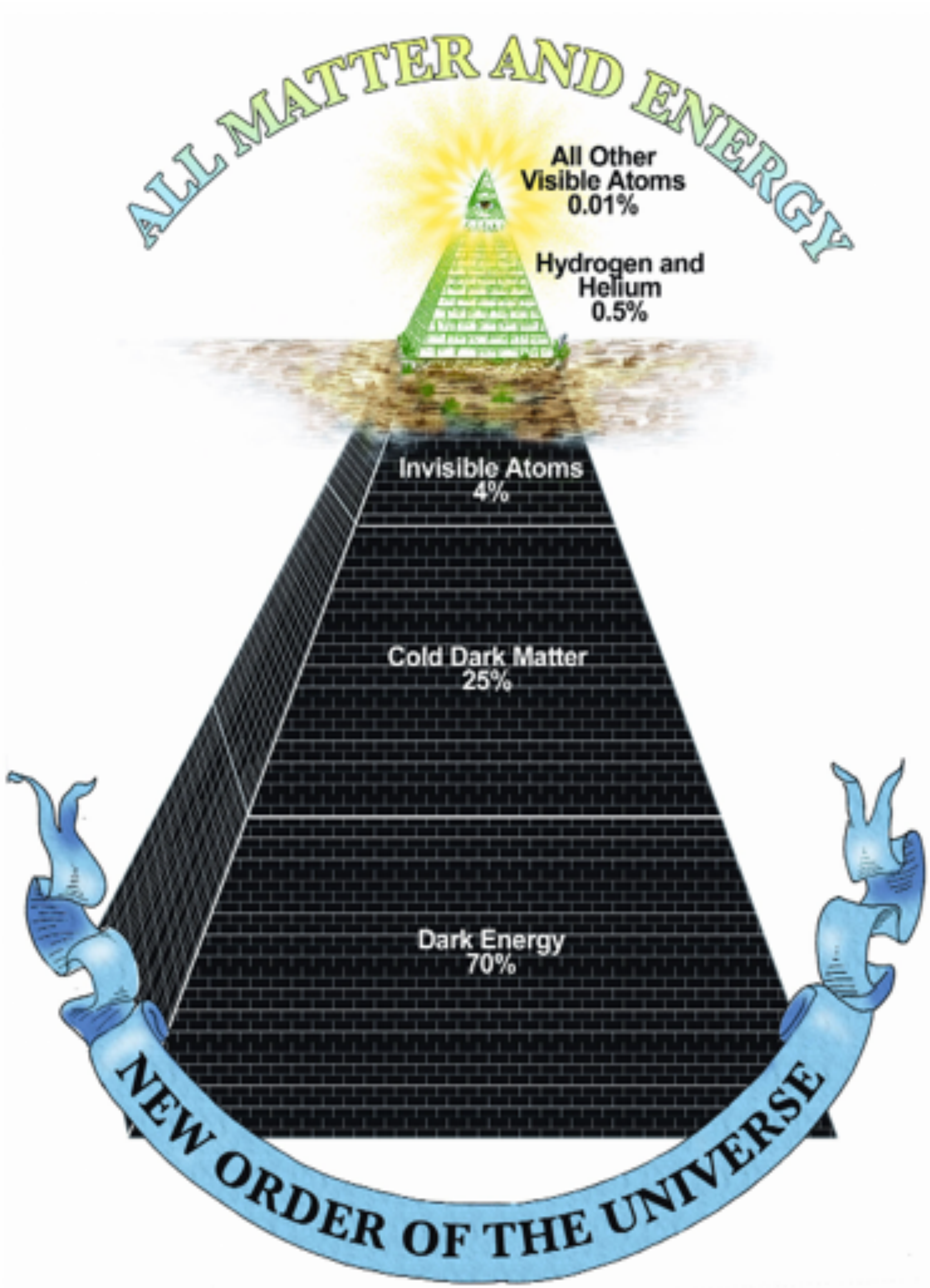
ALL MATTER AND ENERGY
All Other Visible Atoms 0.01%
Hydrogen and Helium 0.5%
Invisible Atoms 4%
Cold Dark Matter 25%
Dark Energy 70%
NEW ORDER OF THE UNIVERSE

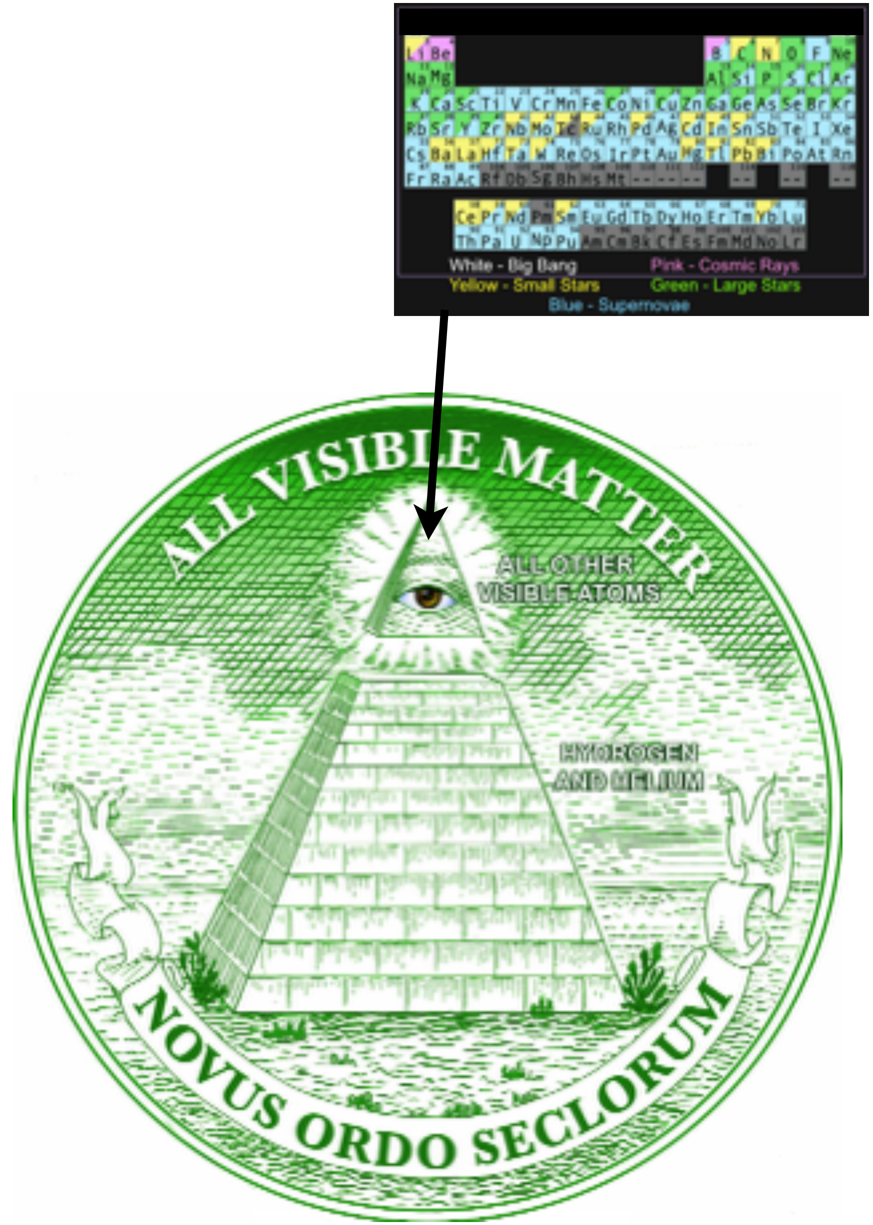
White - Big Bang
Pink - Cosmic Rays
Yellow - Small Stars
Green - Large Stars
Blue - Supernovae
ALL VISIBLE MATTER
ALL OTHER VISIBLE ATOMS
HYDROGEN AND HELIUM
NOVUS ORDO SECLORUM

BBN Predicted vs. Measured Abundances of D, ^{3}He, ^{4}He, and ^{7}Li

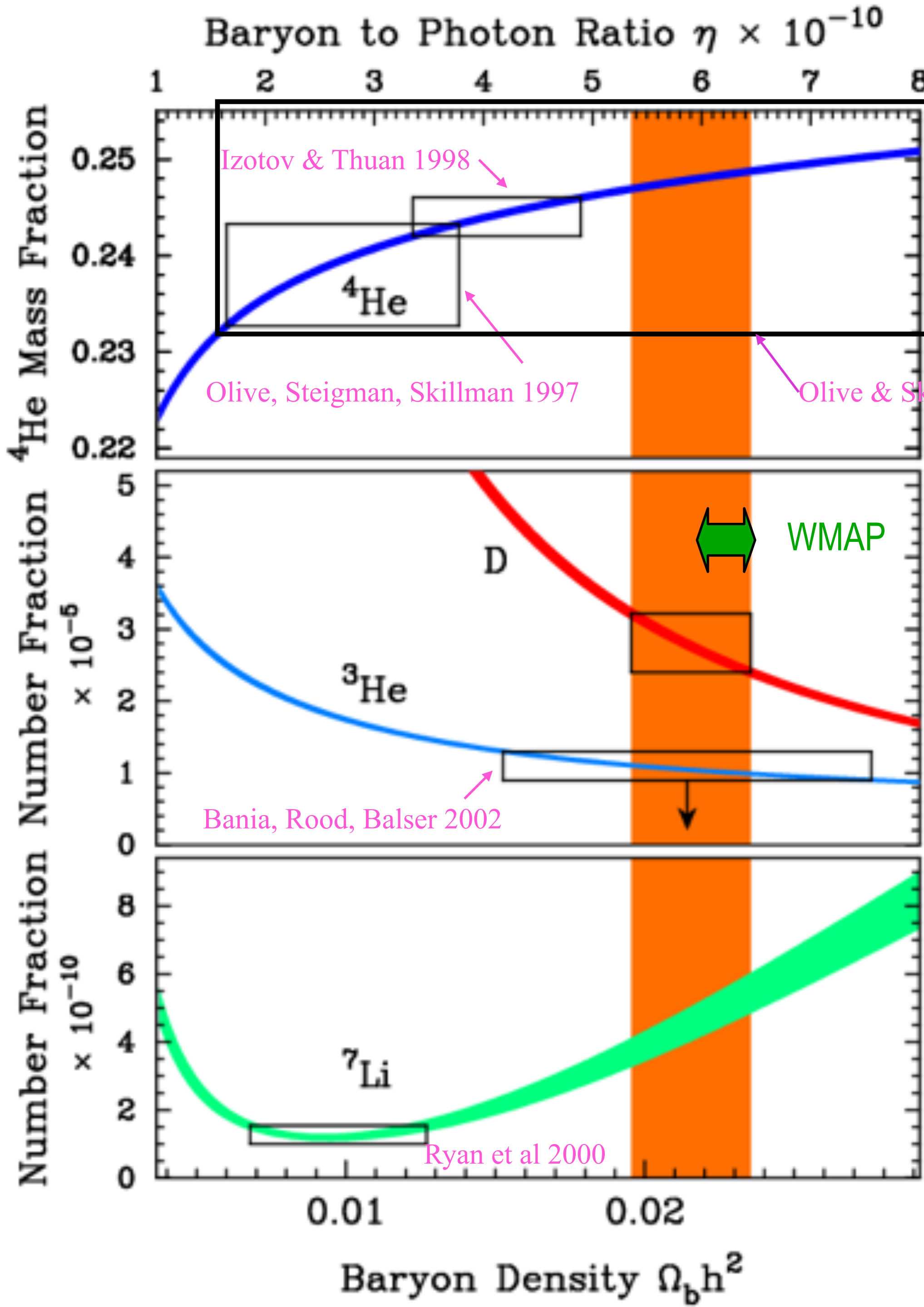

Izotov & Thuan 2004: $\Omega_b h^2$=0.012±0.0025

WMAP (Spergel et al. 2003) says that $\Omega_b h^2$=0.0224±0.0009 (with their running spectral index model)

BBN predictions are from Burles, Nollett, & Turner 2001

D/H is from Kirkman, Tytler, Suzuki, O'Meara, & Lubin 2004, giving $\Omega_b h^2$=0.0214±0.0020

^{7}Li IS NOW DISCORDANT unless stellar diffusion destroys ^{7}Li

Deuterium absorption at redshift 2.525659 towards Q1243+3047

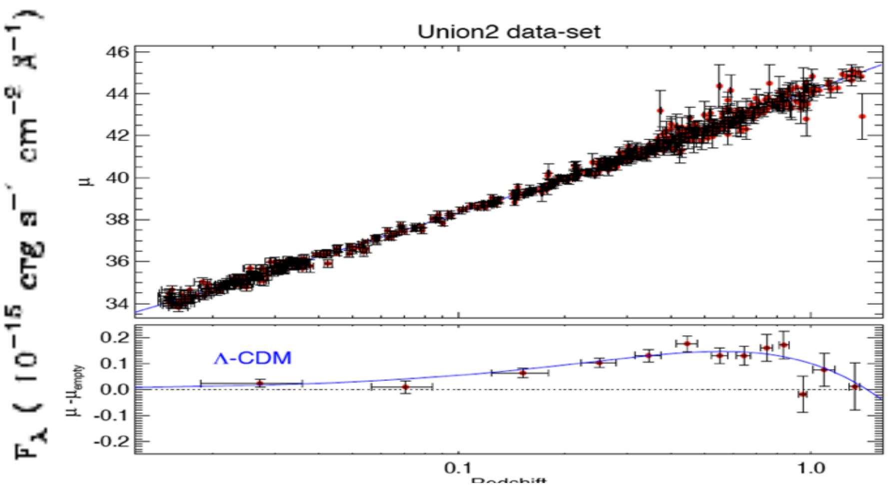

The Lyα absorption near 4285 Å is from the system in which we measure D/H.

The detection of Deuterium and the modeling of this system seem convincing. This is just a portion of the evidence that the Tytler group presented in this paper. They have similarly convincing evidence for several other Lyman alpha clouds in quasar spectra.

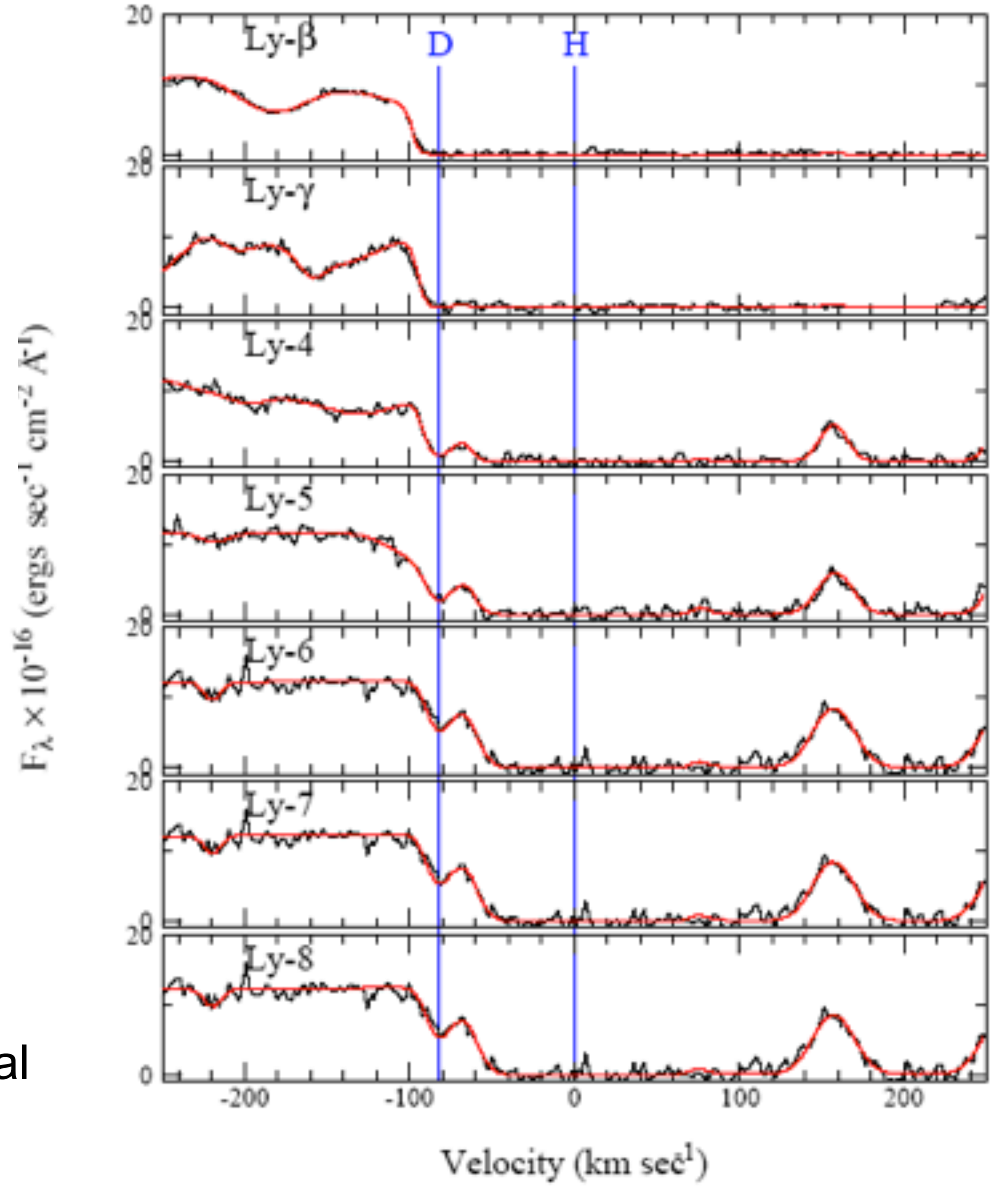

FIG. 7.— The HIRES spectrum of Ly-2 to 8, together with our model of the system, as given in Table 3.

Kirkman, Tytler, Suzuki, O'Meara, & Lubin 2004

Determination of primordial He^4 abundance Y_p by linear regression

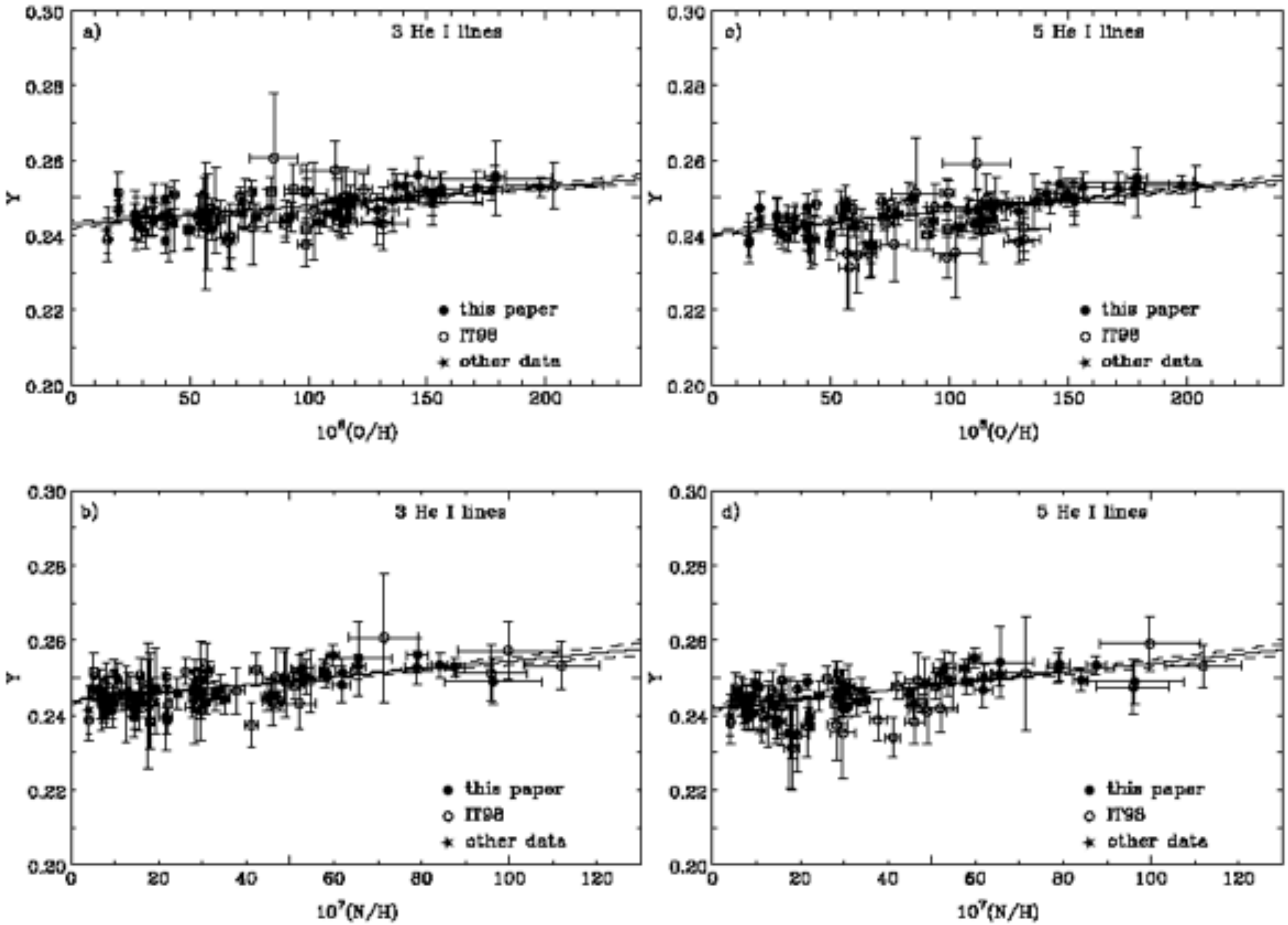

Y = M(^{4}He)/M(baryons), Primordial Y ≡ Yp = zero intercept

Note: BBN plus D/H ⇒ Yp = 0.247± 0.001

Izotov & Thuan 2004

The Li abundance disagreement with BBN may indicate new physics

Did Something Decay, Evaporate, or Annihilate during Big Bang Nucleosynthesis?

Karsten Jedamzik Phys.Rev. D70 (2004) 063524

Laboratoire de Physique Mathématique et Théorique, C.N.R.S.,
Université de Montpellier II, 34095 Montpellier Cedex 5, France

Results of a detailed examination of the cascade nucleosynthesis resulting from the putative hadronic decay, evaporation, or annihilation of a primordial relic during the Big Bang nucleosynthesis (BBN) era are presented. It is found that injection of energetic nucleons around cosmic time 10^3sec may lead to an observationally favored reduction of the primordial ^{7}Li/H yield by a factor $2-3$. Moreover, such sources also generically predict the production of the ^{6}Li isotope with magnitude close to the as yet unexplained high ^{6}Li abundances in low-metallicity stars. The simplest of these models operate at fractional contribution to the baryon density $\Omega_b h^2 \gtrsim 0.025$, slightly larger than that inferred from standard BBN. Though further study is required, such sources, as for example due to the decay of the next-to-lightest supersymmetric particle into GeV gravitinos or the decay of an unstable gravitino in the TeV range of abundance $\Omega_G h^2 \sim 5\times 10^{-4}$ show promise to explain both the ^{6}Li and ^{7}Li abundances in low metallicity stars.

See also “Supergravity with a Gravitino LSP” by Jonathan L. Feng, Shufang Su, Fumihiro Takayama Phys.Rev. D70 (2004) 075019

“Gravitino Dark Matter and the Cosmic Lithium Abundances” by Sean Bailly, Karsten Jedamzik, Gilbert Moultaka, arXiv:0812.0788

The Li abundance disagreement with BBN may be caused by stellar diffusion

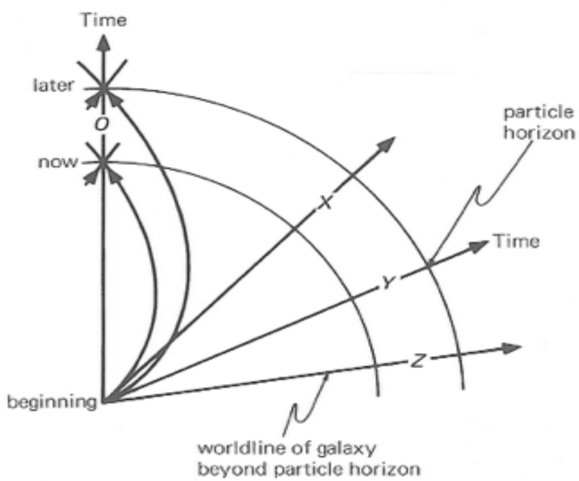

Figure 21.12. At the instant labeled "later" the particle horizon has receded to world line Y. Notice the distance of the particle horizon is always a reception distance, and the particle horizon always overtakes the galaxies and always the fraction of the universe observed increases.

	List of Ingredients
photons:	$\Omega_{\gamma,0} = 5.0 \times 10^{-5}$
neutrinos:	$\Omega_{\nu,0} = 3.4 \times 10^{-5}$
total radiation:	$\Omega_{r,0} = 8.4 \times 10^{-5}$
baryonic matter:	$\Omega_{\mathrm{bary},0} = 0.04$
nonbaryonic dark matter:	$\Omega_{\mathrm{dm},0} = 0.26$
total matter:	$\Omega_{m,0} = 0.30$
cosmological constant:	$\Omega_{\Lambda,0} \approx 0.70$

Lithium abundance in very old stars that formed from nearly primordial gas. The amount of ^{7}Li in these "Spite-plateau" stars (green) is much less than has been inferred by combining BBN with measurements of the cosmic microwave background made using WMAP (yellow band). Our understanding of stellar astrophysics may be at fault. Those Spite-plateau stars that have surface temperatures between 5700 and 6400 K have uniform abundances of ^{7}Li because the shallow convective envelopes of these warm stars do not penetrate to depths where the temperature exceeds that for ^{7}Li to be destroyed ($T_{destruct} = 2.5 \times 10^6$ K). The envelopes of cooler stars (data points towards the left of the graph) do extend to such depths, so their surfaces have lost ^{7}Li to nuclear reactions. **If the warm stars gradually circulate ^{7}Li from the convective envelope to depths where $T > T_{destruct}$, then their surfaces may also slowly lose their ^{7}Li.** From http://physicsworld.com/cws/article/print/30680

Lithium abundances, [Li] ≡ 12+ log(Li/H), versus metallicity (on a log scale relative to solar) from (red) S. Ryan et al. 2000, ApJ, 530, L57; (blue) M. Asplund et al.2006, ApJ, 644, 229. Figure from G. Steigman 2007, ARAA 57, 463.

Korn et al. 2006 find that both lithium and iron have settled out of the atmospheres of these old stars, and they infer for the unevolved abundances, [Fe/H] = –2.1 and [Li] = 2.54 ± 0.10, in excellent agreement with SBBN.

The most stringent constraint on a mixing model is that it must maintain the observed tight bunching of plateau stars that have the same average ^7Li abundance. In a series of papers that was published between 2002 and 2004, Olivier Richard and collaborators at the Université de Montréal in Canada proposed such a mixing model that has since gained observational support. It suggests that all nuclei heavier than hydrogen settle very slowly out of the convective envelope under the action of gravity. In particular, the model makes specific predictions for settling as a star evolves, which are revealed as variations of surface composition as a function of mass in stars that formed at the same time.

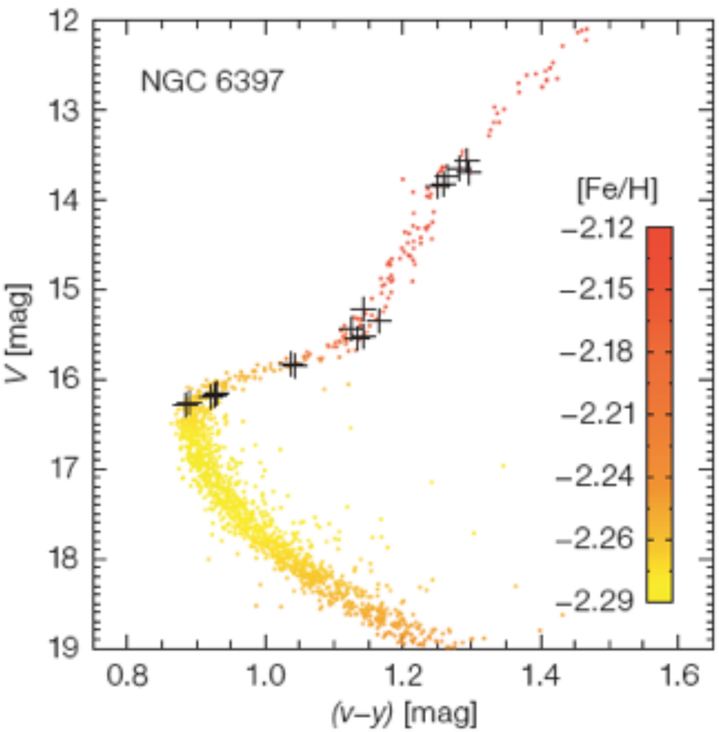

Korn et al. The Messenger 125 (Sept 2006); Korn et al. 2006, Nature 442, 657.

By spring 2006, Andreas Korn of Uppsala University in Sweden and colleagues had used the European Southern Observatory's Very Large Telescope (VLT) in Chile to study 18 chemically primitive stars in a distant globular cluster called NGC 6397 that were known to have the same age and initial composition. From this Korn et al. showed that the iron and lithium abundances in these stars both varied according to stellar mass as predicted by Richard's model. In fact, the model indicated that the observed stars started out with a ^7Li abundance that agrees with the WMAP data. Corroboration of these results is vital because **if the result stands up to scrutiny based on a wide range of data, then we have solved the lithium problem.**

FIGURE 6.5 The scale factor a as a function of time t (measured in units of the Hubble time), computed for the Benchmark Model. The dotted lines indicate the time of radiation-matter equality, $a_{rm} = 2.8 \times 10^{-4}$, the time of matter-lambda equality, $a_{m\Lambda} = 0.75$, and the present moment, $a_0 = 1$.

A probable stellar solution to the cosmological lithium discrepancy

A Korn et al.

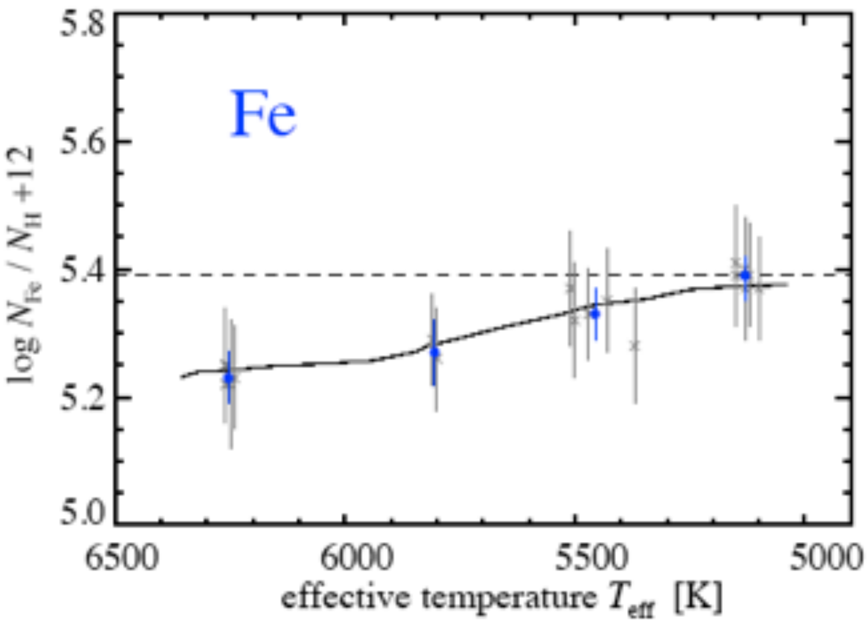

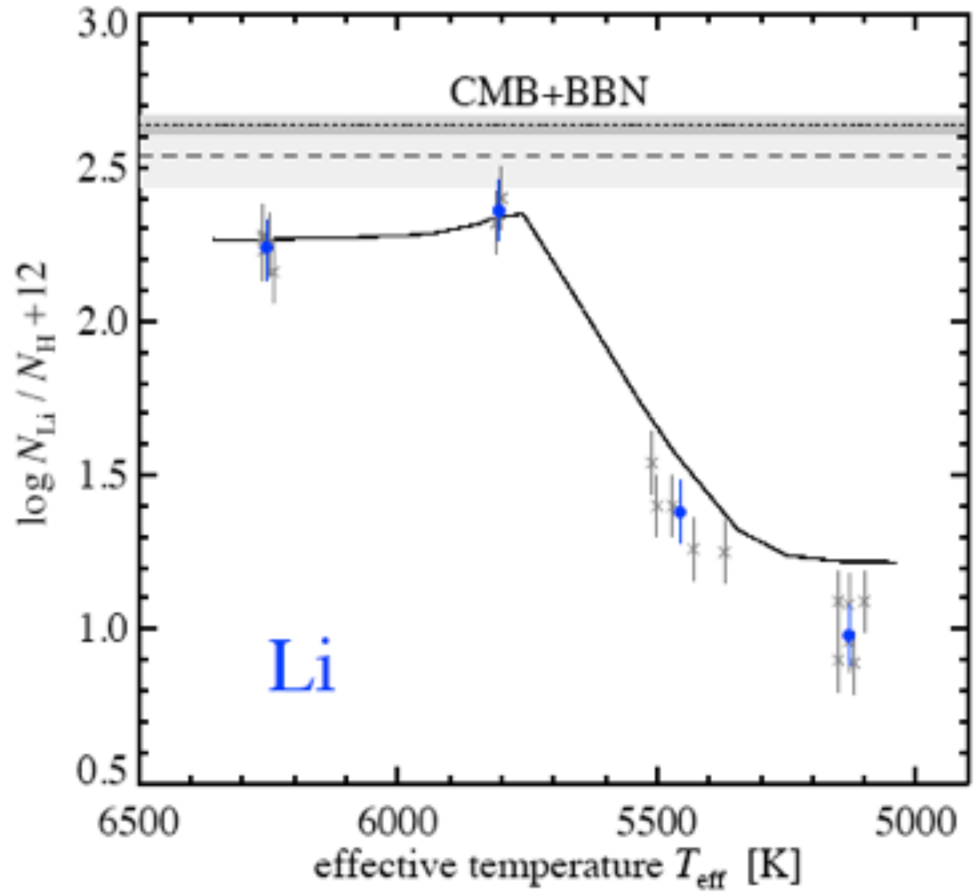

Figure 1: Trends of iron and lithium as a function of the effective temperatures of the observed stars compared to the model predictions. The grey crosses are the individual measurements, while the bullets are the group averages. The solid lines are the predictions of the diffusion model, with the original abundance given by the dashed line. In b, the grey-shaded area around the dotted line indicates the 1σ confidence interval of CMB + BBN[1]: $\log[\varepsilon(\mathrm{Li})] = \log(N_{Li}/N_H) + 12 = 2.64 \pm 0.03$. In a, iron is treated in non-equilibrium[20] (non-LTE), while in b, the equilibrium (LTE) lithium abundances are plotted, because the combined effect of 3D and non-LTE corrections was found to be very small[29]. For iron, the error bars are the line-to-line scatter of Fe I and Fe II (propagated into the mean for the group averages), whereas for the absolute lithium abundances 0.10 is adopted. The 1σ confidence interval around the inferred primordial lithium abundance ($\log[\varepsilon(\mathrm{Li})] = 2.54 \pm 0.10$) is indicated by the light-grey area.We attribute the modelling shortcomings with respect to lithium in the bRGB and RGB stars to the known need for extra mixing[30], which is not considered in the diffusion model.

Another way to determine the amount of ^{7}Li destroyed in stars is to observe the element's other, less stable, isotope: ^{6}Li. ^{6}Li is not made in detectable quantities by BBN but instead comes from spallation: collisions between nuclei in cosmic rays and in the interstellar gas. Since ^{6}Li is even more easily destroyed than ^{7}Li, detecting it allows us to place limits on the destruction of ^{7}Li.

In 2006 Martin Asplund and co-workers at the Mount Stromlo Observatory in Australia made extensive observations of ^{6}Li in plateau stars using the VLT. In each of the nine stars where they found ^{6}Li, roughly 5% of the lithium consisted of this isotope – which was larger than expected although at the limit of what was detectable with the equipment. This has huge implications not only for BBN but also for the history of cosmic rays in the galaxy and for stellar astrophysics. For example, the production of such large amounts of ^{6}Li must have required an enormous flux of cosmic rays early in the history of our galaxy, possibly more than could have been provided by known acceleration mechanisms. Moreover, if the plateau stars have truly destroyed enough ^{7}Li to bring the WMAP prediction of the mean baryon density into agreement with that obtained with the observed Spite plateau, the greater fragility of ^{6}Li implies that the stars initially contained ^{6}Li in quantities comparable to the observed ^{7}Li plateau.

All of these facts make the ^{6}Li observations an uncomfortable fit for BBN, stellar physics and models of cosmic-ray nucleosynthesis – particularly since the production of large amounts of ^{6}Li via cosmic rays has to be accompanied by a similar production of ^{7}Li. Although ^{6}Li can be produced in some exotic particle-physics scenarios, it is vital that we independently confirm Asplund's results. Indeed, the hunt for primordial lithium (of both isotopes) is currently ongoing at the VLT, as well as at the Keck Observatory and the Japanese Subaru Telescope, although such observations are right at the limit of what can be achieved.

Recent references on BBN and Lithium

M Asplund et al. 2006, "Lithium isotopic abundances in metalpoor halo stars" ApJ 644 229–259

M Asplund and K Lind, "The light elements in the light of 3D and non-LTE effects" Light elements in the Universe (Proceedings IAU Symposium No. 268, 2010) C. Charbonnel, M. Tosi, F. Primas & C. Chiappini, eds. (arXiv:1002.1993v1)

T Beers and N Christlieb 2005, "The discovery and analysis of very metal-poor stars in the galaxy" Ann. Rev. Astron. Astrophys. 43, 531–580

A Korn et al. 2006 "A probable stellar solution to the cosmological lithium discrepancy" Nature 442, 657–659; 2007 "Atomic Diffusion and Mixing in Old Stars. I. Very Large Telescope FLAMES-UVES Observations of Stars in NGC 6397" ApJ 671, 402

C Charbonnel 2006, "Where all the lithium went" Nature 442, 636-637

K Nollett 2007, "Testing the elements of the Big Bang" physicsworld.com

R H Cyburt, B D Fields, K A Olive 2008, "An update on the big bang nucleosynthesis prediction for 7Li: the problem worsens" JCAP 11, 12 (also arXiv:0808.2818)

A J Korn 2008 "Atomic Diffusion in Old Stars --- Helium, Lithium and Heavy Elements" ASPC 384, 33

BBN is a Prototype for Hydrogen Recombination and DM Annihilation

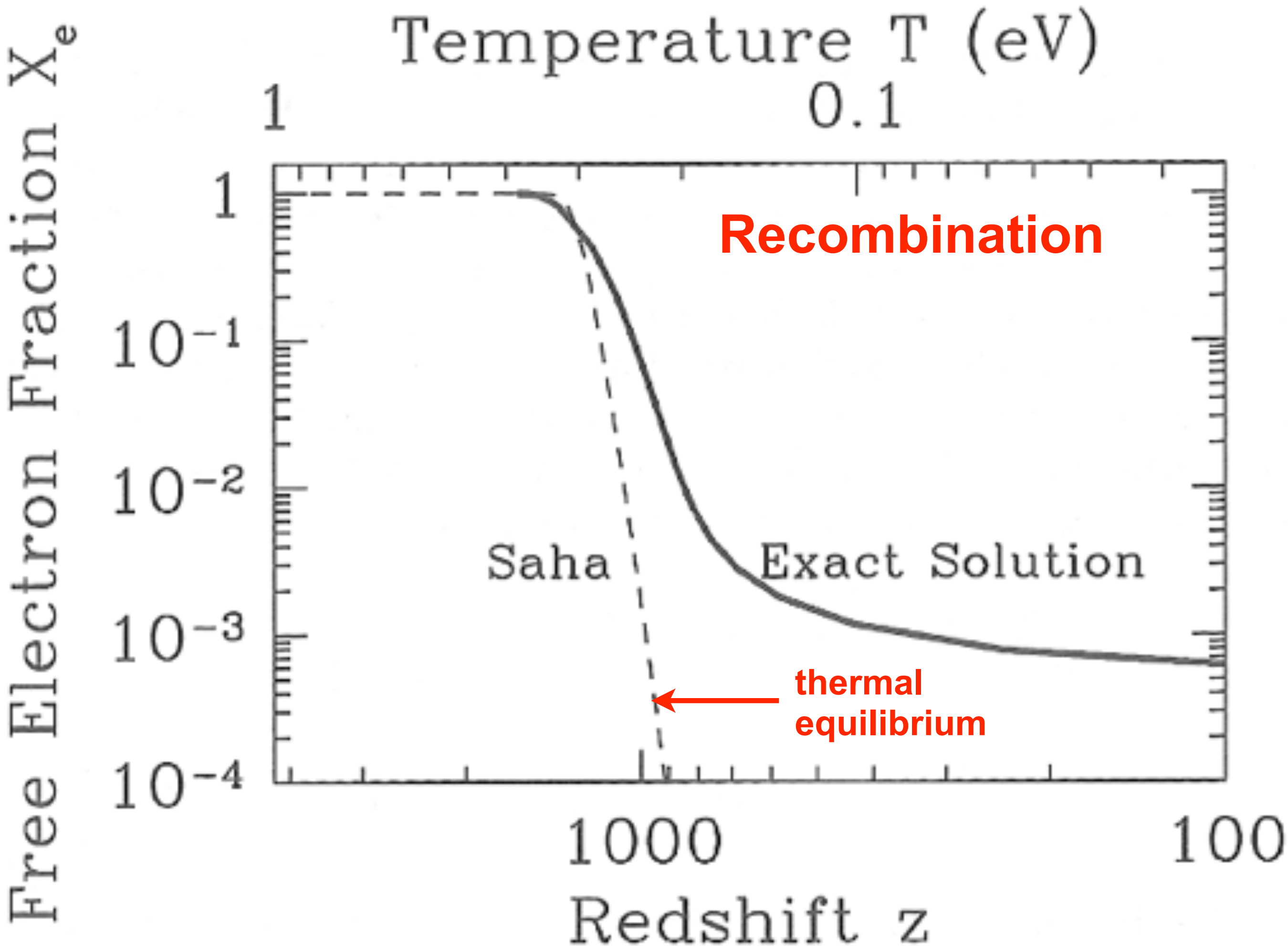

Figure 3.4. Free electron fraction as a function of redshift. Recombination takes place suddenly at $z \sim 1000$ corresponding to $T \sim 1/4$ eV. The Saha approximation, Eq. (3.37), holds in equilibrium and correctly identifies the redshift of recombination, but not the detailed evolution of X_e. Here $\Omega_b = 0.06, \Omega_m = 1, h = 0.5$.

Dodelson, *Modern Cosmology*, p. 72

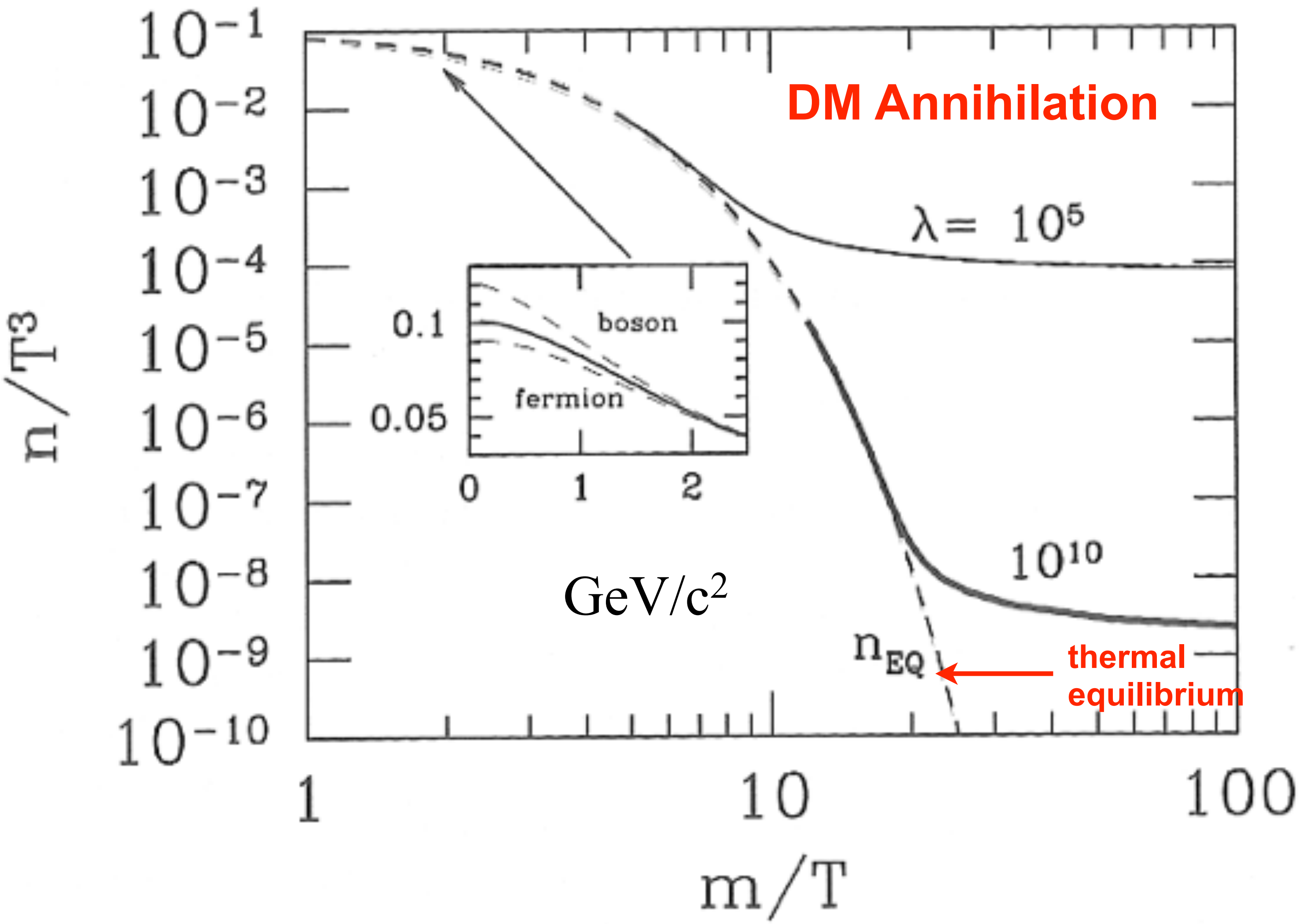

Figure 3.5. Abundance of heavy stable particle as the temperature drops beneath its mass. Dashed line is equilibrium abundance. Two different solid curves show heavy particle abundance for two different values of λ, the ratio of the annihilation rate to the Hubble rate. Inset shows that the difference between quantum statistics and Boltzmann statistics is important only at temperatures larger than the mass.

Dodelson, *Modern Cosmology*, p. 76